CAPTURING MOLECULES WITH TEMPLATED MATERIALS: ANALYSIS AND RATIONAL DESIGN OF MOLECULARLY IMPRINTED POLYMERS

A Thesis
Presented to
The Academic Faculty

by

Shuting Wei

In Partial Fulfillment
of the Requirements for the Degree
Doctor of Philosophy in the
School of Chemistry and Biochemistry

Georgia Institute of Technology
August 2007

CAPTURING MOLECULES WITH TEMPLATED MATERIALS: ANALYSIS AND RATIONAL DESIGN OF MOLECULARLY IMPRINTED POLYMERS

Approved by:

Dr. Boris Mizaikoff, Advisor
School of Chemistry and Biochemistry
Georgia Institute of Technology

Dr. Andrew L. Lyon
School of Chemistry and Biochemistry
Georgia Institute of Technology

Dr. Ching-hua Huang
School of Civil & Environmental Engineering
Georgia Institute of Technology

Dr. David M. Collard
School of Chemistry and Biochemistry
Georgia Institute of Technology

Dr. Facundo M. Fernandez
School of Chemistry and Biochemistry
Georgia Institute of Technology

Date Approved: May 18, 2007

ACKNOWLEDGEMENTS

My dearest thanks and deepest respect go to my supervisor *Professor Boris Mizaikoff* for giving me the great opportunity to do my PhD thesis at the Applied Sensors Laboratory, School of Chemistry and Biochemistry, Georgia Institute of Technology. He and *Dr.Christine Kranz* are an incredible team with outstanding motivation abilities and profound knowledge. Their guidance and inspiration helped me to grow as a scientist and person.

I also would like to express my appreciation and thanks to the members of my committee who have provided me knowledge, insight, and experience helping throughout my work. Especially I would like to thank Dr. Facundo M. Fernandez and Dr. Ching-hua Huang for enabling use of the facilities in their lab as well as the many discussions on the MS studies and the environmental analysis, and our collaborator Dr. Michael Jakusch for enabling use of the computing facilities at the Austrian Research Center Seibersdorf (ARC, Division of Environmental and Life Sciences) and helping with the molecular dynamics simulations.

Many thanks go to both past and present group members of the Applied Sensors Laboratory for their help, support, friendship, and for the many interesting and useful discussions.

Finally, I would like to extend a special thank you to my husband and my parents. I could not have accomplished all that I have without their love and support. I cannot express the depth of my appreciation for their love, understanding, and support for me as I pursued my degree.

TABLE OF CONTENTS

LIST OF TABLES

LIST OF FIGURES

LIST OF SYMBOLS AND ABBREVIATIONS

AIBN	2,2'-Azobis (2-isobutyronitrile)
ATR/FT-IR	Attenuated total reflectance fourier transform infrared spectroscopy
DART	Direct analysis in real time
DVB	Divinylbenzene
E1	Estrone
E2	17β-estradiol
17α-E2	17α-estradiol
E3	Estriol
EDMA	Ethyleneglycol dimethacrylate
EE2	ethynylestradiol
MIPs	Molecular imprinted polymers
MISPE	MIP based solid phase extraction
MAA	Methacrylic acid
MIA	Molecularly imprinted sorbent assays
4-NP	4-nitrophenol
SPE	Solid phase extraction
TIC	Total ion chromatograms
TRIM	Trimethylolpropane trimethacrylate
4-VP	4-vinylpyridine

SUMMARY

Within the last decade, interest in molecularly imprinted polymers (MIPs) has strongly increased, with potential applications ranging from solid phase extraction (SPE) materials to antibody-like sorbent assays and selective recognition layers in sensing devices. Advantages such as chemical, mechanical and thermal stability together with high selectivity for the templated analyte render MIPs interesting alternatives to routinely applied separation materials or antibodies. Nevertheless, many factors such as the choice of functional monomer, cross-linker, and porogenic solvent, as well as the ratio between template, functional monomer, and cross-linker will affect the resulting imprinting efficiency and polymer particle size and morphology. The conventional MIPs synthesized by bulk polymerization methods produce particles with the desired size by grinding and sieving, which is a labor intensive and wasteful process, as a considerable amount of fine particles with broad size distribution is produced, which is of limited suitability for HPLC separations or binding assays. For the synthesis of molecularly imprinted micro- and nanospheres while retaining high selectivity along with control on particle shape and size, a synthetic route avoiding the use of dispersants such as water or protic solvents is demanded. The research described in this thesis contributes to the development of new synthetic strategies for the generation of imprinted micro- and nanospheres for 17β-estradiol (E2) focusing on accurate control and optimization of the governing parameters for precipitation polymerization, including the polymerization temperature and the cross-linker, yielding a one-step synthetic approach with superior control on the bead diameter, shape, monodispersity and imprinting efficiency. Thus synthesized imprinting materials for E2 were successfully applied in HPLC separation, solid phase extraction and

radioligand binding assays. As the optimization of imprinted materials is based on fundamental understanding of the binding site properties, the investigations is aimed at establishing a more rational basis for further tailoring imprinted materials to the desired analytical application. For this purpose, a comparison of the specific binding properties of imprinted polymers prepared by different synthetic routes yielding particulates generated from bulk polymers, microspheres, and nanospheres was obtained. The relationships between the particle porosity and rebinding properties were detailed, providing useful guidelines for controlling the particle properties for the desired application including, SPE pre-concentration, HPLC separations, and biomimetic binding assays. Furthermore, analytical techniques (^{1}H-NMR and IR, etc.) and molecular modeling were combined in this thesis to facilitate advanced understanding of the fundamental principles governing selective recognition of molecularly imprinted polymers at a molecular level. It is assumed that complex formation based on noncovalent interactions between the template analyte, the functional monomer, and the cross-linker is ultimately responsible for a successful imprint. However, confirmation of the proposed mechanisms is essential for the development of optimized MIPs. The molecular interactions involved in the templating process of molecularly imprinted polymers based on the self-assembly approach were simulated in molecular dynamic simulation model by building a modeling system include all the imprinting components with correct ratio, which has never been reported before. Molecular level interactions such as hydrogen bonding, π-π stacking interactions as well as the free energy governing complex formation of E2 with the functional monomers 4-vinylpyridine (4VP) and methacrylic acid (MAA), and the cross-linker divinylbenzene (DVB) were discussed. The accuracy of these results needs to be

confirmed by thorough experimental analysis establishing the validity of the developed models. ^{1}H-NMR titration experiments suggested the formation of hydrogen-bonding complexes between E2 and MAA in the pre-polymerization mixture. The presence of specific functionalities of the imprinted polymer to the template molecule is validated by the results obtained from attenuated total reflectance fourier transform infrared spectroscopy (ATR/FT-IR) measurements of the imprinted polymer matrix as well as the control polymer matrix.

CHAPTER 1

INTRODUCTION

1.1 Molecular Imprinted Polymers as Synthetic Receptors

The selective recognition of biologically relevant molecules governs many essential biological interactions. Hence, the creation of synthetic, tailor-made receptors capable of recognizing molecular targets of interest with high affinity and selectivity continues to be a long-term goal for scientists in the field of chemical, biological, and pharmaceutical research. Compared to natural receptors, synthetic receptors promise simplified synthesis, production, and processing, less costs, and more robust receptor architectures. During recent decades, molecular imprinting or templating techniques have been adopted as versatile synthetic strategies providing a variety of synthetic routes to achieve these goals. Among the variety of approaches for generating synthetic receptors, molecular imprinting techniques offer a number of distinct advantages, which include (i) the comparative straightforwardness of the preparation of molecularly imprinted polymers, (ii) the inherent robustness of such recognition elements, and (iii) the chemical, mechanical, and thermal stability of the obtained templated materials[1, 2]. Many relatively small molecules have successfully been imprinted for a variety of applications aiming at the unambiguous detection and quantification of the template molecule, and include the application of the derived recognition materials in biomimetic sensors[3-5], affinity chromatography[6-8], solid phase extraction[9-16], and (immuno)assays[17-19]. A remaining challenge for the next generation of MIPs is the synthesis of deliberately designed and highly efficient receptor architectures, and a more rational understanding of the principles

underlying the formation of binding sites by investigating molecular level interactions between the molecular building blocks involved in the imprinting procedure.

1.2 Scope of This Work

Highly selective sorbent materials for a large number of analytes of environmental and pharmaceutical interest have been prepared by molecular imprinting[1]. Within the various imprinting strategies briefly introduced later in this thesis, non-covalent molecular imprinting relies on the nature and stability of the complex formed between target analyte and functional monomer building blocks prior to radical polymerization, as well as the number, distribution, and accessibility of thus generated specific binding sites within the resulting polymeric recognition material. Therefore, fundamental understanding of the interactions responsible for complex formation and complex stability during the imprinting procedure at a molecular level is crucial for rationally devising the development of next-generation designed biomimetic recognition materials. Consequently, **the aim of this thesis** was to develop molecular imprinted materials suitable for recognizing biologically relevant molecules for applications in affinity separations and biomimetic assays, with focus on the synthesis of size- and shape-uniform particles facilitating reproducibility, improved binding site accessibility, and enhanced affinity. Furthermore, deeper understanding on the fundamental interactions governing imprinting, and rational understanding of the imprinting mechanism was detailed by the combination of analytical/spectroscopic techniques with molecular dynamics simulations for assessing the dominating parameters responsible for successful non-covalent imprinting at a molecular level.

Original contributions of this thesis:

• The development of MIP synthesis methods for 17β-estradiol including bulk material, microsphere (3 μm), and nanosphere (400 nm) formats, along with the characterization and analytical application of these imprinted materials in affinity separations and biomimetic assays (Chapter 3).

• The comprehensive investigation of different imprinted polymer formats enabled correlating the obtained porosities with differences observed during rebinding studies (Chapter 3).

• Experimental analysis of the nature of non-covalent imprinting mechanisms by spectroscopic and spectrometric techniques, in particular NMR, IR, and MS (Chapter 3).

• Development of the first models and molecular dynamics simulations for theoretically describing the interaction between the molecular building blocks involved in non-covalent molecular imprinting at the pre-polymerization stage (Chapters 4).

This thesis is organized as follows:

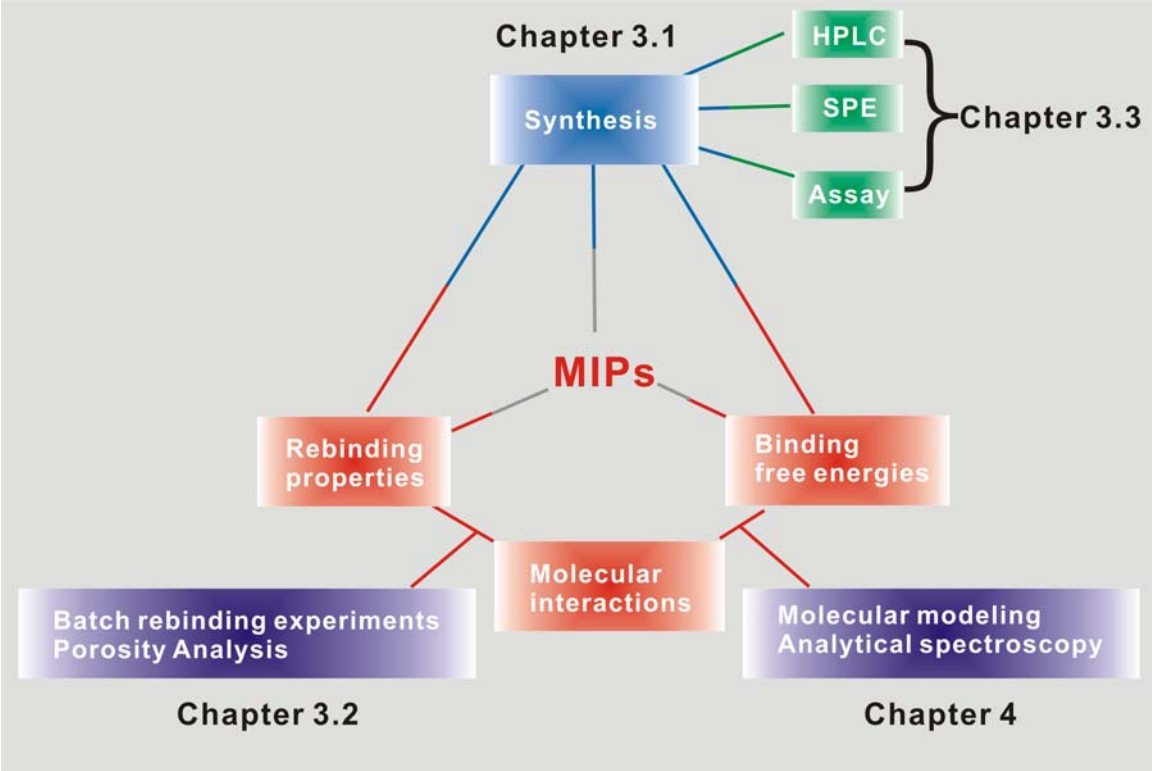

Figure 1.1 Overview of the main contributions of this thesis and their connection.

Chapter 2 of this thesis provides the background and theory on the principles of molecular imprinting techniques, along with a discussion of the main factors affecting the recognition properties of MIPs. Furthermore, an introduction to the application of imprinted materials in liquid chromatography, solid phase extraction, and ligand binding assays is provided. Finally, current techniques for monitoring molecular interactions involved in the binding site formation including spectroscopic/spectrometric techniques and computational modeling are introduced.

Chapter 3 focuses on the synthesis and characterization of imprinted materials for 17β-estradiol in affinity separations and biomimetic assays. The developed particular bulk

imprinted polymers and monodisperse imprinted microspheres were synthesized and then characterized by application as stationary phase material in HPLC experiments for estrogen separation. Furthermore, the most suitable candidate among the synthesized imprinted polymers was determined in comparison studies, and successfully applied as stationary phase in solid phase extraction based sample preparation for environmental water analysis. Finally, nanospheres with diameters of approximately 400 nm were synthesized by optimization of the polymerization conditions, and subsequently applied in biomimetic ligand binding assays.

Chapter 4 A computational model including all the imprinting components was established for the first time, thereby providing detailed understanding on the strength and type of interactions between the involved molecular species, including the porogenic solvent. The interactions involved in molecular imprinting at molecular level were confirmed by analytical characterization of the pre-polymerization complexes, as well as the polymer matrix. The binding free energies of the MIP systems compared in this study were calculated by treating the template molecule as a guest, and all the other imprinting components as host. The free energy calculation results are in acceptable agreement with the chromatographic performance (separation ability for optical isomers of the template molecule) of the corresponding MIP materials.

Chapter 5 summarizes the contributions of the present studies on non-covalent molecular imprinting techniques, and provides an outlook for future investigations.

1.3 References

1. Sellergren, B., Molecularly Imprinted Polymers: Man-Made Mimics of Antibodies and Their Applications in Analytical Chemistry. Amsterdam, Elsevier.: 2001.

2. Molinelli, A.; Janotta, M.; Mizaikoff, B., Molecularly Imprinted Polymers for Biomolecular Recognition (Protein Nanotechnology: Protocols, Instrumentation and Applications). Humana Press: Totowa, NJ 2005; Vol. 300, p 243-254.

3. Kriz, D.; Ramstroem, O.; Svensson, A.; Mosbach, K., A Biomimetic Sensor Based on a Molecularly Imprinted Polymer as a Recognition Element Combined with Fiber-Optic Detection**.** *Anal. Chem.* **1995,** 67, 2142-2144.

4. Jakusch, M.; Janotta, M.; Mizaikoff, B.; Mosbach, K.; Haupt, K., Molecularly Imprinted Polymers and Infrared Evanescent Wave Spectroscopy. A Chemical Sensors Approach. *Anal. Chem.* **1999,** 71, 4786-4791.

5. Greene, N. T.; Shimizu, K. D., Colorimetric molecularly imprinted polymer sensor array using dye displacement**.** *J. Am. Chem. Soc.* **2005,** 127, 5695-5700.

6. Kempe, M.; Mosbach, K., Separation of amino acids, peptides and proteins on molecularly imprinted stationary phases. *J. Chromatogr., A* **1995,** 691, 317-323.

7. Haginaka, J.; Sanbe, H., Uniformly sized molecularly imprinted polymer for (S)-naproxen. Retention and molecular recognition properties in aqueous mobile phase. *J. Chromatogr., A* **2001,** 913, 141-146.

8. Watabe, Y.; Hosoya, K.; Tanaka, N.; Kubo, T.; Kondo, T.; Morita, M., Novel surface modified molecularly imprinted polymer focused on the removal of interference in environmental water samples for chromatographic determination. *J. Chromatogr., A* **2005,** 1073, 363-370.

9. Sellergren, B., Direct Drug Determination by Selective Sample Enrichment on an Imprinted Polymer. *Anal. Chem.* **1994,** 66, (9), 1578-1582.

10. Muldoon, M. T.; Stanker, L. H., Molecularly Imprinted Solid Phase Extraction of Atrazine from Beef Liver Extracts. *Anal. Chem.* **1997,** 69, (5), 803-808.

11. Stroink, T.; Paarlberg, E.; Waterval, J. C.; Bult, A.; Underberg, W. J., On-line sample preconcentration in capillary electrophoresis, focused on the determination of proteins and peptides. *Electrophoresis* **2001,** 22, (12), 2375-2383.

12. Zhu, Q.-Z.; Degelmann, P.; Niessner, R.; Knopp, D., Selective trace analysis of sulfonylurea herbicides in water and soil samples based on solid-phase extraction

using a molecularly imprinted polymer. *Environ. Sci. Technol.* **2002,** 36, (24), 5411-5420.

13. Molinelli, A.; Weiss, R.; Mizaikoff, B., Advanced Solid Phase Extraction Using Molecularly Imprinted Polymers for the Determination of Quercetin in Red Wine. *J. Agric. Food Chem.* **2002,** 50, (7), 1804-1808.

14. Caro, E.; Marce, R. M.; Cormack, P. A. G.; Sherrington, D. C.; Borrull, F., On-line solid-phase extraction with molecularly imprinted polymers to selectively extract substituted 4-chlorophenols and 4-nitrophenol from water. *J. Chromatogr., A* **2003,** 995, (1-2), 233-238.

15. Zhu, X.; Yang, J.; Su, Q.; Cai, J.; Gao, Y., Selective solid-phase extraction using molecularly imprinted polymer for the analysis of polar organophosphorus pesticides in water and soil samples. *J. Chromatogr., A* **2005,** 1092, (2), 161-169.

16. Perez-Moral, N.; Mayes, A. G., Direct rapid synthesis of MIP beads in SPE cartridges. *Biosens. Bioelectron.* **2006,** 21, (9), 1798-1803.

17. Vidyasankar, S.; Ru, M.; Arnold, F. H., Molecularly imprinted ligand-exchange adsorbents for the chiral separation of underivatized amino acids. *J. Chromatogr., A* **1997,** 775, 51-63.

18. Hennion, M.-C.; Pichon, V., Immuno-based sample preparation for trace analysis. *J. Chromatogr., A* **2003,** 1000, 29-52.

19. Wei, S.; Molinelli, A.; Mizaikoff, B., Molecularly imprinted micro and nanospheres for the selective recognition of 17b-estradiol. *Biosens. Bioelectron.* **2006,** 21, (10), 1943-1951.

CHAPTER 2

2. BACKGROUND

2.1 The Non-covalent Approach to Molecular Imprinting

2.1.1 Introduction

Molecular imprinting is based on the co-polymerization of a template-functional monomer (vinylic, acrylic, methacrylic) complex forming a binding pocket with an excess of cross-linking di- or tri-vinyl (vinylic, acrylic, methacrylic) monomers, thereby resulting in networked porous organic materials. The template can be linked to the functional monomer by cleavable covalent bonds, metal ion coordination, or non-covalent bonds. Two main approaches to molecular imprinting have emerged to date, however, with a wide variety of modifications and combinations published: (i) the covalent approach pioneered by the group of Wulff[1], and the non-covalent approach initially developed by the group of Mosbach[2]. While the well-defined stoichiometry associated with the covalent approach certainly has its merits, non-covalent imprinting and recognition techniques are dominating literature, as they facilitate readily adaptable and rapid synthesis, close resemblance to the molecular recognition mechanisms of natural receptors, and the availability of substantial functional monomer libraries reported in literature. However, the complexity and variety of weak interactions in non-covalent imprinting needs to be carefully considered to control the recognition properties of non-covalent MIPs. In addition, the heterogeneity of binding sites produced by non-covalent imprinting prevents non-covalent MIPs from behaving like a highly organized layer of antibodies. Consequently, non-covalent MIP applications need to take advantage of a

separation path-length or incubation time, as provided in separation applications and assays. In contrast, the use of non-covalent MIPs in chemical sensing technology, which requires rapid and highly selective signal generation, appears less applicable. Given the versatility and closest resemblance to naturally occurring recognition mechanisms, the discussion in the remainder of this thesis will focus on non-covalent imprinting, as schematically shown in Figure 2.1.

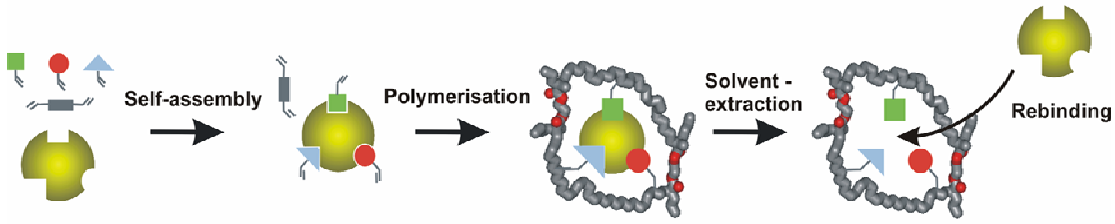

Figure 2.1 Fundamental principles of non-covalent molecular imprinting

2.1.2 Factors influencing the recognition properties of MIPs

To obtain MIPs with adequate molecular recognition properties, it is important to stabilize the template-monomer complex by increasing the strength and number of imprinted sites, and by minimizing non-specific binding sites. Furthermore, the template-functional monomer complex should be at least in part maintained during and after the polymerization resulting in selective binding pockets. In the following, we will discuss the factors that need to be considered prior to designing the synthetic strategy for imprinting any particular template molecule.

2.1.2.1 Choice of functional monomer and cross-linker

In order to improve the overall efficiency of MIPs, functional monomers are needed to facilitate the formation of increasingly robust complexes with template molecules. The widespread use of methacrylic acid (MAA) as functional monomer is related to the fact that carboxylic acid (the functional group) can act as a hydrogen bond and proton donor, as well as a hydrogen bond acceptor[3]. In general, templates containing Brönsted-basic or hydrogen bonding functional groups are potentially suitable for the MAA/EDMA (ethyleneglycol dimethacrylate) system[4]. However, in many cases, the recognition capabilities of MIPs are not as selective as expected even after optimization of the synthesis conditions, which is related to the weak interactions between template and functional monomers. Derived from this consideration, an excess of functional monomer is usually applied to ensure the formation of the template-functional monomer complex. However, a large amount of low affinity or non-specific binding sites may result from an excess of functional monomer (Figure 2.2).

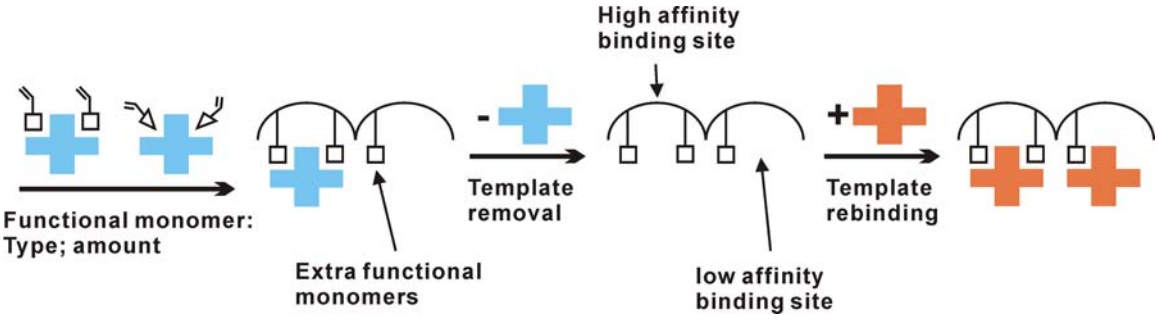

Figure 2.2 Schematic selection of the type and amount of functional monomer

The issue of binding site heterogeneity has been addressed by inactivating low affinity binding sites via esterification with appropriate blocking reagents such as diazomethane or phenyldiazomethane[5]. In this process, the template molecule is used as an in-situ protecting reagent shielding the high affinity binding sites. However, while the average binding affinity has reportedly increased by this strategy, the binding capacity of the synthesized MIPs was not improved.

An interesting strategy to improve the molecular recognition properties is to synthesize new functional monomers based on the structural features of the target templates[6]. However, the synthesis of new functional monomers is time-consuming and not applicable to all templates. An alternate approach is to combine two or more functional monomers in the imprinting process[7, 8]. However, the competition of monomer-monomer associations with template-monomer associations needs to be particularly considered, if two or more functional monomers are used. Spectroscopic studies on the pre-polymerization solution for fundamentally understanding the involved template-monomer interactions facilitate the choice of monomers prior to synthesis, as discussed in section 2.3.2, although this is not yet common practice in molecular imprinting.

The cross-linking monomer stabilizes the template-functional monomer complex during the polymerization process, thereby creating 3-D binding cavities, which are available for rebinding. Cross-linkers with two (e.g., DVB or EDMA), and three (e.g., trimethylolpropane trimethacrylate (TRIM)) vinyl groups have been intensely evaluated throughout the molecular imprinting literature. From this large body of work, a broadly applicable system has emerged based on copolymers of EDMA-MAA, which provides

adequate recognition properties and mechanical/thermal stability for MIPs. However, this system is not a universal solution for the generation of acceptable imprinting properties. For obtaining MIPs with the desired recognition properties, the choice of cross-linker also needs to consider the binding site rigidity, swelling properties, wettability, and mass transfer properties for a particular target system.

2.1.2.2 Role of polymerization conditions: temperature and porogen

The preparation of MIPs requires careful selection of appropriate solvents, which should (i) preferably not interfere with and rather strengthen the inter-molecular interactions between functional monomers and templates during the self-assembly, (ii) create porous structures within the synthesized polymer matrix, (iii) support the preparation of MIPs as monolith or in bead format, and (iv) provide sufficient solubility for the template molecules and the involved polymeric building blocks. In particular, Sellergren *et al*.[9] performed a detailed study on the influence of the solvent properties on the recognition properties of the L-phenylalanine-MIPs indicating that the polymers prepared using solvents with poor hydrogen bonding capacity exhibited higher selectivity than those prepared using solvents with pronounced hydrogen bonding capacity (i.e., average of donor and acceptor capacity). In general, optimum recognition (i.e., re-binding) during the application of MIPs in separations can be achieved in the same solvent used as porogenic solvent during the polymerization. Nevertheless, MIPs prepared in aprotic solvents have also demonstrated recognition in entirely aqueous solutions[10, 11], where ionic and hydrophobic interactions are primarily contributing to the recognition properties of the MIP material.

In aprotic/non-polar solvents, monomers and templates containing polar groups assemble via electrostatic interaction, which will be favored by decreasing the polymerization temperature. But in the case where monomers and templates are strongly solvated, the association of template-monomer may lead to a net increase in entropy. Therefore, the template-monomer interaction will be favored by increasing the polymerization temperature. However, during the application of MIPs, the temperature effect becomes less critical as most of the imprinted polymers are quite stable under ambient temperature.

2.1.3 Synthesis strategies

2.1.3.1 Block polymer by bulk polymerization

Conventionally, MIPs are synthesized by bulk polymerization methods in a porogenic solvent[2, 12, 13]. A significant number of studies has shown that the separation of the template from its structural analogues was achieved with MIP-based HPLC[14-19], or SPE[20-24]. Although the bulk polymerization is technically straightforward, particles with the desired size are then obtained by grinding and sieving, which is a labor intensive and wasteful process, as a considerable amount of fine particles with broad size distribution is produced, which are of limited suitability for HPLC separations or binding assays. Furthermore, this method yields particles with limited control on particle size and shape. Although the porosity of MIPs prepared by bulk polymerization can be tuned by using different porogenic solvents or different monomer concentrations, the choice of solvents is limited by the solubility of the template molecule, and the stability of the template-monomer complex. In addition, the heterogeneity of the pore size distribution reduced the accessibility of the analyte to the binding sites. Therefore, next-generation MIPs will be

characterized by improved control on the particle size, as well as the binding site accessibility (polymer porosity and density).

2.1.3.2 Polymer spheres synthesized by precipitation polymerization

For chromatographic evaluation (e.g., HPLC) or solid phase extraction (SPE), MIP particles with dimensions ranging from 10 to 25 μm are usually applied[25]. In binding assays, or when immobilized as biomimetic recognition element at a chemical sensing interface, smaller particles (less than 1 μm) with a narrow size distribution are required[26]. Several attempts have been reported producing monodisperse molecularly imprinted polymer particles applying methods such as suspension polymerization in water[27], liquid perfluorocarbon[28], or mineral oil[29], by dispersion polymerization[30], and via aqueous two-step swelling polymerization[31]. However, these techniques suffer from the need of water or highly polar organic solvents during the polymerization procedure, which frequently decreases specific interactions between functional monomers and template molecules in most commonly applied non-covalent imprinting mixtures[28]. Hence, for the synthesis of molecularly imprinted micro- and nanospheres while retaining high selectivity along with control on particle shape and size, a synthetic route avoiding the use of dispersants such as water or protic solvents is demanded.

Precipitation techniques have been applied for the preparation of imprinted nanospheres for a variety of different analytes and applications[32-36]. Most obtained spherical particles have diameters ranging from 0.1 to 1 μm with the diameter dispersity usually narrowed by centrifugation. The dimensions and morphologies of these spheres are ideal for radioligand binding assays[32], capillary electrophoresis[34], or sensing materials[36], however, less suitable for HPLC and SPE applications due to the resulting

backpressure of columns packed with such small particles. Hence, the synthesis of larger particles by simple precipitation polymerization yielding monodisperse MIP-based stationary phase materials requires the development of novel synthetic routes.

The synthesis of imprinted polymer beads for MIP-based stationary phase materials can frequently be realized by adapting synthetic routes for generating conventional (non-imprinted) polymeric micro- and nanospheres[37, 38] to the required conditions ensuring non-covalent complex formation between the template and functional monomer building blocks. The disadvantages of this approach include the usually reduced porosity of the polymer beads, thereby limiting appreciable flow of the mobile phase at acceptable back pressures, and the limitation in functional monomers and cross-linkers to species amenable to bead synthesis recipes.

In summary, the specificity and selectivity of MIP beads requires fine-tuning by careful selection of the polymerization conditions for obtaining comparable results to irregularly shaped MIP particles prepared by bulk polymerization. Again, this selection process benefits from deeper insight on the governing mechanisms underlying MIP synthesis at a molecular level. Although reportedly the chromatographic efficiency appears improved when using MIPs in bead format, the obtained selectivity is at best on par, but not superior to materials obtained from bulk polymerization. However, comparing to the wasteful and slow processing procedures required for block polymers, the direct production of imprinted beads is comparatively fast and provides quantitative yields of directly usable particles. In addition, beads are physically more robust, and facilitate efficient template recovery. Finally, to commercialize MIPs it is necessary to

scale up the polymer production, which is certainly attractive by direct production of MIP beads in lieu of laborious additional particulate preparation of MIP materials.

2.1.4 Characterization methods for MIPs

2.1.4.1 The rebinding properties of MIPs

In this thesis, the binding properties of MIPs were studies using Freundlich isotherm affinity distribution (FIAD) analysis, which has been used in the past to determine the binding affinity and heterogeneity of MIPs. The group of Shimizu has introduced the method of modeling the adsorption isotherms of non-covalent imprinted polymers[39]. Compared to the 2-binding site model[40], the Freundlich isotherm is a heterogeneous binding model, which can inherently accommodate and evaluate the heterogeneity of MIPs. Fitting of experimental isotherms to the Freundlich model provided excellent agreement for MIPs against L-phenylalanine anilide[41], aminoantipyrine[42], hemoglobin[43], and monocrotophos[44]. Furthermore, it was demonstrated that this model is applicable to isotherms measured at low concentration or sub-saturation levels[45, 46]. The empirical form of the Freundlich isotherm[47] has been widely used for modeling heterogeneous surfaces including activated carbon[48], silica[49], sediment materials[50], and β-cyclodextrin polymer[51]. The Freundlich isotherm describes the relationship of the concentration of bound (B) and free (F) guest molecules in MIPs following

$$B = aF^m, \qquad (1)$$

where *a* is related to the median binding affinity constant K_0 ($K_0 = a^{1/m}$), and *m* is the heterogeneity index. The value of m ranges from 0 to 1, and increases as the heterogeneity of the MIP increases. The fitting constants *a* and *m* are then applied in

$$N(K) = 2.303\ am\ (1-m^2)\ e^{-2.303\ m \log K}\ (K_{min} = 1/F_{max},\ K_{max} = 1/F_{min}). \qquad (2)$$

This equation is only valid in a certain range of binding affinities with K_{min} and K_{max} set by the free concentrations (F_{max} and F_{min}) in the binding experiments.

2.1.4.2 The porosity of MIPs

During the polymerization process, the solvent properties largely determine the pore structure of the resultant polymers. In the presence of a poor solvent, an earlier phase separation of the polymer occurs. The new phase swells with the monomers thermodynamically preferential than the porogenic solvent. As a result, the local concentration of monomers in the swollen gel nuclei is higher than that in the surrounding solution. The newly formed nuclei obtained in solution are likely to be adsorbed by large pre-globules formed earlier due to coalescence of many nuclei, and will further increase in size. Overall, the globules that are formed in such a system are larger, and consequently, the voids between them (pores) are larger as well. While the good solvent competes with monomers for the solvation of nuclei, the local monomer concentration is lower, and the globules are smaller. As a result, the porogenic solvent controls the porous properties of the monolith via solvation of the polymer chains in the reaction medium during the early stages of the polymerization. Solvents with pore-forming properties are called porogens. In general, micropores less than 20 Å will result

in slow diffusion for small molecules. Polymers prepared by bulk polymerization usually provide pores from 20-2000 Å, in dependence on the applied polymerization conditions. An increase of the amount of porogen, or decrease of the amount of cross-linker will therefore lead to an increase of large pores. The pore structure in dry state can be characterized by gas sorption measurements[52-57], or mercury penetration methods[55, 58]. The following parameters can be determined: surface area, pore volume, and pore size distribution. However, a porous polymer in a liquid medium will swell to varying extents depending on the solvation and swelling degree of the polymer in a particular solvent. Therefore, the rebinding properties of MIPs will be different in different media, due to the effect of the solvent on the pore structure of the polymer leading to variations in binding site accessibility and mass transfer characteristics of the MIP.

2.2 Application of MIPs in Separation and Pre-concentration

2.2.1 Introduction

Most biological processes are governed by molecular recognition such as immuno response, ligand-receptor interactions, etc., which involve biological hosts specifically binding to certain analytes. The development of synthetic receptors capable of recognizing target analytes with high specific affinity is particularly desirable, if natural receptors are not available, or expensive and/or laborious to obtain. Consequently, research in molecularly imprinted polymers (MIPs) has rapidly increased, and is nowadays considered a straightforward and versatile technique for the generation of synthetic receptors for small organic constituents, and most recently even for large (bio)macromolecules[75]. Among the most promising applications for molecularly imprinted materials are affinity separations, with the MIP serving as stationary phase, or

biomimetic assays utilizing MIPs as synthetic antibodies. In this context, most of the imprinting systems reported in literature take advantage of non-covalent recognition techniques, due to facile preparation procedures, and a large library of available functional monomers used throughout literature.

MIPs created by non-covalent imprinting are usually characterized by a comparatively small fraction of highly selective binding sites, and the majority of binding sites providing a wide range of binding affinities[59]. In principle, this circumstance is considered detrimental to the application of MIPs in affinity-based chromatography, such as HPLC. However, it has been suggested that low affinity binding sites may play an important role in chromatographic separation due to their fast binding kinetics[59].

In order to improve the overall efficiency of MIPs, functional monomers are in demand that facilitate the formation of increasingly robust complexes with template molecules. However, from another point of view the heterogeneity of binding site affinities may in fact contribute to a broad – i.e., flexible - "separation window" for a variety of analytes within a single MIP matrix. For example, it has been shown that a (S)-timolol imprinted MAA-EGDMA polymer was able to resolve not only racemic timolol mixtures, but also racemic propranolol solutions[60]. This effect is especially useful in MIP-based SPE for separating a group of structurally or chemically related constituents, rather than individual analytes from a sample matrix. Hence, while optimizing a MIP formulation for a selection of templates and/or functional monomers, these effects need to be taken into account in view of the desired final application and separation performance. It should be noted that the binding site heterogeneity is not detrimental for

MIPs used in pseudoimmunoassays, if the binding conditions are optimized, as discussed in Section 2.2.4.

2.2.2 MIPs as stationary phase for HPLC

Predominantly, MIPs are prepared using conventional free radical bulk polymerization providing particles between 10-25 μm in diameter, which are finally packed as stationary phase into HPLC or SPE columns. A significant body of literature has demonstrated that baseline separation of templates from their structure analogues is achievable with MIP-based HPLC columns, documented here with few selected examples[14-19]. Substantial interest on the development of imprinted polymers for biologically active constituents has provided the impetus for designing an increasing number of MIP-based stationary phases. However, more widespread application of MIP-based HPLC stationary phases in commercial products is still limited by the drawbacks of band broadening and tailing resulting from sub-optimal particles obtained during conventional bulk polymerization, and to date limited rational design of the synthetic route for flexibly creating the desired retention properties for a wide range of templates.

2.2.3 MIPs in solid phase extraction

Since the first application of MIPs for SPE (also referred to as 'MISPE') for the extraction of pentamidine in urine[61], MISPE has been applied to selective clean-up and pre-concentration from a wide variety of sample matrices including biological fluids[62-64], environmental matrices[65-67], and food/beverages[68-72]. In MISPE, the solid phase particle size is less critical, with main emphasis on (i) rapid and complete but separate elution of interferents and target analyte(s), and (ii) elimination of template leaking from the MIP matrix, which is of particular importance when using MISPE for pre-concentration in

quantitative trace analysis. The majority of the reported studies on MISPE apply the cartridges off-line with subsequent downstream analytical separation. For example, red wine samples from a French Merlot spiked with 8.8 mg per liter quercetin were directly applied onto MISPE cartridges, and selective extraction of quercetin was achieved[69]. Consequently, it would be advantageous combining a MIP column directly with a detector providing integrated separation and identification. The first reported on-line MISPE approach was demonstrated for 4-nitrophenol from environmental water samples[73] using solvent switching.

2.2.4 MIPs in competitive ligand binding assays

Biomimetic molecularly imprinted sorbent assays (MIA) based on the competition between target analyte and a labeled probe have been developed for a number of constituents of clinical and environmental interest utilizing MIPs in lieu of antibodies. Frequently, comparable performance to their biological analogues in terms of selectivity and limit of detection has been obtained. Usually lower cost of preparation, and superior chemical and mechanical stability render MIA a potentially useful immunoassay strategy complementing antigen-antibody type assays, if antibodies are not available or laborious and thus expensive to isolate. Figure 2.3 shows a general scheme for a competitive biomimetic MIP assay.

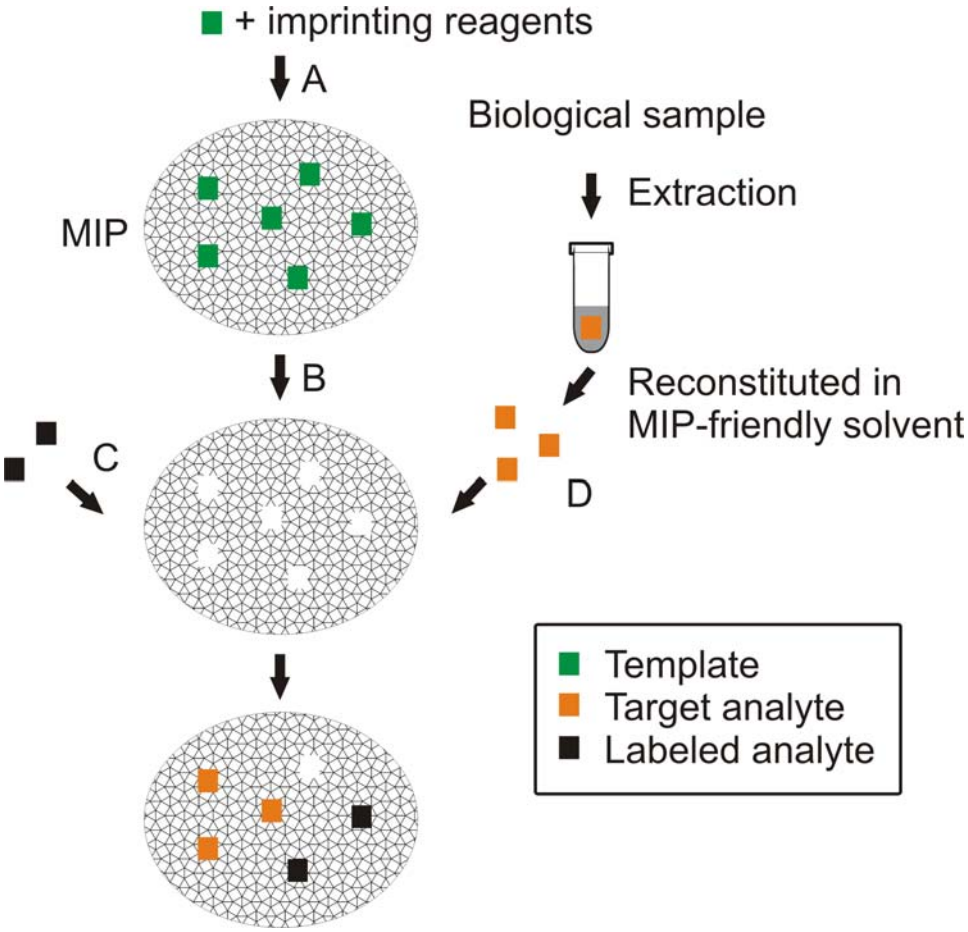

Figure 2.3 Schematic of biomimetic competitive assay based on molecular imprints. (A) Preparation of molecularly imprinted polymer; (B) Removal of template from MIP leaving selective binding cavities; (C) Addition of labeled analyte; (D) Addition of target analyte (identical to the template) competing with the labeled analyte.

The group of Mosbach has reported the first competitive MIP assay for theophylline and diazepam in human serum[74]. The advantages of MIA over natural antibodies include (i) that MIPs are resilient to extreme conditions (e.g., non-aqueous media, mechanical forces, etc.), (ii) that they are compatible with harsher regeneration chemistry, (iii) that their synthetic variability facilitates flexible direct synthesis of receptors for a wide variety of small molecules, which otherwise have to be coupled to a carrier protein prior to inoculation for raising natural antibodies), and (iv) that they provide a route toward

receptors for highly toxic compounds or immunosupressants. However, the more widespread application of MIA is still limited by (i) the lack of reliable imprinting methodology for large (bio)molecules such as proteins[75], and (ii) the fact that even for small molecules the imprinting methodology requires further improvement avoiding synthesis based on trial-and-error (e.g., increasing the fraction of high affinity binding sites, improving binding site accessibility, etc.).

The synthesis of MIPs for assays may be adapted to different requirements demanded by assays vs. chromatographic separations. Surface imprinting generating easily accessible binding sites at the seed particle surface are a promising approach for preparing particles useful to MIP assays, in particular if large (bio)molecules are templated. In general, smaller MIP particles (< 500 nm) are preferable for assay applications to obtain faster equilibration, and to keep particles in suspension. Although the broad distribution of binding site affinities appears detrimental to the performance of MIPs in chromatography (i.e., peak broading and tailing), this is not as crucial in MIA, if the strongest interactions between the binding sites and the target analytes are sufficiently selective. In an optimized MIA assay, the low affinity binding sites are essentially ignored due to superior control on the binding conditions by optimizing the amount of MIP and solvent in tandem[76]. In fact, it has been confirmed that MIA assays work equally well with MIPs prepared at a template:functional monomer ratio of 1:1000, and of 1:4[77]. Hence, the amount of template required for the MIA assays can be greatly reduced, while still achieving sufficient performance. In practice, to avoid template leaking and to save on expensive template, a lower template:functional monomer ratio (e.g., 1:1000), or a dummy template can be used.

Similar to chromatographic separations, the selection of the most appropriate solvent for an assay usually starts with the same solvent utilized during the initial MIP synthesis. If a MIP is prepared in several steps, the type of template:functional monomer interactions need to be considered. In general, if the MIP is prepared based upon non-covalent interactions, organic solvents that are less interruptive to the template-functional monomer complex are used. If the MIP was prepared in aqueous phase, a buffer solution with pH=7 was used as the starting solvent for MIA. Usually, a modifier is added minimizing non-specific interactions or reducing the surface tension between MIP and solvent. In addition, the percentage of bound probe (e.g., ^{3}H-labeled version of the analyte) needs to be controlled in the range of 0-80 % to achieve reliable quantification[76], as the sensitivity would be reduced if more probe is applied. As MIPs are characterized by heterogeneous affinity distribution of the binding sites (i.e., a range of binding strengths and selectivities), the probe ideally only binds to high affinity binding sites. Hence, the amount of MIP per assay, the amount of probe (B/I; *B* and *I* are bound probe and initial probe amount, respectively), and the type of solvent reducing or enhancing the strengths of the binding interactions need to be optimized in synchronicity.

2.3 Probing the Nature of Recognition towards MIP Optimization

2.3.1 Introduction

Non-covalent interactions are usually considered weak interactions easily affected by different imprinting conditions, such as solvent and temperature. Furthermore, the selectivity and affinity of thus synthesized polymers is intimately related to the initial strength/integrity of the template-monomer complex[78]. Consequently, the optimization of a MIP formulation demands considering the governing interactions between template and

functional monomer, as well as with the porogenic solvent. To this end, better understanding of MIP synthesis by computational prediction orchestrated with the application of appropriate analytical techniques is essential for enabling efficient development of optimized MIP-based receptors; in the following, the most prevalent approaches on modeling-assisted MIP development are briefly discussed.

2.3.2 Rational MIP design: computational approaches for understanding how MIPs work

Computational modeling enables studying complex systems or processes by considering small replications of the investigated systems, generating optimized configurations, and providing structural and thermodynamic properties on the target complex. Such approaches have demonstrated potential for rapid evaluation of molecular imprinting parameters, and for facilitating rational design of MIP synthesis, which is particularly important when working with costly or rare templates. Table 2.1 lists the primary reported approaches of computational modeling assisting MIP synthesis, which are discussed in detail in the remainder of this section.

Table 2.1 Summary of molecular modeling approaches reported in literature for studying pre-polymerization solutions as the first step during MIP synthesis.

Approach		**Wei *et al.*[79, 80]**	**Takeuchi *et al.*[81]**	**Piletsky *et al.*[82]**	**Pavel *et al.*[83, 84]**
Software	**Name**	AMBER 8 or 9	MacroModel4.5	SYBYL 6.7	Cerius^2 version 10.0
	Design. for	Biomacromoles	Organic/bioorganic molecules	Drug design	Material sciences

Table 2.1 continued

Modeling protocol	NVE dynamic simulations; simulated annealing	Conformational search	LEAPFROG algorithm; simulated annealing	NVT dynamic simulations
Modeling system	Template, functional monomers, cross-linkers, solvents	Template, functional monomers	Template, functional monomers	Template, functional monomers or short polymer chains
Data analysis	Hydrogen bonding and π-π stacking interactions; interaction energies of template – all imprinting components	Conformation of template-functional monomer	Template–monomer binding energies	Template–monomer/polymer chain binding energies

Takeuchi *et al.*[81] have estimated the template-monomer complex conformation by docking of the most stable conformers using an intermolecular Monte Carlo-based conformational search to obtain the conformation of the most stable snapshot. However, there is no analysis or classification performed on the multitude of possible interactions, which is related to the wide range of possible binding sites created in MIPs.

Molecular modeling was applied by the group of Pilesky[82, 85, 86] to create virtual libraries of functional monomers, and subsequent screening a selected template against interactions with the monomers contained in this library. The binding energy for each virtual pair of functional monomer and template was compared providing information on the potentially most suitable monomer for that particular template. A similar method was developed by Sode and co-workers[87] for designing molecularly imprinted catalysts. Recently, modeling of clusters including up to 10 monomers, or polymer chains was reported[83, 84]. It was shown that among the various intermolecular energies extracted from the total energy, the electrostatic energy term provides the most significant contribution, which may result from hydrogen bonding between template and monomers.

A novel strategy currently pursued by our research group and collaborators aims at studying the fundamental interactions of template molecules, functional monomer building blocks, and explicit solvent at molecular level detail using AMBER, a suite of programs for molecular modeling and molecular dynamics simulations, which was initially developed for modeling biomolecular interactions[88]. In this thesis, we have applied AMBER for the first time to simulating interactions between template and functional monomers, and for confirming hydrogen bonding and π-π stacking interactions during molecular dynamics simulations[79, 89].

2.3.2.1 The applicability of molecular modeling for MIPs

To facilitate the selection of imprinting conditions, computational predictions based on combinatorial screening approaches calculating the binding energies[82, 86, 90], or stabilization energies[91] of the selected template with different functional monomers have been described. Thereby, selection of the most suitable functional monomer with the

potentially highest binding energy to the target molecule in the pre-polymerization solution is facilitated.

In this work, the potential of using molecular dynamics (MD) simulations for selecting the most suitable monomers via hydrogen bonding analysis during the modeling process is explored. Compared to currently reported binding energy calculations, hydrogen bonding analysis more directly provides access to the bond strengths within the template-monomer complex at molecular level. Furthermore, conformational changes of the template and/or monomer are accessible during these simulations. In the present study, a library of nine monomers with different functionalities was screened. Experimental evidence from previously reported batch rebinding studies support that the selectivity of the synthesized MIP is strongly related to the initial stability of the template-monomer complex in the pre-polymerization solution. Methacrylic acid has been proven as an effective functional monomer for imprinting 17β-estradiol[56].

2.3.2.2 The development of modeling strategies for MIPs

Recently, we have developed a general strategy targeting more fundamental understanding on the template-functional monomer interactions during molecular dynamics (MD) simulations[89]. We hypothesize that a suitable description of the electrostatic and Van der Waals interactions governing non-covalent assembly of the pre-polymerization complex at the force field level provides a viable model for describing the pre-polymerization system. This method has been developed in the present work by constructing a more realistic pre-polymerization complex with all the imprinting species at the correct ratios, which is a unique approach to date. Simulated annealing was performed to obtain the states with minimum possible energy. To estimate the interaction

between different species, the binding free energy of the template-receptor complex (receptor: all the imprinting components except template molecule) was calculated. In the present work, 17β-estradiol was used as the model target molecule due to its relevance in ongoing studies related to endocrine disrupting compounds (EDCs)[32, 92-95] . The use of MIPs in SPE for selective pre-concentration is appealing to a wide variety of analytical applications given that sufficient selectivity and affinity of the synthesized MIPs to target compounds is provided. To achieve MIPs with high selectivity and binding capacity, the initial imprinting formulation needs to be optimized by rational selection of functional monomers and cross-linkers at the correct ratios providing sufficiently strong interactions with the target molecule.

Hence, an approach to simulate a more realistic pre-polymerization complex including all the imprinting components for 17β-estradiol is proposed, combing molecular dynamics simulated annealing, pairwise interaction analysis, and free energy estimation based on the Molecular Mechanics - Generalized Born - Surface Area (MM-GBSA) framework[96] for evaluating the inter-molecular interactions of the imprinting components in molecular modeling. In analyzing individual complex configurations generated via simulated annealing, the hydrogen bonding and π- π stacking interactions are primary parameters to evaluate the stability of the template-receptor complex. The obtained results indicate that both functional monomer and cross-linker contribute to the functionality of the binding sites created by imprinting. The comparison of the free energy calculated from the MM-GBSA method shows that the E2-MAA-DVB system is more stable than the E2-4VP-DVB system, which is confirmed by its superior

performance during chromatographic studies using MIP-based HPLC with both material systems for the separation of E2 and 17α-E2.

2.3.3 Rational MIP design: spectroscopic analysis for understanding how MIPs work

While computational predictions provide detailed insight on molecular interactions, the accuracy of these results needs to be confirmed by thorough experimental analysis establishing the validity of the developed models. So far, template-monomer interactions have predominantly been monitored via ^{1}H-NMR for investigating the extent of complex formation in pre-polymerization solutions[97-101]. UV titration studies have been performed for spectroscopically tracing the saturation of template molecules with functional monomer building blocks by recording changes of absorbance spectra or differential absorption[78]. Recently, IR spectroscopy on pre-polymerization complexes has provided additional complementary information to UV/Vis and NMR studies by probing the vibrational signatures of the involved molecules and complexes[89]. In addition, isothermal titration calorimetry (ITC) enables insight into the thermodynamics of the binding properties of molecularly imprinted polymers[102, 103], or of the pre-polymerization complexes[104]. Most recently, X-ray crystallographic studies[105, 106] were preformed to understand the conformation of pre-polymerization complexes, which may serve as initial configurations for computational modeling studies. In summary, currently applied analytical methods provide useful information for extensive systematic studies on the binding mechanisms involved in the pre-polymerization complex formation. Combining the results of spectroscopic studies with increasingly accurate computational molecular models ensures more conclusive information on binding interactions and stoichiometries

ultimately governing the achievable selectivity, and is essential to the development of next-generation MIP technology.

2.4 References

1. Wulff, G.; Sarhan, A., Use of polymers with enzyme-analogous structures for the resolution of racemates. *Angew. Chem., Int. Ed. Engl.* **1972,** 11, (4), 341.

2. Arshady, R.; Mosbach, K., Synthesis of substrate-selective polymers by host-guest polymerization. *Macromol. Chem. Phys.* **1981,** 182, (2), 687-692.

3. Abraham, M. H.; Duce, P. P.; Prior, D. V.; Barrat, D. G.; Morris, J. J.; Taylor, P. J., Hydrogen bonding. Part 9. Solute proton-donor and proton-acceptor scales for use in drug design. *J. Chem. Soc. Perkin Trans. II* **1989**, 1355-1375.

4. Sellergren, B.; Lepistoe, M.; Mosbach, K., Highly enantioselective and substrate-selective polymers obtained by molecular imprinting utilizing noncovalent interactions. NMR and chromatographic studies on the nature of recognition. *J. Am. Chem. Soc.* **1988,** 110, (17), 5853-5860.

5. Umpleby, R. J., II; Rushton, G. T.; Shah, R. N.; Rampey, A. M.; Bradshaw, J. C.; Berch, J. K., Jr.; Shimizu, K. D., Recognition Directed Site-Selective Chemical Modification of Molecularly Imprinted Polymers. *Macromolecules* **2001,** 34, (24), 8446-8452.

6. Oezcan, A. A.; Say, R.; Denizli, A.; Ersoez, A., L-Histidine Imprinted Synthetic Receptor for Biochromatography Applications. *Anal. Chem.* **2006,** 78, (20), 7253-7258.

7. Takeuchi, T.; Fukuma, D.; Matsui, J., Combinatorial Molecular Imprinting: An Approach to Synthetic Polymer Receptors. *Anal. Chem.* **1999,** 71, (2), 285-290.

8. Ramstroem, O.; Andersson, L. I.; Mosbach, K., Recognition sites incorporating both pyridinyl and carboxy functionalities prepared by molecular imprinting. *J. Org. Chem.* **1993,** 58, (26), 7562-7564.

9. Sellergren, B.; Shea, K. J., Influence of polymer morphology on the ability of imprinted network polymers to resolve enantiomers. *J. Chromatogr.* **1993,** 635, (1), 31-49.

10. Chapuis, F.; Pichon, V.; Lanza, F.; Sellergren, S.; Hennion, M.-C., Optimization of the class-selective extraction of triazines from aqueous samples using a molecularly imprinted polymer by a comprehensive approach of the retention mechanism. *J. Chromatogr., A* **2003,** 999, 23-33.

11. Janotta, M.; Weiss, R.; Mizaikoff, B.; Bruggemann, O.; Ye, L.; Mosbach, K., Molecularly imprinted polymers for nitrophenols - an advanced separation material for environmental analysis. *Int. J. Environ. Anal. Chem.* **2001,** 80, (2), 75-86.

12. Wulff, G.; Grobe-Einsler, R.; Vesper, W.; Sarhan, A., Enzyme-analog built polymers, 5. The specificity distribution of chiral cavities prepared in synthetic polymers. *Makromolekulare Chemie* **1977,** 178, (10), 2817-2825.

13. Vlatakis, G.; Andersson, L. I.; Muller, R.; Mosbach, K., Drug assay using antibody mimics made by molecular imprinting. *Nature* **1993,** 361, (6413), 645-647.

14. Remcho, V. T.; Tan, Z. J., MIPs as chromatographic stationary phases for molecular recognition. *Anal. Chem.* **1999,** 71, (7), 248A-255A.

15. Buchmeiser, M. R., New synthetic ways for the preparation of high-performance liquid chromatography supports. *J. Chromatogr., A* **2001,** 918, (2), 233-266.

16. Haginaka, J., HPLC-based bioseparations using molecularly imprinted polymers. *Bioseparation* **2002,** 10, (6), 337-351.

17. Turiel, E.; Martin-Esteban, A., Molecularly imprinted polymers: towards highly selective stationary phases in liquid chromatography and capillary electrophoresis. *Anal. Bioanal. Chem.* **2004,** 378, (8), 1876-1886.

18. Mahony, J. O.; Nolan, K.; Smyth, M. R.; Mizaikoff, B., Molecularly imprinted polymers-potential and challenges in analytical chemistry. *Anal. Chim. Acta* **2005,** 534, (1), 31-39.

19. Ansell, R. J., Molecularly imprinted polymers for the enantioseparation of chiral drugs. *Adv. Drug Delivery Rev.* **2005,** 57, (12), 1809-1835.

20. Olsen, J.; Martin, P.; Wilson, I. D., Molecular imprints as sorbents for solid phase extraction: potential and applications. *Anal. Commun.* **1998,** 35, (10), 13H-14H.

21. Stevenson, D., Molecular imprinted polymers for solid-phase extraction. *TrAC, Trends Anal. Chem.* **1999,** 18, (3), 154-158.

22. Andersson, L. I., Selective solid-phase extraction of bio- and environmental samples using molecularly imprinted polymers. *Bioseparation* **2001,** 10, (6), 353-364.

23. Pyrzynska, K.; Pobozy, E., On-line coupling of solid phase extraction sample processing with high-performance liquid chromatography. *Crit. Rev. Anal. Chem.* **2002,** 32, (3), 227-243.

24. Mullett, W. M.; Pawliszyn, J., The development of selective and biocompatible coatings for solid phase microextraction. *J. Sep. Sci.* **2003,** 26, (3/4), 251-260.

25. Kempe, M., Antibody-Mimicking Polymers as Chiral Stationary Phases in HPLC. *Anal. Chem.* **1996,** 68, (11), 1948-1953.

26. Ye, L.; Surugiu, I.; Haupt, K., Scintillation Proximity Assay Using Molecularly Imprinted Microspheres. *Anal. Chem.* **2002,** 74, (5), 959-964.

27. Lai, J. P.; Lu, X. Y.; Lu, C. Y.; Ju, H. F.; He, X. W., Preparation and evaluation of molecularly imprinted polymeric microspheres by aqueous suspension polymerization for use as a high-performance liquid chromatography stationary phase. *Anal. Chim. Acta* **2001,** 442, (1), 105-111.

28. Mayes, A. G.; Mosbach, K., Molecularly Imprinted Polymer Beads: Suspension Polymerization Using a Liquid Perfluorocarbon as the Dispersing Phase. *Anal. Chem.* **1996,** 68, (21), 3769-3774.

29. Kempe, H.; Kempe, M., Novel method for the synthesis of molecularly imprinted polymer bead libraries. *Macromol. Rapid Commun.* **2004,** 25, 315-320.

30. Say, R.; Birlik, E.; Ersoz, A.; Yilmaz, F.; Gedikbey, T.; Denizli, A., Preconcentration of copper on ion-selective imprinted polymer microbeads. *Anal. Chim. Acta* **2003,** 480, (2), 251-258.

31. Piscopo, L.; Prandi, C.; Coppa, M.; Sparnacci, K.; Laus, M.; Lagana, A.; Curini, R.; D'Ascenzo, G., Uniformly sized molecularly imprinted polymers (MIPs) for 17b-estradiol. *Macromol. Chem. Phys.* **2002,** 203, (10/11), 1532-1538.

32. Ye, L.; Weiss, R.; Mosbach, K., Synthesis and Characterization of Molecularly Imprinted Microspheres. *Macromolecules* **2000,** 33, (22), 8239-8245.

33. Zhang, Z.; Liu, Y.; Long, Y.; Nie, L.; Yao, S., Effect of the size of molecularly imprinted polymers sensing materials on piezoelectric quartz crystal sensor performance. *Anal. Sci.* **2004,** 20, (2), 291-295.

34. de Boer, T.; Mol, R.; de Zeeuw, R. A.; de Jong, G. J.; Sherrington, D. C.; Cormack, P. A. G.; Ensing, K., Spherical molecularly imprinted polymer particles: A promising tool for molecular recognition in capillary electrokinetic separations. *Electrophoresis* **2002,** 23, (9), 1296-1300.

35. Li, P.; Rong, F.; Yuan, C., Morphologies and binding characteristics of molecularly imprinted polymers prepared by precipitation polymerization. *Polym. Int.* **2003,** 52, (12), 1799-1806.

36. Zhang, Z.-H.; Long, Y.-M.; Liu, Y.-J.; Yao, S.-Z., Microspheres sensor based on molecularly imprinted polymer synthesized by precipitation polymerization. *Chinese J. Chem.* **2003,** 21, (5), 550-555.

37. Funke, W.; Okay, O.; Joos-Muller, B., Microgels-intramolecularly crosslinked macromolecules with a globular structure. *Adv. Polym. Sci.* **1998,** 136, (Microencapsulation, Microgels, Iniferters), 138-234.

38. Li, W.-H.; Stover, H. D. H., Porous monodisperse poly(divinylbenzene) microspheres by precipitation polymerization. *J. Polym. Sci. Pol. Chem.* **1998,** 36, (10), 1543-1551.

39. Umpleby, R. J.; Baxter, S. C.; Bode, M.; Berch, J. K.; Shah, R. N.; Shimizu, K. D., Application of the Freundlich adsorption isotherm in the characterization of molecularly imprinted polymers. *Anal. Chim. Acta* **2001,** 435, (1), 35-42.

40. Matsui, J.; Miyoshi, Y.; Doblhoff-Dier, O.; Takeuchi, T., A molecularly imprinted synthetic polymer receptor selective for atrazine. *Anal. Chem.* **1995,** 67, (23), 4404-4408.

41. Szabelski, P.; Kaczmarski, K.; Cavazzini, A.; Chen, Y. B.; Sellergren, B.; Guiochon, G., Energetic heterogeneity of the surface of a molecularly imprinted polymer studied by high-performance liquid chromatography. *J. Chromatogr., A* **2002,** 964, (1-2), 99-111.

42. Yang, G.; Wang, D.; Li, Z.; Zhou, S.; Chen, Y., Adsorption isotherms on aminoantipyrine imprinted polymer stationary phase. *Chromatographia* **2003,** 58, (1/2), 53-58.

43. Guo, T. Y.; Xia, Y. Q.; Hao, G. J.; Song, M. D.; Zhang, B. H., Adsorptive separation of hemoglobin by molecularly imprinted chitosan beads. *Biomaterials* **2004,** 25, (27), 5905-5912.

44. Zhu, X.; Yang, J.; Su, Q.; Cai, J.; Gao, Y., Molecularly imprinted polymer for monocrotophos and its binding characteristics for organophosphorus pesticides. *Annali di chimica* **2005,** 95, (11-12), 877-884.

45. Rampey, A. M.; Umpleby, R. J., II; Rushton, G. T.; Iseman, J. C.; Shah, R. N.; Shimizu, K. D., Characterization of the Imprint Effect and the Influence of Imprinting Conditions on Affinity, Capacity, and Heterogeneity in Molecularly Imprinted Polymers Using the Freundlich Isotherm-Affinity Distribution Analysis. *Anal. Chem.* **2004,** 76, (4), 1123-1133.

46. Rushton, G. T.; Karns, C. L.; Shimizu, K. D., A critical examination of the use of the Freundlich isotherm in characterizing molecularly imprinted polymers (MIPs). *Anal. Chim. Acta* **2005,** 528, (1), 107-113.

47. Freundlich, H., Colloid and Capillary Chemistry. Methuen: London, 1926.

48. Khan, A. R.; Riazi, M. R.; Al-Roomi, Y. A., A thermodynamic model for liquid adsorption isotherms. *Sep. Purif. Technol.* **2000,** 18, 237-250.

49. Burris, D. R.; Antworth, C. P.; Stauffer, T. B.; Macintyre, W. G., Humic acid-modified silica as a model aquifer material. *Environ. Toxicol. Chem.* **1991,** 10, 433-440.

50. Brownawell, B. J.; Chen, H.; Zhang, W. J.; Westall, J. C., Sorption of Nonionic Surfactants on Sediment Materials. *Environ. Sci. Technol.* **1997,** 31, 1735-1741.

51. Murai, S.; Imajo, S.; Takasu, Y.; Takahashi, K.; Hattori, K., Removal of phthalic acid esters from aqueous solution by inclusion and adsorption on b-cyclodextrin. *Environ. Sci. Technol.* **1998,** 32, 782-787.

52. Piletsky, S. A.; Matuschewski, H.; Schedler, U.; Wilpert, A.; Piletska, E. V.; Thiele, T. A.; Ulbricht, M., Surface Functionalization of Porous Polypropylene Membranes with Molecularly Imprinted Polymers by Photograft Copolymerization in Water. *Macromolecules* **2000,** 33, (8), 3092-3098.

53. Karlsson, J. G.; Karlsson, B.; Andersson, L. I.; Nicholls, I. A., The roles of template complexation and ligand binding conditions on recognition in bupivacaine molecularly imprinted polymers. *Analyst* **2004,** 129, (5), 456-462.

54. Gill, R. S.; Marquez, M.; Larsen, G., Molecular imprinting of a cellulose/silica composite with caffeine and its characterization. *Microporous Mesoporous Mater.* **2005,** 85, (1-2), 129-135.

55. Courtois, J.; Fischer, G.; Sellergren, B.; Irgum, K., Molecularly imprinted polymers grafted to flow through poly(trimethylolpropane trimethacrylate) monoliths for capillary-based solid-phase extraction. *J. Chromatogr., A* **2006,** 1109, (1), 92-99.

56. Wei, S.; Molinelli, A.; Mizaikoff, B., Molecularly imprinted micro and nanospheres for the selective recognition of 17β-estradiol *Biosens. Bioelectron.* **2006,** 21, (10), 1943-1951.

57. Farrington, K.; Magner, E.; Regan, F., Predicting the performance of molecularly imprinted polymers: Selective extraction of caffeine by molecularly imprinted solid phase extraction. *Anal. Chim. Acta* **2006,** 566, (1), 60-68.

58. Zhang, J.; He, L.; Fu, Q., Chromatographic features and molecular recognition mechanism of a strychnine monolithic molecularly imprinted polymer. *Chromatographia* **2005,** 62, (5/6), 319-323.

59. Wei, S.; Mizaikoff, B., Binding Site Characteristics of 17β-Estradiol Imprinted Polymers. *Biosens. Bioeletron.* **2007**, In press.

60. Fischer, L.; Mueller, R.; Ekberg, B.; Mosbach, K., Direct enantioseparation of b-adrenergic blockers using a chiral stationary phase prepared by molecular imprinting. *J. Am. Chem. Soc.* **1991,** 113, (24), 9358-9360.

61. Sellergren, B., Direct Drug Determination by Selective Sample Enrichment on an Imprinted Polymer. *Anal. Chem.* **1994,** 66, (9), 1578-1582.

62. Xia, Y.; McGuffey James, E.; Bhattacharyya, S.; Sellergren, B.; Yilmaz, E.; Wang, L.; Bernert John, T., Analysis of the tobacco-specific nitrosamine 4-(methylnitrosamino)-1-(3-pyridyl)-1-butanol in urine by extraction on a molecularly imprinted polymer column and liquid chromatography/atmospheric pressure ionization tandem mass spectrometry. *Anal. Chem.* **2005,** 77, (23), 7639-7645.

63. Ariffin, M. M.; Miller, E. I.; Cormack, P. A. G.; Anderson, R. A., Molecularly Imprinted Solid-Phase Extraction of Diazepam and Its Metabolites from Hair Samples. *Anal. Chem.* **2007,** 79, (1), 256-262.

64. Xu, X.; Zhu, L.; Chen, L., Separation and screening of compounds of biological origin using molecularly imprinted polymers. *J. Chromatogr., B: Anal. Technol. Biomed. Life Sci.* **2004,** 804, (1), 61-69.

65. Han, D.-M.; Fang, G.-Z.; Yan, X.-P., Preparation and evaluation of a molecularly imprinted sol-gel material for on-line solid-phase extraction coupled with high performance liquid chromatography for the determination of trace pentachlorophenol in water samples. *J. Chromatogr., A* **2005,** 1100, (2), 131-136.

66. Chapuis, F.; Mullot, J.-U.; Pichon, V.; Tuffal, G.; Hennion, M.-C., Molecularly imprinted polymers for the clean-up of a basic drug from environmental and biological samples. *J. Chromatogr., A* **2006,** 1135, (2), 127-134.

67. Urraca, J. L.; Moreno-Bondi, M. C.; Hall, A. J.; Sellergren, B., Direct Extraction of Penicillin G and Derivatives from Aqueous Samples Using a Stoichiometrically Imprinted Polymer. *Anal. Chem.* **2007,** 79, (2), 695-701.

68. Weiss, R.; Molinelli, A.; Jakusch, M.; Mizaikoff, B., Molecular imprinting and solid phase extraction of flavonoid compounds. *Bioseparation* **2001,** 10, (6), 379-387.

69. Molinelli, A.; Weiss, R.; Mizaikoff, B., Advanced Solid Phase Extraction Using Molecularly Imprinted Polymers for the Determination of Quercetin in Red Wine. *J. Agric. Food Chem.* **2002,** 50, (7), 1804-1808.

70. Weiss, R.; Molinelli, A.; Jakusch, M.; Mizaikoff, B., Molecular imprinting and solid phase extraction of flavonoid compounds. *Bioseparation* **2002,** 10, (6), 379-387.

71. Weiss, R.; Freudenschuss, M.; Krska, R.; Mizaikoff, B., Improving methods of analysis for mycotoxins: molecularly imprinted polymers for deoxynivalenol and zearalenone. *Food Addit. Contam.* **2003,** 20, (4), 386-395.

72. Krska, R.; Welzig, E.; Berthiller, F.; Molinelli, A.; Mizaikoff, B., Advances in the analysis of mycotoxins and its quality assurance. *Food Addit. Contam.* **2005,** 22, (4), 345-353.

73. Masqué, N.; Marcé, R. M.; Borrull, F.; Cormack, P. A. G.; Sherrington, D. C., Synthesis and evaluation of a molecularly imprinted polymer for selective on-line solid-phase extraction of 4-nitrophenol from environmental water. *Anal. Chem.* **2000,** 72, 4122-4126.

74. Vlatakis, G.; Andersson, L. I.; Mueller, R.; Mosbach, K., Drug assay using antibody mimics made by molecular imprinting. *Nature* **1993,** 361, (6413), 645-647.

75. Wei, S.; Jakusch, M.; Mizaikoff, B., Capturing molecules with templated materials - Analysis and rational design of molecularly imprinted polymers. *Anal. Chim. Acta* **2006,** 578, (1), 50-58.

76. Ansell, R. J., Molecularly imprinted polymers in pseudoimmunoassay. *J. Chromatogr., B: Anal. Technol. Biomed. Life Sci.* **2004,** 804, (1), 151-165.

77. Yilmaz, E.; Mosbach, K.; Haupt, K., Influence of functional and cross-linking monomers and the amount of template on the performance of molecularly imprinted polymers in binding assays. *Anal. Commun.* **1999,** 36, (5), 167-170.

78. Andersson, H. S.; Nicholls, I. A., Spectroscopic evaluation of molecular imprinting polymerization systems. *Bioorg. Chem.* **1997,** 25, (3), 203-211.

79. Wei, S.; Jakusch, M.; Mizakoff, B., Investigating the Mechanisms of 17b-Estradiol Imprinting by Computational Prediction and Spectroscopic Analysis. *Anal. Bioanal. Chem.* **2007**, In press.

80. Wei, S.; Jakusch, M.; Mizaikoff, B., Understand the Mechanism of Selectivity in Molecular Imprinted Polymers by Molecular Dynamic Simulation. manuscript in preparation.

81. Takeuchi, T.; Dobashi, A.; Kimura, K., Molecular Imprinting of Biotin Derivatives and Its Application to Competitive Binding Assay Using Nonisotopic Labeled Ligands. *Anal. Chem.* **2000,** 72, (11), 2418-2422.

82. Piletsky, S. A.; Karim, K.; Piletska, E. V.; Day, C. J.; Freebairn, K. W.; Legge, C.; Turner, A. P. F., Recognition of ephedrine enantiomers by molecularly imprinted polymers designed using a computational approach. *Analyst* **2001,** 126, (10), 1826-1830.

83. Pavel, D.; Lagowski, J., Computationally designed monomers and polymers for molecular imprinting of theophylline and its derivatives. Part I. *Polymer* **2005,** 46, (18), 7528-7542.

84. Pavel, D.; Lagowski, J., Computationally designed monomers and polymers for molecular imprinting of theophylline-part II. *Polymer* **2005,** 46, (18), 7543-7556.

85. Subrahmanyam, S.; Piletsky, S. A.; Piletska, E. V.; Chen, B.; Karim, K.; Turner, A. P., "Bite-and-Switch" approach using computationally designed molecularly imprinted polymers for sensing of creatinine. *Biosens. Bioelectron.* **2001,** 16, (9-12), 631-637.

86. Chianella, I.; Lotierzo, M.; Piletsky, S. A.; Tothill, I. E.; Chen, B.; Karim, K.; Turner, A. P. F., Rational design of a polymer specific for microcystin-LR using a computational approach. *Anal. Chem.* **2002,** 74, (6), 1288-1293.

87. Meng, Z.; Yamazaki, T.; Sode, K., A molecularly imprinted catalyst designed by a computational approach in catalysing a transesterification process. *Biosens. Bioelectron.* **2004,** 20, (6), 1068-1075.

88. Pearlman, D. A.; Case, D. A.; Caldwell, J. W.; Ross, W. S.; Cheatham, T. E., III; DeBolt, S.; Ferguson, D.; Seibel, G.; Kollman, P., \"AMBER\", a package of computer programs for applying molecular mechanics, normal mode analysis, molecular dynamics and free energy calculations to stimulate the structural and energetic properties of molecules. *Comput. Phys. Commun.* **1995,** 91, (1-3), 1-42.

89. Molinelli, A.; O'Mahony, J.; Nolan, K.; Smyth, M. R.; Jakusch, M.; Mizaikoff, B., Analyzing the Mechanisms of Selectivity in Biomimetic Self-Assemblies via IR and NMR Spectroscopy of Prepolymerization Solutions and Molecular Dynamics Simulations. *Anal. Chem.* **2005,** 77, (16), 5196-5204.

90. Wu, L.; Sun, B.; Li, Y.; Chang, W., Study properties of molecular imprinting polymer using a computational approach. *Analyst* **2003,** 128, (7), 944-949.

91. Dineiro, Y.; Menendez, M. I.; Blanco-Lopez, M. C.; Lobo-Castanon, M. J.; Miranda-Ordieres, A. J.; Tunon-Blanco, P., Computational approach to the rational design of molecularly imprinted polymers for voltammetric sensing of homovanillic acid. *Anal. Chem.* **2005,** 77, (20), 6741-6746.

92. Rachkov, A.; McNiven, S.; El'skaya, A.; Yano, K.; Karube, I., Fluorescence detection of b-estradiol using a molecularly imprinted polymer. *Anal. Chim. Acta* **2000,** 405, (1-2), 23-29.

93. Piscopo, L.; Prandi, C.; Coppa, M.; Sparnacci, K.; Laus, M.; Lagana, A.; Curini, R.; D'Ascenzo, G., Uniformly sized molecularly imprinted polymers (MIPs) for 17b-estradiol. *Macromol. Chem. and Phys.* **2002,** 203, (10/11), 1532-1538.

94. Dong, H.; Tong, A.-j.; Li, L.-d., Syntheses of steroid-based molecularly imprinted polymers and their molecular recognition study with spectrometric detection. *Spectrochim. Acta, Part A* **2003,** 59A, (2), 279-284.

95. Sanbe, H.; Haginaka, J., Uniformly sized molecularly imprinted polymers for bisphenol A and b-estradiol: retention and molecular recognition properties in hydro-organic mobile phases. *J. Pharm. Biomed. Anal.* **2003,** 30, (6), 1835-1844.

96. Kollman, P. A.; Massova, I.; Reyes, C.; Kuhn, B.; Huo, S.; Chong, L.; Lee, M.; Lee, T.; Duan, Y.; Wang, W.; Donini, O.; Cieplak, P.; Srinivasan, J.; Case, D. A.; Cheatham, T. E., III, Calculating Structures and Free Energies of Complex Molecules: Combining Molecular Mechanics and Continuum Models. *Accounts Chem. Res.* **2000,** 33, (12), 889-897.

97. Lancelot, G., Hydrogen bonding between nucleic acid bases and carboxylic acids. *J. Am. Chem. Soc.* **1977,** 99, (21), 7037-7042.

98. Quaglia, M.; Chenon, K.; Hall, A. J.; De Lorenzi, E.; Sellergren, B., Target analogue imprinted polymers with affinity for folic acid and related compounds. *J. Am. Chem. Soc.* **2001,** 123, (10), 2146-2154.

99. Dong, X.; Sun, H.; Lue, X.; Wang, H.; Liu, S.; Wang, N., Separation of ephedrine stereoisomers by molecularly imprinted polymers. Influence of synthetic conditions and mobile phase compositions on the chromatographic performance. *Analyst* **2002,** 127, (11), 1427-1432.

100. O'Mahony, J.; Molinelli, A.; Nolan, K.; Smyth, M. R.; Mizaikoff, B., Towards the rational development of molecularly imprinted polymers: 1H NMR studies on hydrophobicity and ion-pair interactions as driving forces for selectivity. *Biosens. Bioelectron.* **2005,** 20, (9), 1884-1893.

101. O'Mahony, J.; Molinelli, A.; Nolan, K.; Smyth, M. R.; Mizaikoff, B., Anatomy of a successful imprint: Analysing the recognition mechanisms of a molecularly imprinted polymer for quercetin. *Biosens. Bioelectron.* **2006,** 21, (7), 1383-1392.

102. Weber, A.; Dettling, M.; Brunner, H.; Tovar, G. E. M., Isothermal titration calorimetry of molecularly imprinted polymer nanospheres. *Macromol. Rapid Commun.* **2002,** 23, (14), 824-828.

103. Kirchner, R.; Seidel, J.; Wolf, G.; Wulff, G., Calorimetric Investigation of Chiral Recognition Processes in a Molecularly Imprinted Polymer. *J. Inclusion Phenom. Macrocyclic Chem.* **2002,** 43, (3-4), 279-283.

104. Fish, W. P.; Ferreira, J.; Sheardy, R. D.; Snow, N. H.; O'Brien, T. P., Rational design of an imprinted polymer: Maximizing selectivity by optimizing the monomer-template ratio for a cinchonidine MIP, prior to polymerization, using microcalorimetry. *J. Liq. Chromatogr. Relat. Technol.* **2005,** 28, (1), 1-15.

105. O'Mahony, J.; Wei, S.; Molinelli, A.; Mizaikoff, B., Imprinted Polymeric Materials. Insight into the Nature of Prepolymerization Complexes of Quercetin Imprinted Polymers. *Anal. Chem.* **2006,** 78, (17), 6187-6190.

106. O'Mahony, J.; Karlsson, B. C. G.; Mizaikoff, B.; Nicholls, I. A., Mechanisms Underlying a Non-Covalent Imprinted Polymer System: New Detail from Correlated Theoretical, Spectroscopic and X-ray Crystallographic Studies of Pre-polymerisation Events. *Analyst* **2007**, In press.

CHAPTER 3

MIPS FOR 17β-ESTRADIOL: ANALYSIS AND APPLICATIONS

3.1 MIPs for 17β-estradiol Analysis

3.1.1 Introduction

Natural estrogens such as 17β-estradiol (E2), 17α-estradiol (17α-E2), estriol (E3), and estrone (E1), as well as the synthetic hormone 17α-ethynylestradiol (EE2) (Figure 3.1) are suspected of having adverse effects on the endocrine system in wildlife[1] and humans[2].

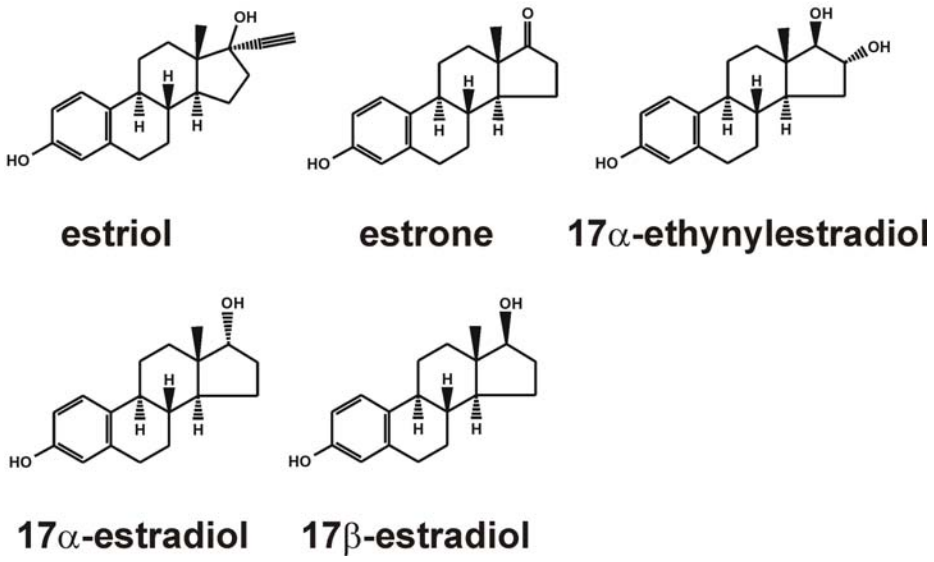

Figure 3.1 Molecular structures of E2 and its structure analogues.

Therefore, considerable interest is focused on developing cost-effective analytical methods for determining these constituents in environmental samples at low concentration levels[3, 4]. Nowadays, non-covalent molecularly imprinted polymers (MIPs)

have increasingly been developed as mimics of natural molecular receptors[5, 6], aiming at the unambiguous detection and quantification of the target analytes in affinity chromatography[7-9], solid phase extraction[10-17], and (immuno)assays[18-20].

However, more widespread application of MIP-based HPLC stationary phases in commercial products is still limited by the drawbacks of band broadening and tailing resulting from sub-optimal particles obtained during conventional bulk polymerization, and to date limited rational design of the synthetic route for flexibly creating the desired retention properties for a wide range of templates. In MISPE, the solid phase particle size is less critical, with main emphasis on (i) rapid and complete but separate elution of interferants and target analyte(s), and (ii) elimination of template leaking from the MIP matrix, which is of particular importance when using MISPE for pre-concentration in quantitative trace analysis. The majority of the reported studies on MISPE apply the cartridges off-line with subsequent downstream analytical separation. Methods for preparing imprinted polymer monoliths inside a column, or imprinted polymer beads providing monodisperse particles with regular geometries have attracted substantial interest. The synthesis of imprinted polymer beads can frequently be realized by adapting synthetic routes for generating conventional (non-imprinted) polymeric micro- and nanospheres[21, 22] to the required conditions for ensuring non-covalent complex formation between the template and functional monomer building blocks.

The present study focuses on a novel synthetic route for the generation of imprinted micro- and nanospheres for E2 providing accurate control and optimization of the governing parameters for precipitation polymerization, including the polymerization temperature and the cross-linker, and yielding a one-step synthetic approach with superior

control on the bead diameter, shape, monodispersity, and imprinting efficiency. In a first step, the synthetic conditions for E2 imprinted bulk polymers were optimized by selecting a variety of functional monomers, cross-linkers, and molar ratios between template, monomer, and cross-linker. In a second step, the optimized synthetic conditions for bulk polymers were adapted for the preparation of imprinted microspheres for E2 operating in more dilute solutions. Finally, imprinted nanospheres were synthesized using EGDMA as cross-linker, reproducibly yielding imprinted nanospheres with a diameter of approx. 400 nm. The obtained monodispersity enabled direct analytical application of the synthesized micro- and nanospheres without further size selection. The molecule specific recognition properties of thus synthesized imprinted micro- and nanospheres were investigated in HPLC separation and radioligand binding assays studies.

3.1.2 Experimental section

3.1.2.1 MIP synthesis

Methacrylic acid (MAA), 4-vinylpyridine (4-VP), ethylene glycoldimethacrylate (EDMA), divinylbenzene (DVB), and trimethylolpropane trimethacrylate (TRIM) were purchased from Sigma-Aldrich (Milwaukee, WI) and purified by distillation. 2,2'-Azobis (2-isobutyronitrile) (AIBN) was purchased from Sigma-Aldrich (Milwaukee, WI), and purified by recrystallization. Figure 3.2 shows the monomer structures in the present study. E2, 17α-E2, and E1 were purchased from Sigma-Aldrich (Milwaukee, WI), and used as supplied. Radiolabeled E2, [6,7-^{3}H(N)]estradiol (specific activity 40-60 Ci/mmol) was purchased from American Radiolabeled Chemicals, Inc. (St. Louis, MO), and used as supplied. The scintillation liquid Ecoscint O was obtained from National Diagnostics

(Atlanta, GA). All solvents were of HPLC grade from VWR International Inc. (Suwannee, GA).

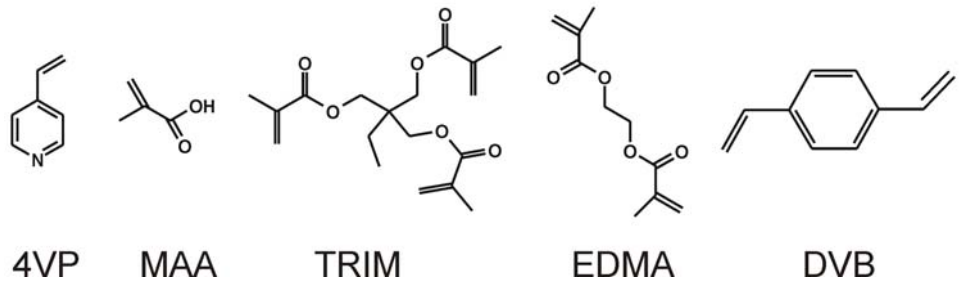

Figure 3.2 Molecular structures of functional monomers and cross-linkers used in the present study.

For the synthesis of molecular imprinted polymers for E2, E2, the functional monomer MAA or 4-VP, and the cross-linker EDMA, TRIM or DVB were dissolved in the porogen following to the molar ratios listed in Table 3.1. After addition of AIBN (2 wt % of the total amount of monomer used), the solutions were sonicated and deoxygenated with nitrogen for 5 min, and then thermally polymerized at 60 ºC for 24 h with the exception of ESTR11 and 12, which were thermally polymerized at 70 ºC to obtain microspheres with the desired dimensions. The resulting bulk polymers (ESTR1 - 10) were ground, and wet-sieved/collected with acetone through a 25 µm sieve. The fine particles were removed by repetitive sedimentation in acetone.

Table 3.1 Composition of the synthesized molecularly imprinted polymers for E2.

Polymer	Template	Functional monomer	Molar Ratio*	Cross-linker	Porogen
ESTR1	E2	MAA	1:6:30	EDMA	acetone and acetonitrile (12 ml, 1:1 v:v)
ESTR2	None	MAA	0:6:30	EDMA	acetone and acetonitrile (12 ml, 1:1 v:v)
ESTR3	E2	4VP	1:6:30	EDMA	acetone and acetonitrile (12 ml, 1:1 v:v)
ESTR4	None	4VP	0:6:30	EDMA	acetone and acetonitrile (12 ml, 1:1 v:v)
ESTR5	E2	MAA	1:6:30	TRIM	acetone and acetonitrile (12 ml, 1:1 v:v)
ESTR6	None	MAA	0:6:30	TRIM	acetone and acetonitrile (12 ml, 1:1 v:v)
ESTR7	E2	MAA	1:8:40	EDMA	acetone and acetonitrile (12 ml, 1:1 v:v)
ESTR8	None	MAA	0:8:40	EDMA	acetone and acetonitrile (12 ml, 1:1 v:v)
ESTR9	E2	MAA	1:8:40	DVB	Acetone (6 ml)
ESTR10	None	MAA	0:8:40	DVB	Acetone (6 ml)
ESTR11	E2	MAA	1:8:40	DVB	mixture of toluene and acetonitrile (60 ml, 1:3 v:v)
ESTR12	None	MAA	0:8:40	DVB	mixture of toluene and acetonitrile (60 ml, 1:3 v:v)
ESTR13	E2	MAA	1:8:6.7	EGDMA	acetone and acetonitrile (40 ml, 1:3 v:v)
ESTR14	None	MAA	0:8:6.7	EGDMA	acetone and acetonitrile (40 ml, 1:3 v:v)

Polymerization solutions were prepared by dissolving the template molecule E2 (1 mmol), MAA (8 mmol), EGDMA (6.7 mmol) or DVB (40 mmol), and AIBN (2 wt % of total monomer) in the porogenic solvent. All polymerizations were performed at 60 ºC for 24 h, with the exception of ESTR11 and 12, which were polymerized at 70 ºC. *Molar ratio describes the proportion between template, functional

Table 3.1 continued

monomer and cross-linker.

The composition of imprinted micro- and nanospheres (ESTR11, 13) is given in Table 3.1. For the preparation of ESTR11, the solution was continuously stirred during the polymerization with a magnetic stirrer. The obtained beads were separated from the reaction medium by filtration or centrifugation, successively washed three times with methanol:acetic acid (100 mL, 85:15 v/v), methanol and acetonitrile, respectively. The microspheres (ESTR11 and 12) were collected by filtration using a funnel with a fritted disc. The nanospheres (ESTR 13 and 14) were collected by centrifugation for 5 min at 10,000 rpm using a Beckman centrifuge. The particles were dried at 40 ºC for 12 h.

As a control, non-imprinted bulk polymers and micro-/nanospheres were prepared by exactly the same synthetic routes in absence of the template molecule.

3.1.2.2 Characterization of MIP morphology: scanning electron microscopy and optical microscopy

Imprinted micro- and nanospheres were deposited onto silicon slides, and coated with 15 nm of gold using a thermal evaporator (Denton DV-502A, Denton Vacuum, Moorestown, NJ). Scanning electron micrographs were obtained at 25 kV (SEM 1530, thermally-assisted FEG, LEO, Oberkochen, Germany).

Optical micrographs were obtained by depositing the particles onto glass slides, and recording digital images with an optical microscope (BX41, Olympus Optical Co. Ltd., Tokyo, Japan).

3.1.2.3 Characterization of MIPs via HPLC

Bulk polymer particles (ESTR1 - 10) and microspheres (ESTR11 and 12) were suspended in acetone and packed into 150×4.6 mm stainless steel HPLC columns with a slurry packer (Alltech 1666, Deerfield, IL) using acetone as the packing solvent. Chromatographic analysis was performed using a HPLC system equipped with a UV/Vis diode array detector (Dionex P580 pump, UVD 340S Detector, Sunnyvale, CA).

3.1.2.4 Characterization of imprinted nanospheres for competitive ligand binding assays

For saturation studies, MIP nanospheres (ESTR13 and 14) were suspended in acetonitrile and appropriate volumes were incubated with 417 fmol of radioligand [6,7-^{3}H(N)]estradiol in acetonitrile. The final volume was adjusted to 1 ml. The samples were incubated for 20 h and separated by centrifugation. 500 µl of supernatant was added to a scintillation liquid (10 ml, Ecoscint O). The radioactivity was measured with a liquid scintillation counter (LS5000-TD, Beckman Coulter, Fullerton, CA). For competitive assays, 30 mg of MIP nanospheres (ESTR13 and 14) were suspended in acetonitrile and appropriate volumes were added into 1.5 ml polypropylene centrifuge tubes followed by a constant amount of [6,7-^{3}H(N)]estradiol and varying amounts of E2 or 17α-E2. The appropriate amount of acetonitrile was added to maintain a total volume of 1 ml. The samples were incubated for 20 h and the amount of bound radioligand was determined similar to the saturation studies described above.

3.1.3 Results and discussion

3.1.3.1 Optimization of the synthetic conditions of molecular imprinted polymers for 17β-estradiol

Molecular imprinted polymers and the corresponding control polymers for the template E2 were synthesized at a variety of conditions (choice of functional monomers, cross-linkers, template:functional monomer:cross-linker ratio). The optimization of the MIP formulation was performed with one parameter changing at a time. Table 3.1 lists the synthetic conditions for different MIPs and control polymers. Previous studies in our group[23] show that the ratio 1:4:20 and below produces fine and brittle polymers resulting in very high backpressures during column packing after grounding and sieving. MIPs with ratios 1:6:30 to 1:20:100 are characterized by adequate to moderate imprinting effects. Consequently, the ratio 1:6:30 was selected as starting ratio for imprinting of E2. Acetone mixed with acetonitrile was selected as porogen for the preparation of bulk polymers, as E2 is characterized by a very low solubility in non-protonic solvents such as acetonitrile (approx. 0.6 μmol/100 g acetonitrile)[24].

For the choice of functional monomer, it is evident from Table 3.2 that MIPs prepared with 4VP (ESTR3) are characterized by a larger capacity factor, but a moderate separation factor for E2 and 17α-E2, in contrast to MIPs prepared with MAA (ESTR1). As a consequence, MAA was used as functional monomer during the following optimization process. The contribution of the cross-linker to molecular imprinting is mostly related to its ability to provide adequate binding site accessibility and rapid mass transfer. In addition, it has been proven that the cross-linker may provide part of the

binding site functionality to the imprinting, as shown in the subsequent studies of this thesis (Section 4.1). It has been reported that higher load capacities and separation resolution were achieved using trifunctional cross-linkers such as TRIM for the imprinting of Z-L-Tyr-OH[25]. For imprinting of E2, the MIP prepared with TRIM (ESTR5) shows enhanced capacity factors, but moderate separation factors compared to EDMA prepared MIPs (ESTR1). Furthermore, the result from ESTR 7 indicates that increasing the ratio from 1:6:30 to 1:8:40 results in an increase of the separation factor from 1.472 to 1.653, along with a lower capacity factor. This result indicates that sufficient resolution and rapid elution are achieved at the ratio 1:8:40. Next, the cross-linker DVB was replaced with EDMA, while all other optimized conditions remained unchanged. Surprisingly, this MIP (ESTR9) reveals the best performance both in capacity factor and separation factor. The mechanism of the molecular interactions involved in this formulation will be discussed in detail in Chapter 4.

Table 3.2 Capacity factor and separation factor from the HPLC characterization of the synthesized molecularly imprinted polymers for E2.

Polymer	Capacity factor*	Separation factor**
ESTR1	0.939	1.472
ESTR3	1.352	1.282
ESTR5	1.174	1.463
ESTR7	0.782	1.653
ESTR9	1.874	2.040

*Capacity factor $K= (t–t_0)/t_0$, t and t_0 are the retention time of E2 and acetone (void marker), respectively.
**Separation factor = K_β/K_α, K_β and K_α are the capacity factor of E2 and 17α-E2, respectively.

3.1.3.2 Synthesis of imprinted spheres

Several examples of E2 selective MIPs have previously been synthesized using MAA or 4-VP as functional monomer[26-29]. The molar ratio between template, functional monomer, and cross-linker was 1:6:30[27] or 1:8:25[26] for bulk polymers, and 1:2.7:12[29] or 1:7:12.5[28] for spherical particles synthesized by multi-step swelling polymerization procedures. In this thesis, two distinct varieties of imprinted micro- and nanospheres were synthesized using different cross-linkers and porogenic solvents.

In order to synthesize microspheres with diameters suitable for HPLC applications, a series of control beads were prepared to rationalize the influence of the monomer concentration and polymerization temperature on the size and morphology of the obtained polymer beads. Monodisperse spheres were obtained at a monomer content < 11 vol % in the pre-polymerization solution (Figure 3.3 A, B). If more cross-linker (EDMA) was used, coagulation of particles was apparent, instead of the formation of larger spheres (Figure 3.3 C, D). Hence, it is concluded that the mere variation of the EDMA concentration is insufficient to control the diameter of the synthesized microspheres. Since it was reported that there is weak interaction between MAA and EDMA[30], the formation of the polymer network is probably affected by the competition between the propagation reaction, and the cross-linking reaction. As a consequence, the particle size of poly(MAA-co-EDMA) under the restricted conditions for MIPs (the ratio between MAA and EDMA, the monomer concentration, etc.) is relatively small comparing to poly (MAA-co-DVB), where there is no interaction between MAA and DVB. For the trifunctional cross-linker TRIM, the resulting particles (Figure 3.3 E) are ever smaller

than for poly(MAA-co-EDMA), which is related to the fact that the formation of the polymer network is dominated by the cross-linking reaction.

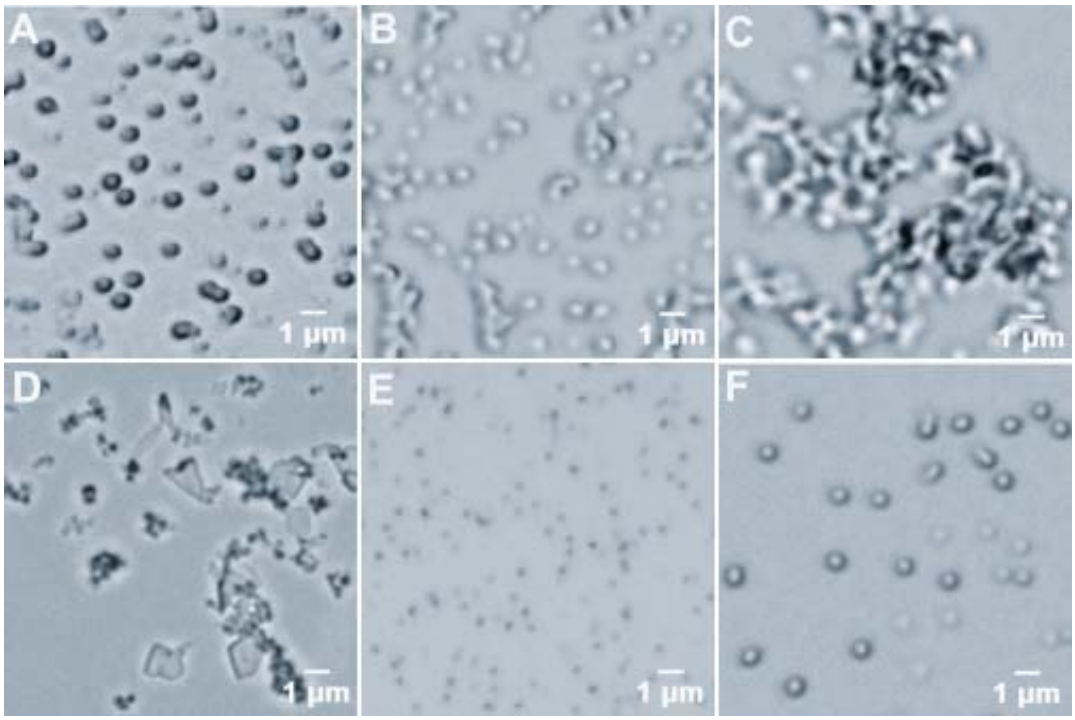

Figure 3.3 Optical micrographs of poly (MAA-co-EGDMA) beads prepared with different monomer ratios (MAA: EGDMA in A: 8:6; B: 8:10; C: 8:14; D: 8:16) and poly (MAA-co-TRIM) beads prepared at different temperatures (E: 60 °C; F: 70 °C) synthesized by precipitation polymerization.

Figures 3.3 E and F show that the polymer particle size increases with an increase of the polymerization temperature. Adapted from the synthesis method for poly(divinylbenzene)[22, 31] using precipitation polymerization techniques, for the preparation of ESTR11 and 12 divinylbenzene has been applied, which cross-links to poly(divinylbenzene) yielding microspheres with diameters ranging from 2 to 5 µm at a polymerization temperature of 70 °C. A solvent mixture of toluene:acetonitrile (1:3, v/v) was used as porogen minimizing the interference of a protic solvents like acetone with

hydrogen bonding, while increasing the porosity of the microspheres. The resulting microspheres with a diameter of ~ 3 μm reveal perfect spherical shapes and a narrow size distribution (see ESTR11, Figure 3.4 B, D). The formation of large particles with DVB is associated with the fact that DVB is a non-polar cross-linker.

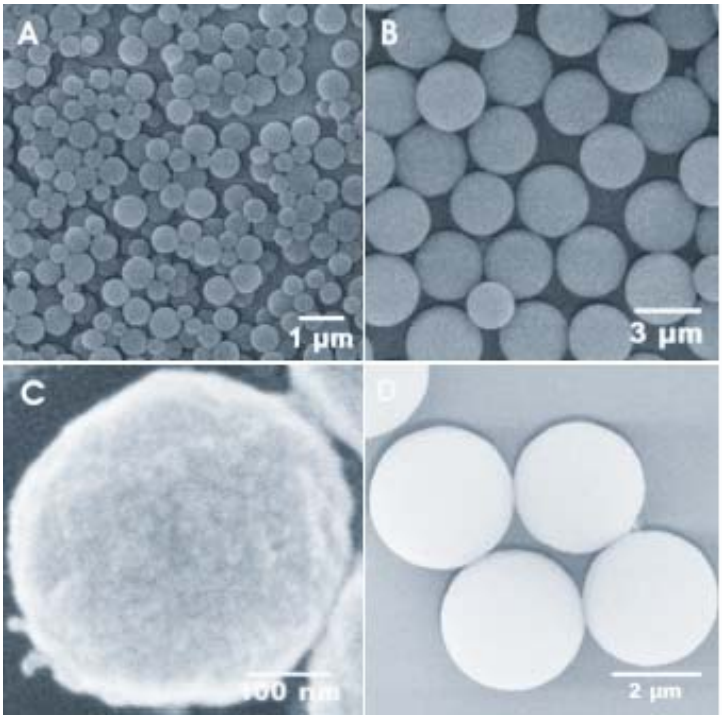

Figure 3.4 Scanning electron micrographs (SEM) of imprinted micro- and nanospheres (A, C: ESTR13; B, D: ESTR11) synthesized by one-step precipitation polymerization.

Therefore, there is no interaction between MAA and DVB, and the formation of poly (MAA-co-DVB) microspheres results from partitioning of DVB between the continuous phase and the mini-monomer droplets of MAA[30]. As a result, the particle size can be increased by increasing of the amount of DVB due to the bridge coagulation of the microspheres.

For the synthesis of nanospheres, the cross-linking polymerization process was initiated from a diluted homogeneous monomer solution. This dilution ensured that as much of the functional monomer and as little of the cross-linker as possible were available for selective binding site formation. EDMA was selected as cross-linker (Table 3.1, ESTR 13) for synthesizing nanospheres, as it provides sufficient wettability in most rebinding media[32], which is essential for the application of thus synthesized nanospheres in binding assays. ESTR13 (Figure 3.4 A,C) was prepared using MAA as functional monomer and EDMA as cross-linker, with significantly less cross-linker in contrast to conventional bulk polymerization[33]. An attractive feature of the obtained nanospheres (ESTR13) is that thus synthesized polymer beads (diam. approx. 400 nm) facilitate dispersion and suspension in solution, which renders them ideal for suspension binding assay applications.

3.1.3.3 MIP based HPLC separation of estrogens

To test the selectivity of E2-imprinted MIPs, both the bulk polymers and microspheres were applied as stationary phase in HPLC experiments for separating structurally related estrogen constituents. Although acetone was used as porogen in the polymerization process, it was not selected as a mobile phase in MIP-based HPLC experiments due to its high UV cut-off (330 nm). Among the various investigated solvents with different polarities (methanol, acetonitrile, water), acetonitrile offered maximum enhancement towards the specific molecular recognition of E2 by the developed MIP matrix. Separation of E2 from other estrogens such as 17α-E2, EE2, E3, and E1, which exhibit similar molecular composition with different functionality at the

17-position, was achieved on the E2 imprinted polymer column operating under simple isocratic conditions (Figure 3.5).

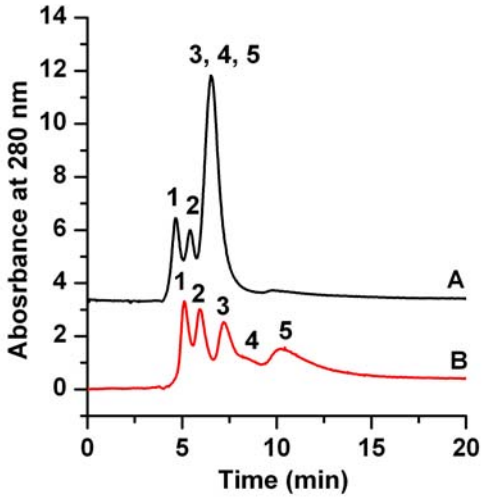

Figure 3.5 Separation of estrogens (1: EE2, 10 mg L^{-1}; 2: E1, 10 mg L^{-1}; 3: 17α-E2, 10 mg L^{-1}; 4: E3, 10 mg L^{-1}, 5:E2, 20 mg L^{-1}) by ESTR10-Control polymer (A), and ESTR9-MIP (B) at identical HPLC conditions (acetonitrile containing 0.5 % of acetic acid at a flow rate of 0.6 mL/min; injected sample amount: 20 μL; detection: @ λ=280 nm).

The size range and spherical shape of ESTR11 and ESTR12 provides ideal particles for chromatographic applications. The recognition ability of imprinted microspheres ESTR11 for E2 was confirmed by HPLC evaluation. First, separation of E2, 17α-E2 and E1 was achieved using ESTR11 as stationary phase in HPLC (Figure 3.6A, solid line). The control experiments were performed using the control polymer ESTR12 (Figure 3.6A, dashed line), and a standard Kromasil 100-5 C_{18} column (Figure 3.6B, dotted line) at identical chromatographic conditions (mobile phase: acetonitrile containing 0.5 % acetic acid; flow rate: 0.6 mL min^{-1}).

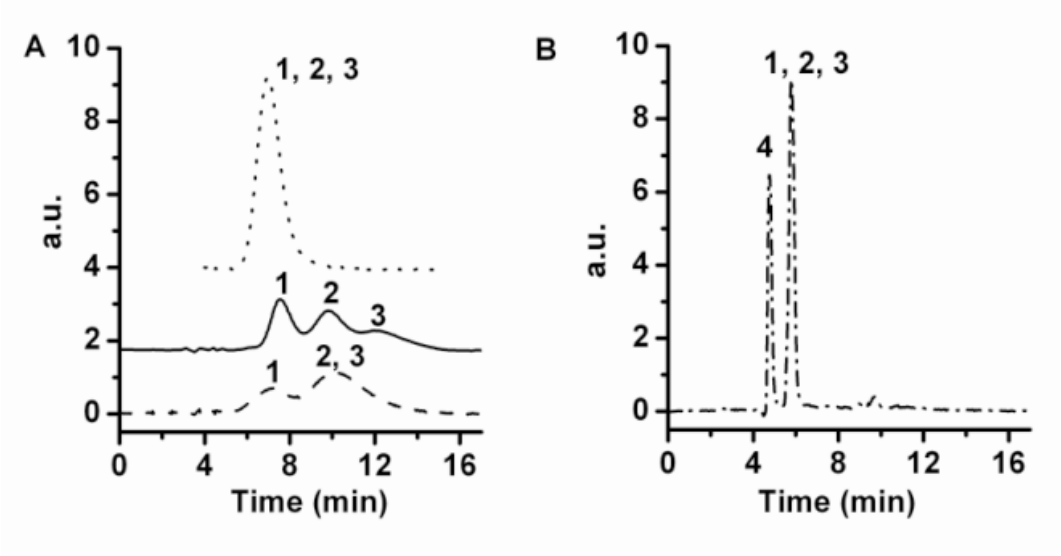

Figure 3.6 Comparison of the chromatographic separation of E1 (peak 1), 17α-E2 (peak 2) and E2 (peak 3) on ESTR3 (A: solid line), ESTR4 (A: dashed line) and Kromasil 100-5 C_{18} column (B: dash dot line; peak 4 is acetone) with acetonitrile containing 0.5 % acetic acid as mobile phase. Chromatographic separation of E1, 17α-E2 and E2 on ESTR3 was also performed with acetonitrile containing 10 % pH 8.5 acetate buffer (A: dotted line) as mobile phase. Flow rate of the mobile phase: 0.6 ml min^{-1}; detection @ 280 nm; 0.2 µg of E1, 0.2 µg of 17α-E2 and 0.4 µg of E2 in 20 µl acetonitrile were injected for each analysis.

To further confirm that the separation is based on an imprinting effect, similar measurements were performed using acetonitrile containing 10 % acetate buffer at pH 8.5 (Figure 3.6A, dashed-dotted line) as mobile phase. In this case, E1, E2, and 17α-E2 were not separated; further studies on these peaks revealed that the peaks for E2 and 17α-E2 are shifted, while the E1 peak remained at the same retention time, therefore resulting in a single peak. Protic solvents and functional monomers compete for specific interactions with the template molecule. Hence, the addition of a protic solvent such as water to the mobile phase or pre-polymerization solution should therefore disable specific interactions such as hydrogen bonding[34]. The disappearance of specific recognition in Figure 3.6A (dashed-dotted line) confirms this hypothesis, and indicates that specific recognition

indeed results from hydrogen bonding interaction between the template E2 and the functional monomer MAA.

Secondly, the efficiency of the synthesized imprinted microspheres was compared to MIPs prepared by conventional bulk polymerization and imprinted microspheres prepared by other polymerization techniques[28, 29]. Table 3.3 illustrates that the performance of imprinted microspheres prepared by the one-step synthetic route developed in the course of this thesis was superior or equal to the performance of microspheres prepared by multi-step swelling/polymerization techniques, as documented by higher separation and selectivity factors against E2 and E1. Hence, the advantages of imprinted microspheres prepared by precipitation polymerization not only include superior performance as HPLC separation matrix, but also the considerably simplified synthetic preparation compared to conventional bulk polymerizations and multi-step swelling/polymerization strategies.

Table 3.3 Chromatographic data obtained from HPLC analysis using imprinted microspheres synthesized via one-step precipitation polymerization as stationary phase in comparison to imprinted microspheres prepared by multi-step swelling/polymerization routes described in literature.

Data Source	Analyte	Capacity factor		Separation Factor	Selectivity Factor
		MIP	Control		
Wei *et al.*[20]	E2	3.01	2.37	1.00	1.00
	17α-E2	2.08	2.14	1.45	1.31
	E1	1.41	1.42	2.13	1.27
Piscopo *et al.*[29]	E2	2.06	0.79	1.00	1.00
	17α-E2	1.76	0.70	1.17	1.04
	E1	1.78	0.80	1.16	1.17

Table 3.3 continued

Sanbe *et al.*[28] *	E2	11.2	4.76	1.00	1.00
	17α-E2	9.16	5.13	1.22	1.31
	E1	6.72	4.09	1.67	1.44

Separation Factor: α = k' (E2)/k' (compound) is the ratio of the capacity factors; Selectivity Factor: $S = \alpha_{imp} / \alpha_{control}$ is the ratio of the separation factors.

HPLC conditions: acetonitrile as mobile phase at a flow rate of 1 ml/min; detection @ 280 nm.
*Sanbe *et al* have used different HPLC conditions: Mobile phase: sodium dihydrogen phosphate and disodium hydrogen phosphate (pH 5.1; 20 mM) - acetonitrile (1:1, v/v); flow rate: 1 ml/min; det. @ 200 nm.

3.1.3.4 Imprinted nanospheres for competitive ligand binding assays

In order to investigate the imprinting efficiency in comparison to the corresponding bulk polymerization methods, the imprinted micro- and nanospheres were evaluated by HPLC analysis and radioligand binding assays. Radioligand binding assays were performed in acetonitrile using [^{3}H] estradiol as a radioligand for evaluating the capacity of the imprinted nanospheres (ESTR13), and the corresponding control nanospheres (ESTR14) (Figure 3.7 A). Figure 3.7 B shows competitive [^{3}H] estradiol binding to the imprinted nanospheres with unlabeled E2 and its optical isomer 17α-E2. Evidently, the imprinted beads bind more [^{3}H] estradiol than the corresponding control material. Furthermore, binding to the imprinted beads is effectively inhibited following the addition of unlabeled E2 but not during the addition of 17α-E2. In addition, the displacement curve of labeled E2 in Figure 3.7 B may be used as calibration graph for the determination of E2 levels in biological or environmental samples.

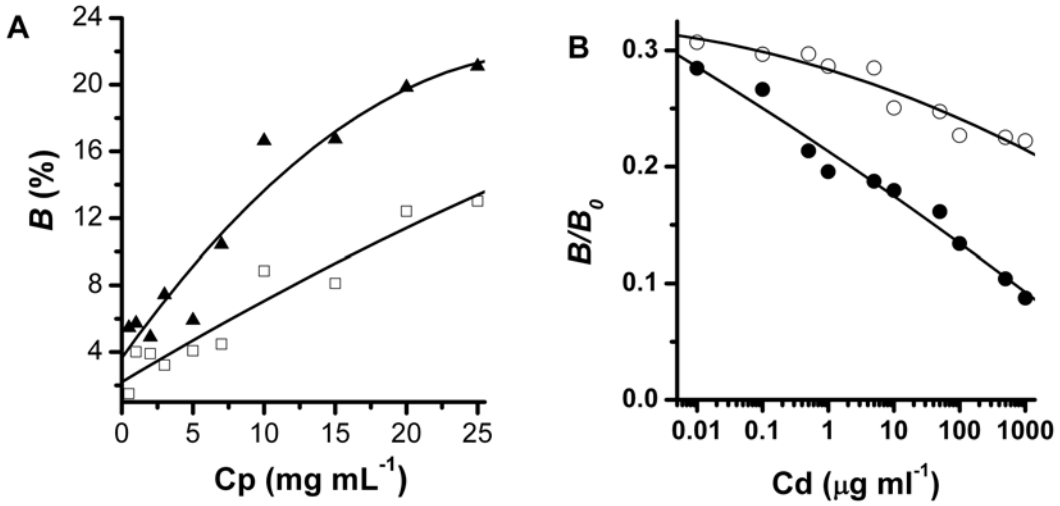

Figure 3.7 Results of radioligand binding assay studies using molecularly imprinted nanospheres synthesized by one-step precipitation polymerization.
A: Binding of [^{3}H]estradiol as a function of the polymer concentration. The data points represent the binding isotherm of ESTR13 (▲) and ESTR14 (□).
B: Displacement of [^{3}H]estradiol binding (X, %) to ESTR13 as a function of the concentration of E2 (●) and 17α-E2 (○). The x-axis (μg/ml) has a logarithmic scale.

3.1.4 Conclusions

In summary, the main synthesis parameters affecting the recognition properties of E2 imprints were assessed. MAA was finally selected as the functional monomer of choice providing polymers with high imprinting effect and rapid elution for E2, which is suitable as stationary phase material for HPLC applications. The best template:functional monomer:cross-linker ratio for E2 imprints was determined at 1:8:40. The use of DVB as cross-linker promises an increased capacity factor, as well as superior separation properties. Furthermore, a one-step precipitation polymerization method has been developed for the preparation of micro- and nanospheres imprinted against E2. With this synthetic strategy the size and morphology of the imprinted spheres can be rationally

controlled by the polymerization conditions, the nature of the cross-linker, the monomer concentration, and the polymerization temperature. The successful synthesis of E2 imprinted polymers with superior control on size and morphology ensures the applicability of molecularly imprinted polymers as selective recognition material for separation and enrichment of E2 in environmental samples, and offers a viable alternative to conventional sample clean-up and pre-concentration methods. However, better understanding of the recognition properties of MIPs at different rebinding conditions is required for the application of MIPs in a variety of media. For example, the MIP-based HPLC and SPE require rapid and complete but separate elution of interferents and target analyte(s), while the mass transfer rate is less critical in the MIP assays. Therefore, the next step in this study was focused on thorough investigations on the rebinding properties of the developed MIPs during equilibrium binding, non-equilibrium binding, and release studies.

3.1.5 References

1. Tashiro, Y.; Takemura, A.; Fujii, H.; Takahira, K.; Nakanishi, Y., Livestock wastes as a source of estrogens and their effects on wildlife of Manko tidal flat, Okinawa. *Mar. Pollut. Bull.* **2003,** 47, (1-6), 143-147.

2. Ingerslev, F.; Vaclavik, E.; Halling-Sorensen, B., Pharmaceuticals and personal care products: A source of endocrine disruption in the environment? *Pure Appl. Chem.* **2003,** 75, (11-12), 1881-1893.

3. Penalver, A.; Pocurull, E.; Borrull, F.; Marce, R. M., Method based on solid-phase microextraction-high-performance liquid chromatography with UV and electrochemical detection to determine estrogenic compounds in water samples. *J. Chromatogr. A* **2002,** 964, (1-2), 153-160.

4. Johnson, A. C.; Sumpter, J. P., Removal of Endocrine-Disrupting Chemicals in Activated Sludge Treatment Works. *Environ. Sci. Technol.* **2001,** 35, (24), 4697-4703.

5. Zhu, L.; Chen, L.; Xu, X., Application of a molecularly imprinted polymer for the effective recognition of different anti-epidermal growth factor receptor inhibitors. *Anal. Chem.* **2003,** 75, (23), 6381-6387.

6. Ramstroem, O.; Ye, L.; Mosbach, K., Artificial antibodies to corticosteroids prepared by molecular imprinting. *Chem. Biol.* **1996,** 3, (6), 471-477.

7. Kempe, M.; Mosbach, K., Separation of amino acids, peptides and proteins on molecularly imprinted stationary phases. *J. Chromatogr., A* **1995,** 691, 317-323.

8. Haginaka, J.; Sanbe, H., Uniformly sized molecularly imprinted polymer for (S)-naproxen. Retention and molecular recognition properties in aqueous mobile phase. *J. Chromatogr., A* **2001,** 913, 141-146.

9. Watabe, Y.; Hosoya, K.; Tanaka, N.; Kubo, T.; Kondo, T.; Morita, M., Novel surface modified molecularly imprinted polymer focused on the removal of interference in environmental water samples for chromatographic determination. *J. Chromatogr., A* **2005,** 1073, 363-370.

10. Sellergren, B., Direct Drug Determination by Selective Sample Enrichment on an Imprinted Polymer. *Anal. Chem.* **1994,** 66, (9), 1578-1582.

11. Muldoon, M. T.; Stanker, L. H., Molecularly Imprinted Solid Phase Extraction of Atrazine from Beef Liver Extracts. *Anal. Chem.* **1997,** 69, (5), 803-808.

12. Stroink, T.; Paarlberg, E.; Waterval, J. C.; Bult, A.; Underberg, W. J., On-line sample preconcentration in capillary electrophoresis, focused on the determination of proteins and peptides. *Electrophoresis* **2001,** 22, (12), 2375-83.

13. Zhu, Q.-Z.; Degelmann, P.; Niessner, R.; Knopp, D., Selective trace analysis of sulfonylurea herbicides in water and soil samples based on solid-phase extraction using a molecularly imprinted polymer. *Environ. Sci. Technol.* **2002,** 36, (24), 5411-5420.

14. Molinelli, A.; Weiss, R.; Mizaikoff, B., Advanced Solid Phase Extraction Using Molecularly Imprinted Polymers for the Determination of Quercetin in Red Wine. *J. Agric. Food Chem.* **2002,** 50, (7), 1804-1808.

15. Caro, E.; Marce, R. M.; Cormack, P. A. G.; Sherrington, D. C.; Borrull, F., On-line solid-phase extraction with molecularly imprinted polymers to selectively extract substituted 4-chlorophenols and 4-nitrophenol from water. *J. Chromatogr., A* **2003,** 995, (1-2), 233-238.

16. Zhu, X.; Yang, J.; Su, Q.; Cai, J.; Gao, Y., Selective solid-phase extraction using molecularly imprinted polymer for the analysis of polar organophosphorus pesticides in water and soil samples. *J. Chromatogr., A* **2005,** 1092, (2), 161-169.

17. Perez-Moral, N.; Mayes, A. G., Direct rapid synthesis of MIP beads in SPE cartridges. *Biosens. Bioelectron.* **2006,** 21, (9), 1798-1803.

18. Vidyasankar, S.; Ru, M.; Arnold, F. H., Molecularly imprinted ligand-exchange adsorbents for the chiral separation of underivatized amino acids. *J. Chromatogr., A* **1997,** 775, 51-63.

19. Hennion, M.-C.; Pichon, V., Immuno-based sample preparation for trace analysis. *J. Chromatogr., A* **2003,** 1000, 29-52.

20. Wei, S.; Molinelli, A.; Mizaikoff, B., Molecularly imprinted micro and nanospheres for the selective recognition of 17b-estradiol. *Biosens. Bioelectron.* **2006,** 21, (10), 1943-1951.

21. Funke, W.; Okay, O.; Joos-Muller, B., Microgels-intramolecularly crosslinked macromolecules with a globular structure. *Adv. Polym. Sci.* **1998,** 136, (Microencapsulation, Microgels, Iniferters), 138-234.

22. Li, W.-H.; Stover, H. D. H., Porous monodisperse poly(divinylbenzene) microspheres by precipitation polymerization. *J. Polym. Sci. Pol. Chem.* **1998,** 36, (10), 1543-1551.

23. Molinelli, A., Ph.D. Thesis. **2004**.

24. Li, J.; Masso, J. J.; Guertin, J. A., Prediction of drug solubility in an acrylate adhesive based on the drug–polymer interaction parameter and drug solubility in acetonitrile *J. Control. Release* **2002,** 83, 211-221.

25. Kempe, M., Antibody-Mimicking Polymers as Chiral Stationary Phases in HPLC. *Anal. Chem.* **1996,** 68, (11), 1948-1953.

26. Rachkov, A.; McNiven, S.; El'skaya, A.; Yano, K.; Karube, I., Fluorescence detection of estradiol using a molecularly imprinted polymer. *Anal. Chim. Acta* **2000,** 405, 23-29.

27. Ye, L.; Weiss, R.; Mosbach, K., Synthesis and Characterization of Molecularly Imprinted Microspheres. *Macromolecules* **2000,** 33, (22), 8239-8245.

28. Sanbe, H.; Haginaka, J., Uniformly sized molecularly imprinted polymers for bisphenol A and b-estradiol: retention and molecular recognition properties in hydro-organic mobile phases. *J. Pharm. Biomed. Anal.* **2003,** 30, (6), 1835-1844.

29. Piscopo, L.; Prandi, C.; Coppa, M.; Sparnacci, K.; Laus, M.; Lagana, A.; Curini, R.; D'Ascenzo, G., Uniformly sized molecularly imprinted polymers (MIPs) for 17b-estradiol. *Macromol. Chem. Phys.* **2002,** 203, (10/11), 1532-1538.

30. Ni, H.; Kawaguchi, H., Mechanism of preparing monodispersed poly(acrylamide/methacrylic acid) microspheres in ethanol. II. *J. Polym. Sci., Part A: Polym. Chem.* **2004,** 42, (11), 2833-2844.

31. Downey, J. S.; Frank, R. S.; Li, W.-H.; Stoever, H. D. H., Growth Mechanism of Poly(divinylbenzene) Microspheres in Precipitation Polymerization. *Macromolecules* **1999,** 32, (9), 2838-2844.

32. Sellergren, B., Molecularly Imprinted Polymers: Man-Made Mimics of Antibodies and Their Applications in Analytical Chemistry. Amsterdam, Elsevier.: 2001; Vol. 5, p 42.

33. Ye, L.; Yu, Y.; Mosbach, K., Towards the development of molecularly imprinted artificial receptors for the screening of estrogenic chemicals. *Analyst* **2001,** 126, (6), 760-765.

34. Mayes, A. G.; Mosbach, K., Molecularly Imprinted Polymer Beads: Suspension Polymerization Using a Liquid Perfluorocarbon as the Dispersing Phase. *Anal. Chem.* **1996,** 68, (21), 3769-3774.

3.2 The Recognition Properties of MIPs

3.2.1 Introduction

In section 3.1, MIP particles with dimensions ranging from 3 to 5 μm were synthesized by precipitation polymerization[1]. Smaller particles (< 1 μm) with narrow size distribution have also been prepared by precipitation polymerization with a lower amount of cross-linker. Aiming at optimizing the experimental conditions for the various applications of the synthesized MIPs, the binding site properties of spherical particles and particular bulk polymers were evaluated during equilibrium binding studies, non-equilibrium binding studies, and release studies.

Improving and thoroughly characterizing the binding properties of MIPs should be an essential component toward next-generation MIP technology. Batch rebinding studies are characterization methods providing first insight into the binding properties of a specific MIP. The most common approach for estimating the binding parameters is to assume a bimodal distribution of binding sites with the binding parameters derived from a Scatchard plot[2-4], where the binding data can be linearly transformed according to the Scatchard equation[5]

$$B/F = (B_{max} - B)/K_D, \quad (1)$$

where B and F are the bound analyte and free analyte, respectively; K_D is an equilibrium dissociation constant and B_{max} is an apparent maximum number of binding sites. When B/F is plotted versus B, K_D and B_{max} can be estimated from the slope and the intercept, respectively. Matsui *et al.*[3] reported on two distinct sections within the plot, which can be

regarded as straight lines assuming that the binding sites can be classified into two distinct groups with specific binding properties. Thereby, two binding affinity constants are obtained from the fitting parameters. However, MIPs are commonly characterized by low average binding affinities, and a high degree of binding site heterogeneity[6]. The degree of heterogeneity is of particular importance for MIP applications in separation techniques, and is a main source of chromatographic peak asymmetry and peak tailing in the resulting chromatograms[7]. Furthermore, binding site heterogeneity is among the main parameters responsible for cross-reactivity in sensing[8] and catalysis[9] applications. Consequently, in this thesis a more universal approach based on the Freundlich isotherm[10] is applied to characterize the binding site heterogeneity, thereby providing a more generic model for MIP materials.

In the present thesis, this strategy was adapted for comparing the binding parameters between different imprinted polymer formats. Furthermore, these results are complemented by pore size and surface area studies at the synthesized imprinted polymer materials, as provided by Brunauer-Emmett-Teller (BET) analysis[1, 11, 12]. Finally, these comprehensive investigations enabled correlating the obtained porosities for different imprinted polymer formats (particulates, microspheres, and nanospheres) with differences observed during rebinding studies, which have not been reported in such a comprehensive format to date.

3.2.2 Experimental section

3.2.2.1 BET analysis of MIPs

The porosity and surface area of the developed micro-/nanospheres and bulk polymers was investigated by nitrogen adsorption/desorption analysis using a nitrogen

surface area analyzer (SA3100, Beckman Coulter, Hialeah, FL). A defined amount of MIP or control polymer (0.03 g) was degassed at 100 ºC for a period of 4 h prior to analysis removing adsorbed gases and moisture.

3.2.2.2 The rebinding properties of MIPs

3.2.2.2.1 Equilibrium binding

Ten different solutions of E2 in acetonitrile spanning a concentration range of 0.01-2 mM were prepared. An aliquot of 1 mL of each solution was added to 20 mg of polymer in 1.5 mL polypropylene centrifuge tubes. The tubes were shaken for 24 h and centrifuged at 9045 g for 15 min using a VWR Galaxy 16 DH centrifuge. UV measurements were taken at 280 nm on the supernatants using an HPLC system with a reverse phase column (Kromasil, C18) to quantify the concentration of free E2 (F). The eluent was acetonitrile/water (77:23). The amount of bound E2 (B) was calculated by subtracting F from the initial E2 concentration. Experimental binding isotherms were analyzed using the FIAD method. The experimentally obtained data were plotted in log B vs. log F format, and a Freundlich isotherm was fitted to the log plot of the experimental adsorption isotherms using the solver function in Microsoft Excel. The coefficient of determination (R^2) was optimized by variation of the fitting parameters (a, m). Finally, an affinity distribution was calculated by inserting the parameters m and a into eq. 2 (Chapter 2). The affinity range is determined by the minimum (F_{min}) and maximum (F_{max}) free concentration of the experimental binding isotherm.

3.2.2.2.2 Non-equilibrium binding

The polymer particles (100 mg) were packed in an empty solid-phase extraction cartridge. Polyethylene frits (Argonaut Technologies, Foster City, CA) were placed at both ends. Prior to and between uses, the cartridges were conditioned successively with 20 mL of methanol containing 15 % of acetic acid, 20 mL of methanol, 20 mL of acetonitrile, and 20 mL of de-ionized water. 1 mL of E2 solution with a concentration ranging from 10 μM to 2 mM in acetonitrile was loaded onto the cartridge, and the polymer was washed with 0.6 mL of acetonitrile to remove and E2 that has non-specifically bound to the polymeric matrix. Then, vacuum was applied for 30 min to dry the cartridges. Finally, the analytes were quantitatively eluted with 1.5 mL of methanol. The obtained fraction was evaporated to dryness and re-dissolved in 0.5 mL of acetonitrile:water (77:23). The loading, washing, and eluting steps were performed at a constant flow rate of 2.5 mL/min. The analyte concentrations in the final fraction, which represent the amount of analyte specifically bound to the polymer (*B*), were determined by HPLC-UV analysis as described in section 3.2.2.2.1. The amount of unbound analyte (*F*) was obtained by subtracting *B* from that of initial analyte concentration of the samples loaded onto the polymers.

3.2.2.2.3 Polymer-estradiol dissociation kinetics

The polymer particles (30 mg) were incubated with 2 mL of 2 mM E2 solution for 24 h. Unbound E2 was separated from the polymer material by locating the polymer solutions in empty SPE cartridges, in which the polymers were dried by passing through dry air for 20 min. In the following, 2 mL of fresh acetonitrile was incubated with the bound polymer particles. The polymer solution was centrifuged at 3120 g for 5 min,

0.6 mL of upper solution was sampled, and the amount of E2 released from the imprinted polymer matrices was determined during time-resolved release experiments quantified by HPLC-UV analysis as described in section 3.2.2.2.1.

3.2.3 Results and discussion

3.2.3.1 The influence of the porosity of MIPs on their recognition properties

The porosities of the developed micro-/nanospheres and particulate bulk polymers were determined by nitrogen adsorption/desorption analysis of Brunauer-Emmett-Teller (BET) multi-point adsorption isotherms (Figure 3.8).

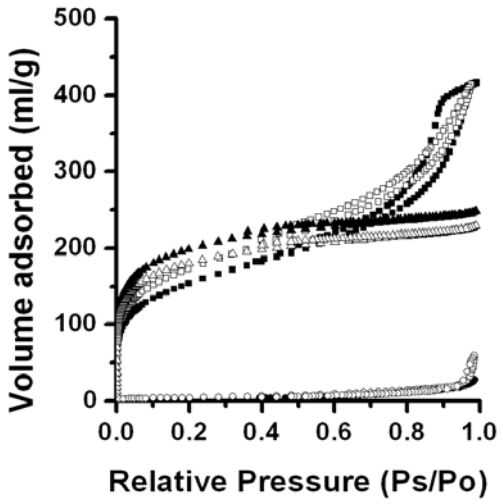

Figure 3.8 Nitrogen adsorption BET isotherms of imprinted nanospheres (●), control nanospheres (○), imprinted microspheres (▲), control microspheres (Δ), particulate bulk imprinted polymer (■), and particulate bulk control polymer (□).

Table 3.4 summarizes the pore volume and specific surface area of the polymer particles derived from the results in Figure 3.8. It is clearly evident that nanospheres are

characterized by a much smaller pore volume and surface area, as compared to bulk polymers and microspheres. The huge difference in porosity between the poly(MAA-co-DVB) (bulk and microspheres) and the poly(MAA-co-EDMA) (nanospheres) is likely due to the reduced effective cross-linker level[13]. Given the low surface area, the amount of gas adsorbed onto nanospheres is relatively low. For the adsorption isotherms recorded at microspheres, small pores apparently slow down the diffusion of gas molecules into the material. The shape of the adsorption isotherm of the particulate bulk polymers indicates that the sorbent is dominated by a mesoporous structure[14].

Table 3.4 Results of BET analysis for molecularly imprinted and control polymers prepared as bulk material, microspheres and nanospheres.

Sample	ESTR1	ESTR2	ESTR3	ESTR4	ESTR5	ESTR6
Size	Bulk	Bulk	3 μm	3 μm	400 nm	400 nm
Total Pore volume ($mL\ g^{-1}$)	0.639	0.689	0.382	0.352	0.038	0.071
BET surface area ($m^2\ g^{-1}$)	552.890	621.160	706.980	639.870	10.298	14.977
Micropore volume ($mL\ g^{-1}$)	0.053	0.067	0.137	0.130	-*	-*
Micropore specific surface area ($m^2\ g^{-1}$)	131.402	163.917	320.040	301.378	-*	-*

*At pore diameters of 7 to 20 Å the micropore volume and specific surface area is not detectable by gas adsorption measurements.

The pore size and surface area are of particular importance for the application of MIPs as stationary phase materials. As shown by Quaglia *et al.*[15], the porosity of the MIP

significantly affects the stationary phase performance in HPLC experiments. Schmidt *et al.*[16] studied the ability of MIP films to rebind target analytes as function of the concentration and molecular weight of the polymer porogen. Figure 3.9 A shows the pore size distribution of the developed microspheres and particulate bulk polymers. The pore size distribution of the synthesized microspheres (Figure 3.9 A, red) reveals that the pore dimensions predominantly cluster in the range of 3.2–5.8 nm, which is too small for efficient diffusion of the E2 molecule. As for HPLC stationary phase, the absence of micro- and meso-pores is very important to provide adequate column efficiency. In arbitrary classification, micro-pores have diameter less than 10 Å, while meso-pores correspond to diameters less than 50 Å. Most of the analyte molecules could not penetrate into micropores, and molecular diffusion into meso-pores is restricted, which significantly reduces or at least slows down mass transfer, and thereby decreases the column efficiency[17]. In addition, the synthesized bulk polymers (Figure 3.9 A, black) cluster more in the range of 10.0-18.7 nm compared to the microspheres. It can be seen from Table 3.4 that the total pore volume of the bulk polymer is higher than that of the microspheres, so it can be concluded that the bulk polymer has much more pores in the range of 10.0-18.7 nm compared to the microspheres. The particle size of the nanospheres is not suitable for conventional HPLC analysis, hence, the performance of nanospheres in HPLC is not discussed here. In general, for sufficient retention and acceptable peak shapes pore sizes in the range of 100-180 Å[18] (i.e., 10-18 nm) is the preferred choice for HPLC analysis of small molecules and biomolecules, also suggesting that the synthesized imprinted bulk polymer is more suitable as HPLC stationary phase.

In addition, the synthesized bulk polymer shows another cluster in the range of 18.7-77.7 nm, which ensure the rapid elution of the analyte from the stationary phase.

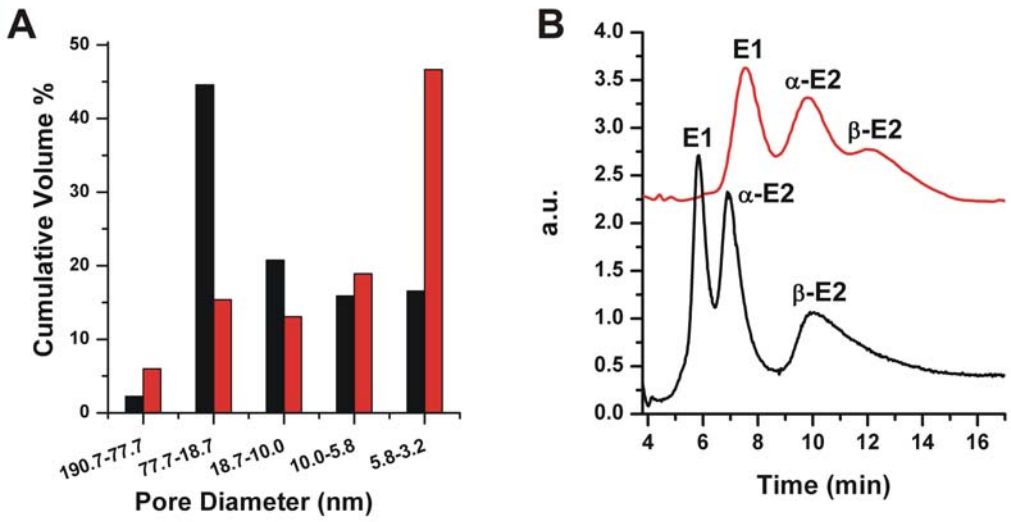

Figure 3.9 (A) Pore sized distribution of particulate bulk imprinted polymer (black), imprinted microspheres (red). (B) Chromatographic separation of E1 (peak 1), 17α-E2 (peak 2) and E2 (peak 3) using the particulate bulk imprinted polymer (red) and the imprinted microspheres (black) as the stationary phase. Acetonitrile containing 0.5% acetic acid was used as the mobile phase at a flow rate of 0.6 ml/min. Analytes were monitored at 280 nm.

Figure 3.9 B shows the chromatographic separation of E1, 17α-E2, and E2 using the bulk imprinted polymer and the imprinted microspheres as stationary phase. On the bulk imprinted polymer, all analytes are subject to rapid elution and complete separation. The small pores (less than 6 nm) of the imprinted microspheres show excellent retention properties for the target analytes, however, the separation of 3 structurally related compounds is inadequate due to slow elution. These findings indicate that the application of MIPs as stationary phase materials should thoroughly consider the pore size distribution within the MIP material for obtaining the desired HPLC performance.

3.2.3.2 The rebinding properties of MIPs

3.2.3.2.1 Equilibrium Binding Studies

For equilibrium binding assays, fixed amounts of imprinted polymers (20 mg) were incubated with different concentrations of E2 in acetonitrile. After 24 h, the supernatant solutions were separated by centrifugation, and the amount of E2 was determined by reversed phase HPLC. Binding isotherms were derived from the amounts of E2 bound to the imprinted polymer material by plotting against the initial concentration of the incubation solution. All equilibrium binding isotherms obtained from imprinted polymers were characterized by linear *log-log* binding relationships. It is also evident that significantly less E2 is bound to the corresponding control polymers (Figure 3.10).

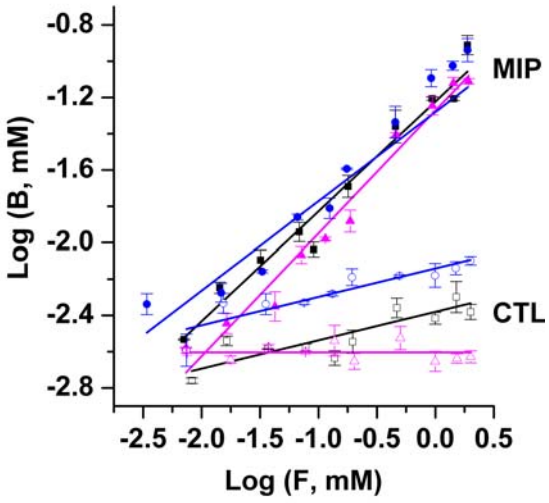

Figure 3.10 Equilibrium binding isotherms for imprinted particulate bulk polymer (■), microspheres (▲), and sub-microspheres (●), as well as control particulate bulk polymer (□), microspheres (Δ), and nanospheres (○) in *log-log* format. (■, ▲, ●, □, Δ, ○ represent the experimental data; lines are Freundlich fitting functions).

Furthermore, the control microspheres (Δ) absorbed less E2 than the controls for the particulate material, and for the nanospheres. This result indicates that there is less non-specific rebinding to the MIP microsphere material, which may result from the formation of porous microspheres with a large number of micropores, thereby reducing the binding site accessibility.

Besides the mechanical forces incident at the bulk material during grinding, the preparation strategy for the bulk polymers and the microspheres were very similar (i.e., similar type of functional monomer and cross-linker, and similar ratio template:functional monomer:cross-linker), and should therefore yield comparable results during binding studies. The experimental data for MIP particles resulting from the bulk polymer, and the microsphere data fits well to the Freundlich model. The goodness of the fit (R^2 value) is used as quantitative descriptor for characterizing the difference between the model and the experimental data following

$$R^2 = 1- \{sum\ [(log\ B-log\ aF^m)^2]/sum[(log\ B-average\ log\ B)^2]\}. \quad (2)$$

The fitting data for the affinity constants and heterogeneity indices are provided in Table 3.5. The obtained R^2 value for the particulate imprinted polymer is 0.969, and 0.973 for the imprinted microspheres, respectively. Following the binding isotherm, it is evident that the microsphere MIP is characterized by a higher median binding affinity constant ($1.3\times10^{-2} \pm 4.8\times10^{-4}$ mM^{-1}), than the particulate MIP generated from bulk polymer synthesis ($9.0\times10^{-3} \pm 5.3\times10^{-4}$ mM^{-1}). Moreover, the microspheres appear more homogeneous than bulk polymer particles, as derived by comparing their heterogeneity indices (0.676 for microspheres and 0.605 for bulk polymer, respectively). The imprinted

nanospheres were prepared with EDMA as cross-linker using a reduced ratio for the cross-linker in the pre-polymerization solution. The equilibrium binding studies reveal a lower median binding affinity constant (0.0025 mM^{-1}) and heterogeneity index (0.492), which indicates that the binding sites provide by imprinted nanospheres have a lower affinity and a higher heterogeneity in comparison to binding sites available in microspheres and particles generated from bulk polymer.

Table 3.5 Freundlich fitting parameters for the investigated imprinted and control polymers.

Fitting Data	Bulk MIP	Bulk Control	Microspheres MIP	Microspheres Control	nanospheres MIP	nanospheres Control
a (STD)*	0.060 (0.003)	0.0042 (NM)**	0.053 (0.002)	- (NM)**	0.052 (0.004)	0.0072 (NM)**
m (STD)*	0.606 (0.001)	0.157 (NM)**	0.673 (0.004)	- (NM)**	0.492 (0.008)	0.157 (NM)**
R^2	0.969 (0.021)	0.693 (NM)**	0.973 (0.023)	- (NM)**	0.940 (0.053)	0.811 (NM)**
K_0 (mM^{-1})	0.010 (0.00053)	7.3E-16 (NM)**	0.013 (0.00048)	-	0.0025 (0.00045)	2.3E-14 (NM)**

(STD)*: Standard deviation

(NM)**: Not measured

The corresponding control polymers for each synthetic route were analyzed by precisely the same equilibrium binding procedure. The heterogeneity index (Table 3.5) reveals that the control polymers are generally more heterogeneous than the imprinted polymers, which is in contrast to results reported by Rampey *et al*[10]. In their studies, the

imprinted polymers appear more heterogeneous than the control polymers. This circumstance confirms the importance of thorough analytical studies for each MIP approach, as templated materials prepared by different synthetic routes and for different templates apparently yield different results. Moreover, the binding results also indicate that the control polymers have very small binding affinities, with only minimal fluctuations (ranging from 1.7×10^{-3} to 4.1×10^{-3} mM), if the initial concentration of the binding solution changes from 0.01 to 2 mM. This indicates that the control polymers are saturated within this concentration range. The experimental data obtained for the control polymers does not fit well to a Freundlich binding isotherms, as indicated by a R^2 value < 0.9. This result is consistent with the expected deviation of the experimental binding isotherm from the Freundlich model at higher analyte-to-polymer ratios, as this model is only valid at low concentrations or at sub-saturation levels[10, 19].

Based on the studies reported in this thesis, we infer a correlation between the binding site properties derived from the Freundlich model based on equilibrium binding assays, and the porosities of the imprinted materials, which has not been reported to date. Interestingly, Figure 3.11 shows that the binding site distribution generated within differently synthesized materials is apparently quite similar. If the specific binding sites are predominantly located at the surface of the imprinted materials, it is expected that there are less specific binding sites available at particles with smaller pore volume and surface area given similar distribution of the binding sites, as confirmed by the equilibrium binding isotherm studies.

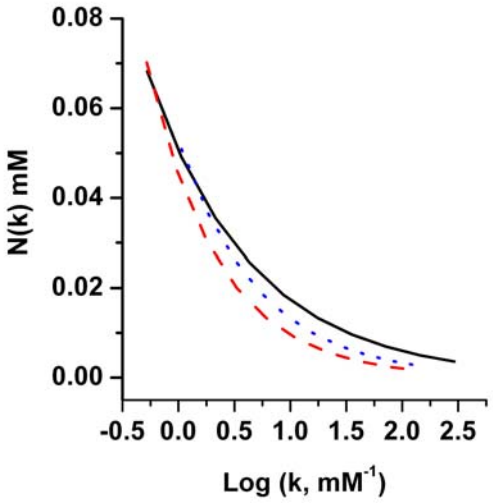

Figure 3.11 Affinity distribution of sub-microspheres (black solid line), microspheres (red dashed line), and particulate bulk polymer (blue dotted line).

To support this hypothesis, the binding affinity constants of the imprinted polymers were compared. As expected, nanospheres provide a lower median binding affinity constant ($2.5\times10^{-3} \pm 4.5\times10^{-4}$ mM^{-1}) than bulk polymers ($9.0\times10^{-3} \pm 5.3\times10^{-4}$ mM^{-1}), and than microspheres ($1.3\times10^{-2} \pm 4.8\times10^{-4}$ mM^{-1}), as derived from the fitting parameters of the Freundlich isotherm. Accordingly, the surface areas of these imprinted particles can be ranked by increasing surface area as nanospheres (10.30 m^2/g), particulates generated from bulk polymers (552.89 m^2/g), and microspheres (706.98 m^2/g), which is consistent with the hypothesis that less specific binding sites are available at particles with smaller surface area considering the binding site distributions are similar. As much less cross linker was used during the synthesis of the templated nanosphere materials, these results suggest that the concentration of the cross linker is crucial to the pore structure of imprinted polymer materials, and to their binding site distribution. With decreasing amounts of cross-linker, apparently less pore volume was created during the

polymerization process. However, it is essential to provide sufficient fractions of cross-linker for maintaining the integrity of the generated binding sites. These findings clearly confirm that optimizing the fraction of cross-linker is essential for maintaining the balance between sufficient rigidity of the material maintaining the structural integrity of binding sites, and sufficient porosity of the resulting polymer material during rational design of next-generation MIP technology.

3.2.3.2.2 Non-Equilibrium Binding Studies

The analysis of equilibrium binding isotherms provides useful information for binding assays, however, is of limited value for non-equilibrium applications of MIPs, such as chromatographic separations including HPLC and SPE. Hence, non-equilibrium binding isotherms have to be established for fully characterizing behavior of the templated material at these conditions. In this thesis, non-equilibrium binding analysis was performed using a molecularly imprinted solid phase extraction (MISPE) set-up. As the filters closing off SPE cartridges have a pore size of 10 µm ensuring rapid flow of solvent through the stationary phase material, only particulates generated from bulk polymers were tested in these experiments. 100 mg of polymer particles were packed into an empty SPE cartridge, and sequentially conditioned with methanol, water, and acetonitrile, respectively. In the following, different concentrations of E2 solutions were percolated through the MISPE cartridge.

E2 during the elution was considered the bound fraction (*B*), while the free concentration (*F*) was calculated by subtracting *B* from the initial E2 concentration in the sample solution. Figure 3.12 shows the Freundlich adsorption isotherms of these non-equilibrium binding experiments. It is evident that the Freundlich model does not fit the

observed binding behavior (R^2 = 0.924) with the same fidelity determined during equilibrium binding. In fact, the Freundlich model is usually used for equilibrium binding, although it is valid for covalent imprinted polymer in very few cases[20]. The specific binding model for non-equilibrium binding in SPE format is not reported. As a first approximation, information on the binding parameters was still derived from these fits. The median binding affinity constant determined during these non-equilibrium experiments (0.061 mM^{-1}) is higher than the affinity constant obtained from the equilibrium experiments (0.010 mM^{-1}). Also, the binding site distribution appears more homogeneous, as reflected in a heterogeneity index of m = 0.725.

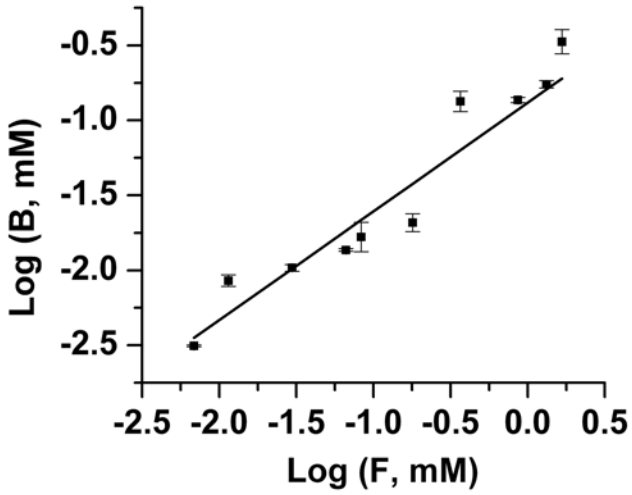

Figure 3.12 Non-equilibrium binding isotherms for particulate bulk imprinted polymer in log-log format.

A possible explanation for this difference in equilibrium vs. non-equilibrium binding is related to the observed binding kinetics. It is hypothesized that the high affinity binding sites are occupied first, followed by the low affinity binding sites. Hence, it is derived

that during non-equilibrium binding conditions a significant fraction of low affinity binding sites remains unoccupied, which explains the higher median binding affinity constant and the higher heterogeneity index derived from these experiments.

3.2.3.2.3 Release Studies

The kinetics of binding experiments were finally also studied by release experiments. The polymer materials, which have been equilibrated with E2, were incubated under shaking with fresh acetonitrile to release the re-bound template, and the released amount was temporally monitored. Figure 3.13 shows the release of E2 from imprinted particulate bulk polymer, microspheres, and nanospheres. There is little evident difference in release kinetics between different polymer particle dimensions at these conditions.

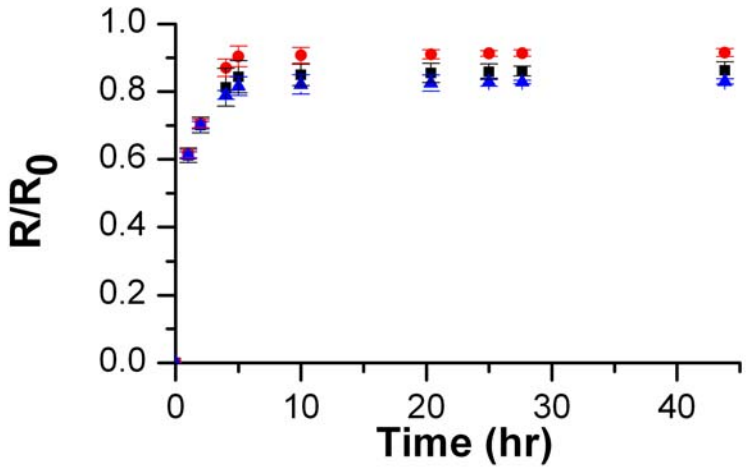

Figure 3.13 Percentage of released E2 (R/R_0) from microspheres (●), nanospheres (■), and particulate bulk polymer (▲).

The pseudo-second order kinetics equation was tested for all polymers considering the differential equation:

$$d[C]/dt = K (C_e-C_t)^2, \quad (3)$$

where C_e is the amount of E2 adsorbed at equilibrium, C_t is the amount of E2 adsorbed at time t and k is the equilibrium rate constant of pseudo-second order sorption. Integrating and applying the boundary conditions $t = 0$ and $t = t$ and $C_t = 0$ and $C_t = C_t$ Eq. (3):

$$t/Ct = 1/(K*C_e^2) + t/C_e. \quad (4)$$

Plotting of t/C_t vs. t allows the kinetics parameters k and C_e to be obtained directly from the intercept and slope, respectively. In Table 3.6 the pseudo-second order kinetic parameters of E2 binding to the imprinted microspheres. nanospheres and particulate bulk polymer are summarized. All the regression coefficients are higher than 0.998, suggests that E2 binding to the studied polymers follows the second-order kinetic model.

Table 3.6 Kinetic data for E2 binding to microspheres, nanospheres, and particulate bulk polymer.

polymer	K (g mmol^{-1} min^{-1})	Ce (mmol g^{-1})	R^2
Bulk polymer	0.6836	0.0213	0.9986
Microspheres	0.8346	0.0289	0.9996
Nanospheres	0.9084	0.0273	0.9995

Microspheres and nanospheres release minutely more E2 than bulk polymer particles, which may results from an increased mobility of the smaller spherical particles in solution providing more advantageous extraction conditions. Furthermore, it is evident for all materials that during the first 2 h, 70 % of E2 were released, which relates to target molecules that have been bound with lowest affinity to the polymer matrix. The more tightly bound molecules were released at a significantly longer timescale after continuous incubation, until complete extraction was achieved after ~ 40 h. From the calculation of binding site distribution (Figure 3.11), it is evident that the number of low affinity binding sites (K = 0.028 mM) is approx. 20-times higher than the number of high affinity binding sites (K = 2.13 mM) for particulates generated from bulk MIPs, which is consistent with the conclusion that there is a dominating amount of low affinity binding sites, as observed from the release experiment. As equal amounts of polymer and solvent were used for the kinetic studies at all MIP formats, it can be concluded that the binding site distribution for the three MIP particle formats studied here are comparable. This conclusion is supported by the results obtained during the equilibrium binding studies, which are shown in Figure 3.11, and confirm that the three types of particles have similar binding site affinity distributions during equilibrium binding.

3.2.4 Conclusions

In summary, a comparison of the specific binding properties of imprinted polymers for E2 prepared by different synthetic routes yielding particulates generated from bulk polymers, microspheres, and nanospheres was obtained. The relationships between the particle porosity and rebinding properties were detailed, providing useful guidelines for controlling the particle properties for the desired application including, SPE pre-

concentration, HPLC separations, and biomimetic binding assays. While microspheres prepared by precipitation polymerization revealed excellent rebinding properties at equilibrium binding conditions, it was also confirmed that the porosity of imprinted polymers plays an important role in their rebinding characteristics. Particulate polymer materials with larger surface area provide superior binding, if the binding site distribution is similar between several generate MIP formats. Furthermore, the importance of an optimized degree of cross-linking was confirmed for maintaining the balance between structural rigidity of the binding sites, and porosity of the resultant polymers. Exemplarily, it was shown that the application of MIPs as HPLC stationary phase material requires particle pore dimensions in the range of 100-180 Å for maintaining the desired retention properties at acceptable elution times, while significant amounts of small pores (<10 nm) would induce slow elution of the target analyte. While these particulate bulk imprinted polymers revealed excellent HPLC performance, their binding affinity was less compared to imprinted microspheres, as determined during equilibrium binding studies. In general, the performed release experiments and the derived binding site distribution revealed that all MIP formats are characterized by a majority of low affinity binding sites. Furthermore, it has been found that the rebinding properties of the synthesized materials are different at equilibrium vs. non-equilibrium conditions confirming that thorough analytical characterization of each MIP system is essential to the final application conditions. As the optimization of imprinted materials is based on fundamental understanding of the binding site properties, the investigations presented here will aid in establishing a more rational basis for further tailoring imprinted materials to the desired analytical application.

3.2.5 References

1. Wei, S.; Molinelli, A.; Mizaikoff, B., Molecularly imprinted micro and nanospheres for the selective recognition of 17b-estradiol. *Biosens. Bioelectron.* **2006,** 21, (10), 1943-1951.

2. Zhu, Q.-Z.; Haupt, K.; Knopp, D.; Niessner, R., Molecularly imprinted polymer for metsulfuron-methyl and its binding characteristics for sulfonylurea herbicides. *Anal. Chim. Acta* **2002,** 468, (2), 217-227.

3. Matsui, J.; Miyoshi, Y.; Doblhoff-Dier, O.; Takeuchi, T., A molecularly imprinted synthetic polymer receptor selective for atrazine. *Anal. Chem.* **1995,** 67, (23), 4404-4408.

4. Subat, M.; Borovik Andrew, S.; Konig, B., Synthetic creatinine receptor: imprinting of a Lewis acidic zinc(II)cyclen binding site to shape its molecular recognition selectivity. *J. Am. Chem. Soc.* **2004,** 126, (10), 3185-3190.

5. Yamamua, H. I.; Enna, S. J.; Kuhar, M. J., Neurotransmitter Receptor Binding. Raven Press: New York, 1985, Chapter 3.

6. Andersson, H. S.; Koch-Schmidt, A. C.; Ohlson, S.; Mosbach, K., Study of the nature of recognition in molecularly imprinted polymers. *J. Mol. Recognit.* **1996,** 9, (5-6), 675-82.

7. Sellergren, B.; Shea, K. J., *J. Chromatogr., A* **1995,** 690, 29-39.

8. Allender, C. J.; Brain, K. R.; Heard, C. M., Binding cross-reactivity of Boc-phenylalanine enantiomers on molecularly imprinted polymers. *Chirality* **1997,** 9, (3), 233-237.

9. Wulff, G., Enzyme-like Catalysis by Molecularly Imprinted Polymers. *Chem. Rev.* **2002,** 102, (1), 1-27.

10. Rampey, A. M.; Umpleby, R. J., II; Rushton, G. T.; Iseman, J. C.; Shah, R. N.; Shimizu, K. D., Characterization of the Imprint Effect and the Influence of Imprinting Conditions on Affinity, Capacity, and Heterogeneity in Molecularly Imprinted Polymers Using the Freundlich Isotherm-Affinity Distribution Analysis. *Anal. Chem.* **2004,** 76, (4), 1123-1133.

11. Piletsky, S. A.; Matuschewski, H.; Schedler, U.; Wilpert, A.; Piletska, E. V.; Thiele, T. A.; Ulbricht, M., Surface Functionalization of Porous Polypropylene Membranes with Molecularly Imprinted Polymers by Photograft Copolymerization in Water. *Macromolecules* **2000,** 33, (8), 3092-3098.

12. Karlsson, J. G.; Karlsson, B.; Andersson, L. I.; Nicholls, I. A., The roles of template complexation and ligand binding conditions on recognition in bupivacaine molecularly imprinted polymers. *Analyst* **2004,** 129, (5), 456-462.

13. Li, W.-H.; Li, K.; Stover, H. D. H., Monodisperse poly(chloromethylstyrene-co-divinylbenzene) microspheres by precipitation polymerization. *J. Polym. Sci. Pol. Chem.* **1999,** 37, (14), 2295-2303.

14. Sellergren, B., *Molecularly Imprinted Polymers: Man-Made Mimics of Antibodies and Their Applications in Analytical Chemistry (Techniques and Instrumentation in Analytical Chemistry, Vol. 23)*. Elsevier: Amsterdam ; New York, 2001; p 52.

15. Quaglia, M.; De Lorenzi, E.; Sulitzky, C.; Caccialanza, G.; Sellergren, B., Molecularly imprinted polymer films grafted from porous or nonporous silica: Novel affinity stationary phases in capillary electrochromatography. *Electrophoresis* **2003,** 24, (6), 952-957.

16. Schmidt, R. H.; Haupt, K., Molecularly Imprinted Polymer Films with Binding Properties Enhanced by the Reaction-Induced Phase Separation of a Sacrificial Polymeric Porogen. *Chem. Mat.* **2005,** 17, (5), 1007-1016.

17. Kazakevich, Y.; McNair, H., HPLC for Pharmaceutical scientists. Wiley: Hoboken, NJ, 2007, Chapter 3.

18. Bolisay, L. D. V.; March, J. F.; Bentley, W. E.; Kofinas, P., Separation of baculoviruses using molecularly imprinted polymer hydrogels. *Materials Research Society Symposium Proceedings* **2004,** 787, (Molecularly Imprinted Materials--2003), 29-33.

19. Rushton, G. T.; Karns, C. L.; Shimizu, K. D., A critical examination of the use of the Freundlich isotherm in characterizing molecularly imprinted polymers (MIPs). *Anal. Chim. Acta* **2005,** 528, (1), 107-113.

20. Gallego-Gallegos, M.; Munoz-Olivas, R.; Camara, C.; Mancheno, M. J.; Sierra, M. A., Synthesis of a pH dependent covalent imprinted polymer able to recognize organotin species. *Analyst* **2006,** 131, (1), 98-105.

3.3 Quantitative Environmental Analysis with MIPs

3.3.1 Introduction

Commonly applied detection methods for E2 usually require extensive sample clean-up procedures. A variety of analytical methods has been developed to determine the concentration level of estrogens in environmental waters by using solid phase extraction (SPE) and derivatization, followed by quantitative detection with gas chromatography coupled to mass spectrometry (GC-MS)[1-5] and GC-MS/MS[6-9], or – without derivatization - by LC-MS[10-12] and LC tandem MS (LC-MS/MS)[13-18]. A novel approach using molecularly imprinted polymers as highly selective separation and enrichment materials will therefore enable the development of high affinity, multiple use solid phase extraction cartridges for the pre-concentration of E2. Sample preparation using MIPs will allow avoiding time-consuming multi-step clean-up procedures, as well as costly immunoaffinity columns.

In this section, we discuss a cost-effective high-throughput analytical methodology for the determination of estrogens spiked into river water samples. An E2-imprinted polymer has been prepared and evaluated both for its use in liquid phase separations, and solid phase extraction of a group of estrogens including E2, 17α-E2, E1, E3, and EE2. In brief, the objectives of this work were (i) the development of analytical methodologies involving molecularly imprinted solid phase extraction (MISPE) for estrogens, (ii) the comparison of the MISPE elution selectivity and recovery with control polymers, as well as conventional sorbents such as C-18, and (iii) the application of the developed MISPE methodology to the analysis of spiked water samples by LC-TOF-MS operated in function-switching mode.

3.3.2 Experimental section

3.3.2.1 Chemicals

E2, 17α-E2, EE2, E1, E3, and 4-NP were purchased from Sigma-Aldrich (Milwaukee, WI), and used as supplied. The HPLC grade solvents acetonitrile, methanol, acetone acetic acid, and water were purchased from VWR International (Suwannee, GA).

3.3.2.2 MIP based solid phase extraction (MISPE)

3.3.2.2.1 Optimization of SPE conditions

Empty SPE cartridges (6 mL; Argonaut Technologies, Foster City, CA) were connected to a multicolumn vacuum manifold operated under negative pressure. 1 g or 500 mg of imprinted or control polymers were suspended in methanol and packed into the SPE cartridges. Polyethylene frits (Argonaut Technologies, Foster City, CA) were placed at both ends. Prior to and between uses, the MISPE cartridges were conditioned successively with 15 % (v/v) acetic acid/methanol (100 mL), methanol (100 mL), acetonitrile (100 mL) and de-ionized water (100 mL). In addition, the cartridges were pre-equilibrated with the loading solvent prior to loading the samples. Different protocols were applied (as described below), utilizing different solvents during loading, washing, and eluting the MISPE cartridge. All obtained fractions were collected and evaporated to dryness at room temperature under a stream of air. The residues were reconstituted in solution with 0.5 mL of mobile phase.

The experimental procedure for the evaluation of MISPE with aqueous standards is described as follows. To optimize the pH of the loading solution, 1 mL of phosphate buffer spiked with 5 mg L^{-1} of E2 (at pH = 8, pH = 8.5, and pH = 9) was loaded onto the

imprinted cartridge, as well as onto the control cartridge (containing either 1 g of MIP or control polymer, respectively). The selectivity of the MIP cartridge was investigated with a mixture of 4-NP, E1 and E2 (5 mg L^{-1} each) in phosphate buffer (pH = 8.5, 5 mM). The analytes were successively eluted from the SPE cartridges using 4×1 mL acetonitrile, 8×0.5 mL 2 % (v/v) acetic acid/acetonitrile and 8×0.5 mL 4 % (v/v) acetic acid/acetonitrile. Each elution fraction was then analyzed by reverse phase liquid chromatography with a Kromasil C-18 column.

River water samples were collected at Quarles plant intake from the Chattahoochee river, and stored at 4 ºC in a refrigerator room before use. After prefiltration through 0.5 μm glass fiber filters, the pH of the river water was adjusted to pH 8.5 with 5 mM phosphate. 500 mL river water samples were spiked with 25 ng of estrogens and preconcentrated with MISPE cartridges. The control polymer and commercially available C-18 cartridges (500 mg, 6 mL, Argonaut Technologies, Foster City, CA) were used for performance comparison. After the samples were loaded, vacuum was applied for 30 min to dry the cartridges. Natural organic matter (NOM) was eluted with 3 mL of acetonitrile, and then estrogens were eluted with 5 mL of methanol.

3.3.2.2.2 HPLC/LC-MS methods for SPE aliquots

Estrogens in each elution fraction were separated and quantified by reverse-phase liquid chromatography using gradient elution and analyte monitoring at 280 nm. The mobile phase was composed of HPLC grade water (containing 1 % (v/v) acetic acid and 0.5 g L^{-1} of KCl) as solvent A, and acetonitrile as solvent B. The flow rate was set at 1 mL/min and the gradient profile was 35 % B at 0 min, 47.5 % B at 10 min (held for

8 min), and 78.1 % B at 25 min. The mobile phase was returned to its initial composition in 5 min. The gradient profile was adapted from Peñalver *et al.*[19]

LC-TOF-MS measurements were performed with an Agilent 1100 system equipped with a solvent degasser, a binary pump, a thermostated column compartment (held at 25 °C), an autosampler, and a diode array detector. This instrument was interfaced to an AccuTOF orthogonal acceleration TOF MS (JEOL, Peabody, MA) via an orthogonal electrospray interface operating at -2 KV. The tune settings for the mass spectrometer ion source optics were switched at a frequency of 4 Hz between four different sets of parameters optimized for each of the estrogens. The optimized mass spectrometer ion source optics settings for E1, 17α-E2 and E2, E3, and EE2 were as follows: inlet orifice: -78, -85, -87, and -84 V; ring electrode: -12, -15, -13, and -12 V, second skimmer: -6, -5, -6, and -5 V, ion guide bias voltage: -27, -28, -27, and -28 V, ion guide peaks voltage:1376, 1330, 1422, and 1766 V, respectively. The nebulizing gas flow rate, the desolvation gas flow rate, the needle chamber temperature and the inlet orifice temperature were 1.0 L/min, 2.5 L/min, 250 °C, and 80 °C, respectively. The MCP detector was set to 2500 V. The TOF repeller extraction voltages were 777 V for the pusher and -777 V for the puller, respectively. The liner voltage was -7000 V and the reflectron voltage was 881 V, producing a mass resolution of R_{FWHM} = 6,000 or better.

The LC was operated at a flow rate of 200 μL min^{-1}, with an injection volume of 20 μL, and a gradient of 35 % to 41 % B for 0-5 min, which was held at 41 % B for 4 min (solvent B: acetonitrile:water 90:10, solvent A: acetonitrile:water 10:90). An Agilent Zorbax 300 Å 300 Extend C18 column of 2.1 mm i.d. and 150 mm length equipped with a pre-column was used in all experiments. Peak areas of mass selected chromatograms of

the $[M-H]^-$ ions with a 0.01 u window were used to construct external calibration curves for quantification and to compute analyte recoveries.

3.3.3 Results and discussion

3.3.3.1 MISPE of aqueous standards

To evaluate the feasibility of using MIP sorbents for SPE of real-world samples containing E2, several parameters were optimized during the SPE procedure. Five standard samples (E1, E2, 17α-E2, E3, EE2) were prepared in pH 8.5 phosphate buffer solution with concentrations ranging from 0.5 to 15 μg/mL to cover the analyte concentration range in the SPE samples. The pH of aqueous samples was adjusted to condition the MIP phase for maximum analyte affinity during the loading step. The MISPE cartridge revealed similar retainment for E2 with the loading solution at different pH levels from 8-9, with the majority of analyte eluted at 8.5 mL of elution solution (Figure 3.14A). In contrast, the elution from the control cartridge was strongly dependent on the pH of the loading solution (Figure 3.14B). Consequently, the MISPE cartridge appears to operate well in the pH range from 8-9, which broadens the available "optimization space" for analytical method development.

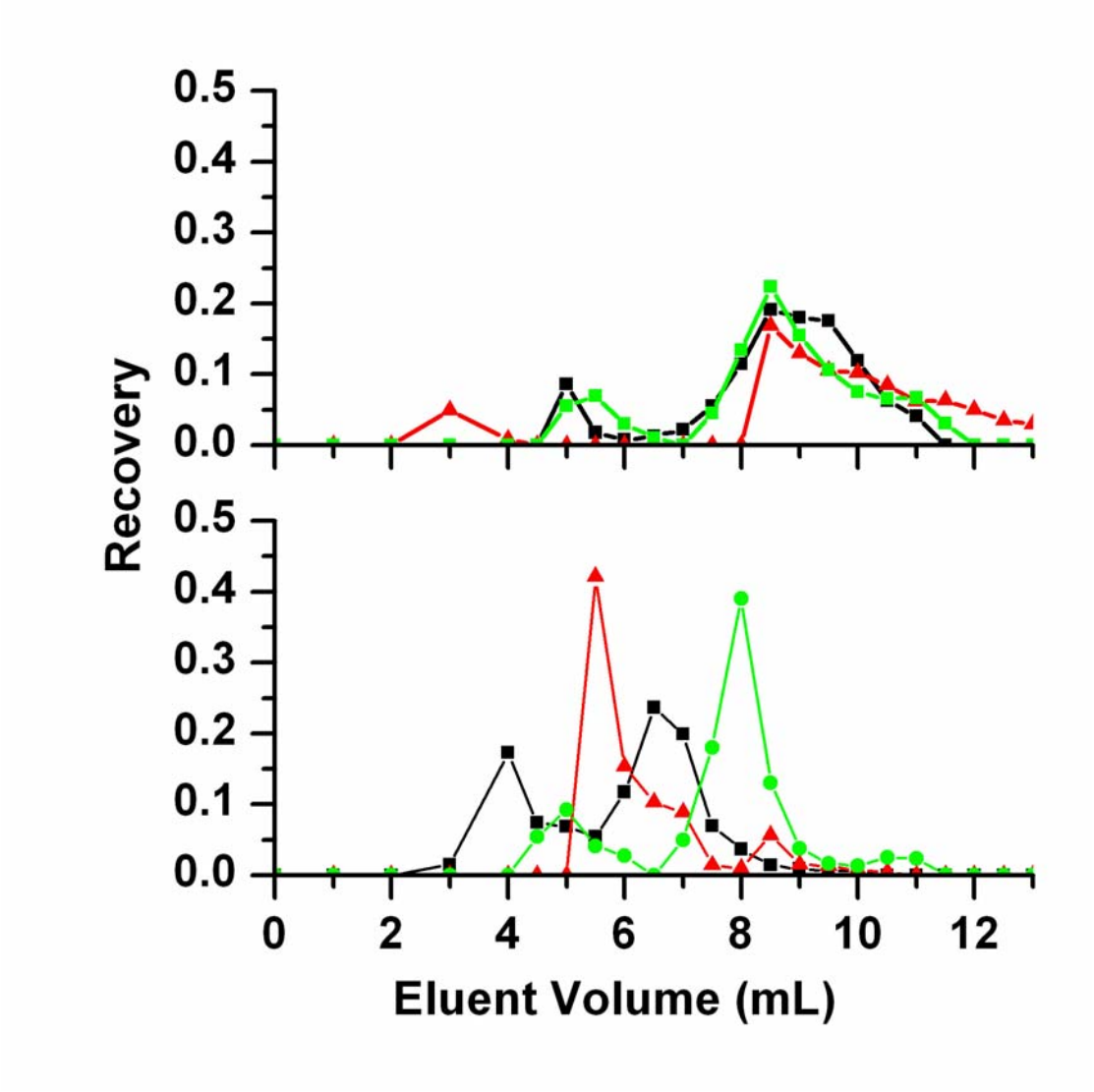

Figure 3.14 Elution of E2 from a MISPE cartridge (A), and a control cartridge (B) with a loading solution at pH = 8 (■), pH = 8.5 (▲), and pH = 9 (●).

During sample loading, the polymer sorbent is expected to operate in a reverse phase mode,[20] since estrogens, as well as other hydrophobic compounds were retained on the cartridges. After the cartridges were thoroughly dried, the elution step was optimized for samples delivered in phosphate buffer to achieve selective binding of E2 to the sorbent, whereas the undesired components were eluted from the cartridges. Acetonitrile (0 %,

2 %, 4 % acetic acid) was selected as eluting solvent, since the HPLC results have revealed that MIPs exhibit the most prominent molecular recognition for the template molecule in acetonitrile. First, most of 4-nitrophenol and estrone was eluted with 4 mL of acetonitrile, followed by E2 and the remaining E1 eluted with 4 mL acetonitrile containing 2 % of acetic acid. Finally, to achieve full recovery of E2, 4 mL acetonitrile containing 4 % of acetic acid was used as eluting solvent. Comparing the elution results obtained from a MIP (Figure 3.15, left A) and a control SPE cartridge (Figure 3.15, left B), a significantly higher affinity of the MIP cartridge for E2 was found. While the affinities of the MIP cartridge to 4-NP and E1 are low, and similar to the affinities of the control cartridge (see also Figure 3.15, left A and B: the maximum elution concentration of 4-nitrophenol and estrone are in the elution fraction after 4 mL acetonitrile washing step). Elution curves (Figure 3.15, right) facilitate the evaluation of the total extraction performance of an SPE sorbent, however, representing the combined contributions of both specific and non-specific interactions. The recoveries from both MIP and control cartridges for all investigated analytes are approximate 90 %. Therefore, the loading and eluting conditions optimized in this study provide an efficient and effective extraction strategy for water samples spiked with estrogens. In order to achieve rapid and complete recovery of E2 during MISPE for real-world samples, methanol was used as eluting solvent after the acetonitrile washing step.

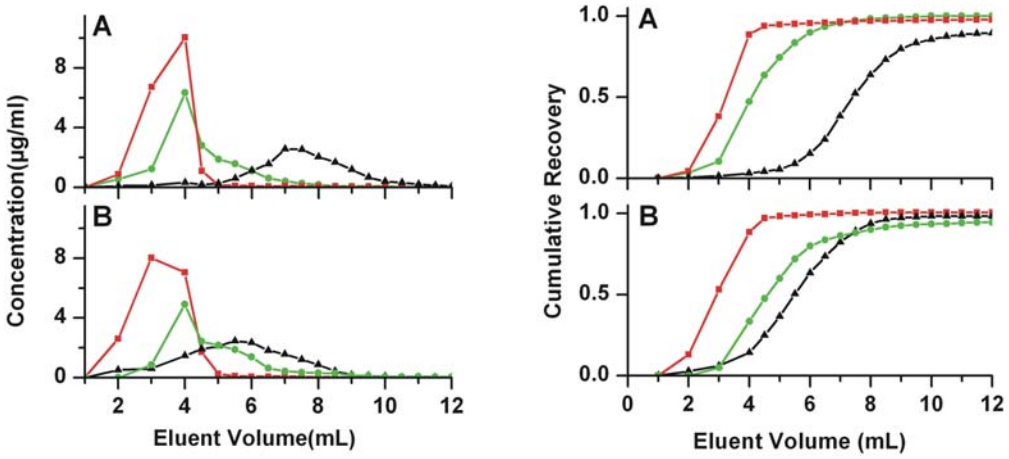

Figure 3.15 (left) Elution of 4-NP (■), E1 (●), and E2 (▲) from a MISPE cartridge (A), and a control SPE cartridge (B). The concentration indicates the amount of analyte recovered from the elution. (right) Recoveries of 4-NP (■), E1 (●), and E2 (▲) from a MISPE cartridge (A), and a control polymer SPE cartridge (B).

3.3.3.2 SPE of spiked river water samples

In order to test the performance of MISPE with real-world samples, 0.8 μg of estrogens were spiked into 500 mL river water samples. To simplify the extraction process, a two step elution procedure was developed for MISPE to separate the estrogens from interferences. In a first step, 3 mL of acetonitrile are applied as washing solvent, which removes interferences but retains the estrogens in the cartridge. The MIP sorbent has a high affinity to estrogens in the presence of acetonitrile, as previously shown during the HPLC characterization of MIPs and MISPE for aqueous standards. In a second step, the estrogens are eluted from the cartridge with 5 mL of MeOH for rapid and complete elution.

During initial MISPE experiments, it was noticed that river water samples spiked with very low levels of estrogens (< 10 ng/L) were affected by leaching of the template

molecule during elution resulting in elevated blank values. In order to minimize template leaching effect during MISPE, a comprehensive post-synthesis MIP extraction procedure was developed, which is also applied prior to MISPE applications. This procedure comprises three steps: (i) the fresh made polymer was packed into a HPLC column and washed with 15 % HAc/MeOH for 24 h; (ii) the polymer was unpacked from the HPLC column and a MIP batch was washed by incubation of 1 g of polymer particles with 200 mL methanol twice for 12 h, followed by decantation and separation of the phases; (iii) the polymer was packed into the SPE cartridge and conditioned with 15 % HAc/MeOH, MeOH, MeCN, and water, respectively. In this procedure, the template washings were performed in both eluting mode and equilibrated releasing mode. To confirm that template leaching did not significantly contribute to the recovery experiments, control experiments were performed extracting from blank river water using an identical MISPE cartridge. No estrogen peaks were detected from both the washing and the elution step (data not shown). Following this careful washing procedure, we have confirmed that template leaching does not significantly contribute to the signal at 50 ng/L estrogen levels. From total ion chromatograms (TIC) and selected ion spectrometry of the SPE samples from MIP (Figure 3.16a), control polymer (Figure 3.16b), and C18 (Figure 3.16c) it is evident that the interferences were significantly reduced after the MISPE (see TIC). Moreover, the insert showing the selected ion chromatograms (271 is the $[M-H]^-$ peak of E2) indicates that the MIP sorbent shows enhanced selectivity toward E2 in comparison to the control polymer.

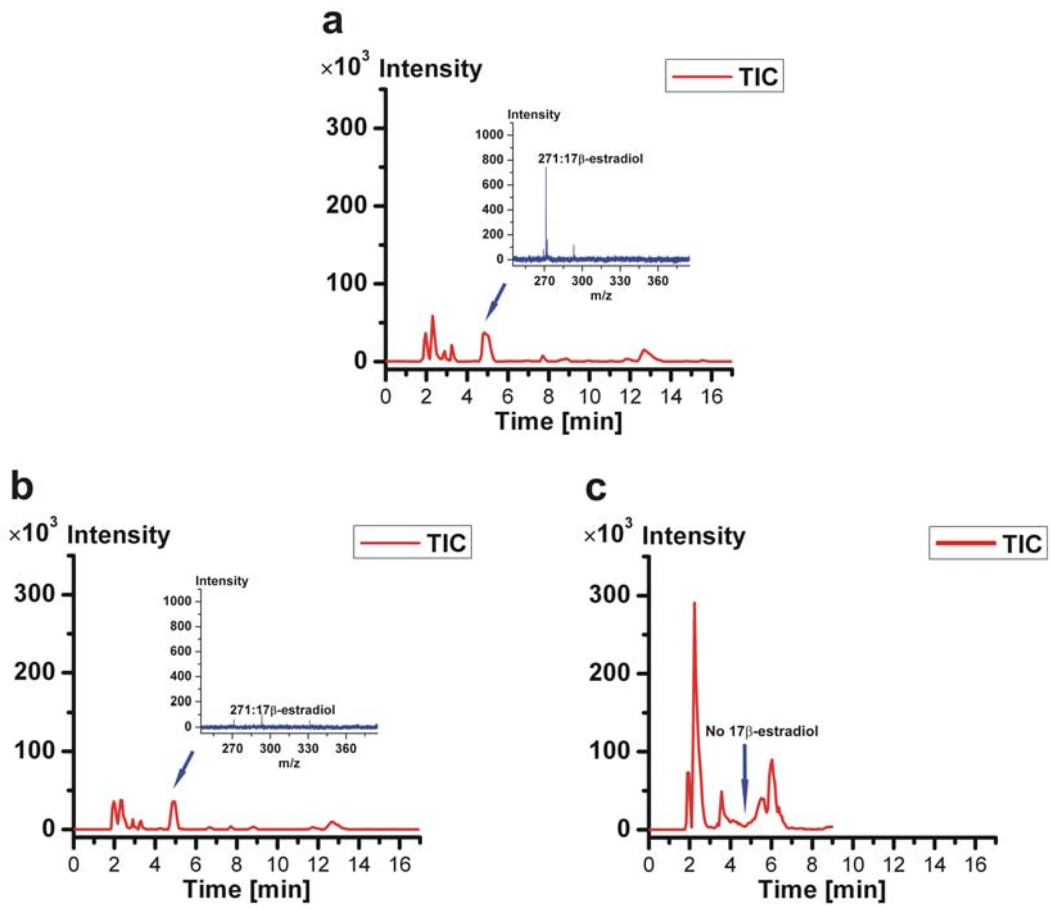

Figure 3.16 Total ion chromatogram (TIC) and mass profile spectrum of estradiol (retention time = 4.85 min) from spiked river water at E2 50 ng/L after MISPE (a), control-SPE (b), and C18-SPE (c).

Humic materials usually present in environmental water samples may act as strong interferant during the analysis of endocrine disrupting compounds in river water using LC with UV or MS detection. Humic acids result in highly complex sample mixtures, due to the limited stability of humic acids during the electrospray ionization process[21], and also produce intense UV/Vis absorption features.[22] To evaluate the extent of adsorption of humic acids onto the MISPE cartridge and their effect on the MISPE cartridge performance, 2 mL of 100 mg/L humic acid solution were loaded onto the cartridge. A

comparison of the chromatograms obtained from the washing fraction, elution fraction, and a humic acid standard solution is shown in Figure 3.17.

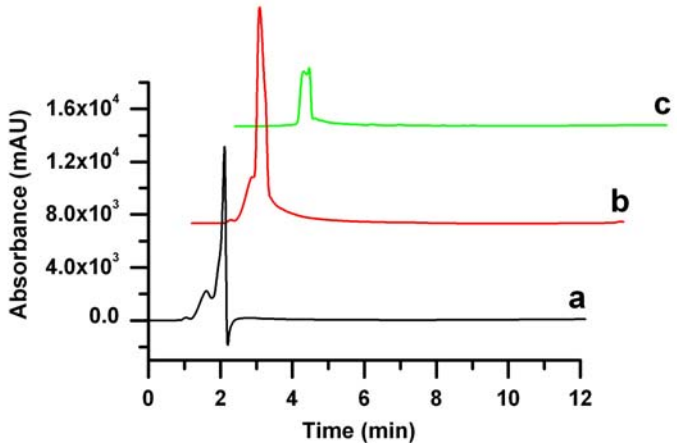

Figure 3.17 Effect of humic acids on the MISPE cartridge performance. A solution of 2 mL of 100 mg/L humic acid was percolated through the MISPE cartridge. The solution of humic acid (100 mg/L) (a), the washing fractions (b), and the eluting fractions (c) were analyzed by HPLC-UV/vis. The waterfall plot clearly shows the reduction in intensity of the signal corresponding to humic acids.

As can be observed, an intense and broad peak was obtained upon direct injection of a solution of humic acids into the HPLC (Figure 3.17a). The fraction corresponding to the washing step shows an equally intense (in mAu), and broad (in min) signal (Figure 3.17b). However, the chromatographic signal of the fraction obtained during the elution step was largely reduced in magnitude (Figure 3.17c). These results indicate that the MIP sorbent selectivity combined with an appropriate washing step is an efficient procedure for removing most of the humic acids from the MIP cartridge. The small amounts of humic acids that still remained on the MISPE sorbent after the washing step did not

significantly affect the subsequent determination of estrogens, due to the added selectivity offered by the MS detector.

To demonstrate the applicability and reliability of this method for real-world environmental samples, river water was spiked with 25 ng of the five estrogens into 500 mL aliquots, and pre-concentrated by SPE using MIP, control polymer, and C18 as sorbents. After LC-TOF-MS analysis of these fractions, the recoveries and LODs for the selected estrogens were determined and summarized in Table 3.7.

Table 3.7 Summary of the recoveries, limits of detection, and RSD of estrogens after SPE of river water (spiked at 50 ng/L) with MIP, control, and C18 as sorbents prior to HPLC-TOF-MS analysis.

	MIP			CTL			C18		
	Recovery	LOD [a] (ng/L)	RSD[b]	Recovery	LOD (ng/L)	RSD	Recovery	LOD (ng/L)	RSD
E1	16.9%	1.51	7.51	ND[c]	ND	ND	21.2%	1.45	6.84
17α-E2	ND	ND	ND	6.8%	1.13	11.0	ND	ND	ND
E2	94.7%	5.65	10.3	13.7%	3.45	8.92	ND	ND	ND
E3	ND	ND	ND	ND	ND	ND	ND	ND	ND
EE2	ND	ND	ND	ND	ND	ND	ND	ND	ND

[a] LOD defined as the limit when the signal-to-noise ratio is 3.

[b] RSD is calculated when n=3.

[c] ND: not detectable

Optimum sensitivity was obtained by appropriately adjusting the TOF mass windows (actual masses ± 0.01). Clearly, the MISPE cartridge reveals the highest affinity for E2 after the washing step. Only estrone shows some cross-reactivity. The other estrogenic

compounds were either not retained by the cartridge sorbent, or eliminated by washing during the cleaning step. The control polymer only retains a very small amount of E2, as well as 17α-E2, but reveals no affinity to the other estrogens. The control polymer SPE samples show similar LODs as MIPs, which is hypothesized to result from the fact that the control polymer has less affinity to the estrogen-like interferences; hence, the chemical noise decreases. In contrast, the C18 sorbent only retained estrone (21.2 %) in the cartridge. This is not surprising considering the fact that estrogens are easily removed from the sorbents by acetonitrile, if no specific interactions provide for increased sorbent affinity to selected constituents.

Table 3.8 summarizes the most prevalent reported methods for the determination of estrogens in environmental samples. It is clearly evident that the results obtained in this thesis are comparable to the reported studies using SPE-immunoassays[23], SPE-LC-MS[24], and nano-LC coupled to direct-electron ionization mass spectrometry.[25] Lower detection limits (~ 0.1 ng/L) were only obtained by enzyme-linked immunosorbent assays (ELISA),[26] or by derivatization prior to HRGC-(NCI)-MS analysis.[27] However, we expect that the next generation of MIP sorbent materials currently developed in our research group will be able to compete even with these ultra-trace detection limits.

Table 3.8 The most prevalent reported methods for the determination of estrogens in environmental samples.

	method	sample	analyte	LOD (ng/L)	Quantification (ng/L)
Huang *et al.*[26]	SPE-HPLC GC/MS/MS ELISA	Waste water	E2	0.1	1.9
			EE2	0.1	0.6
Zhao *et al.*[23]	SPE, immunoassay	Spiked double distilled water	E2	1.5	2.5-50
			E1	NA[a]	NA
Rodriguez-Mozaz *et al.*[24]	SPE-LC-MS	Spiked river water	E2	2.5	50
			E1	2.5	50
Famiglini *et al.*[25]	SPE, nanoLC-Direct-EI-MS	Spiked marine water	E2	7.0	NR[b]
			E1	NR	NR
Kuch *et al.*[27]	SPE, Derivatization, HRGC-(NCI)-MS	River water	E2	0.15	0.3 (median)
			E1	0.10	0.4 (median)
Lagana *et al.*[13]	SPE, LC-MS-MS	Spiked river water/sewage treatment plant water	E2	0.2-1.9	100
			E1	0.1-1.2	100
Wei *et al.*[28] (present study)	MISPE, HPLC-TOF-MS	Spiked river water	E2	5.65	50
			E1	1.51	50

[a]NA: not applicable
[b]NR: not reported

Except for the methods discussed in Table 3.8, the application of MIPs for direct estradiol removal from environmental water has been reported. However, the quantification concentration levels are several orders of magnitude higher (for 17α-estradiol MIPs[29], mg L^{-1}; for 17β-estradiol MIPs[30], μg L^{-1}) than reported in the present study (ng L^{-1}). The later method[30] also reported that 17β-estradiol MIP can remove estradiol from waste water sample at 22.4 ng/L, but with the use of a transformed yeast strain containing the human estrogen receptor, which is costly and is not repeated and optimized.

3.3.4 Conclusions

In summary, during this study non-covalently imprinted polymers for E2 have been synthesized, and applied for the first time to molecularly imprinted solid phase extraction (MISPE) of aqueous mixtures containing up to five estrogenic compounds. It was demonstrated that the loading and washing step requires careful optimization for suppressing non-specific interactions, and for achieving reproducible quantitative recovery rates. The developed MISPE-LC-TOF-MS method was tested with river water samples spiked with trace levels of estrogens at realistic levels. Furthermore, the separation of estrogens from natural organic matter (NOM) was obtained in a simple two-step extraction procedure. The target molecule E2 was selectively recovered from river water spiked with 50 ng L^{-1} of five estrogens by the developed MISPE strategy. In conclusion, it has been demonstrated that the developed MIP sorbents favorably compare to commercially available C18-based SPE materials in terms of selectivity and recovery, providing an advanced sample preparation tool for selective direct extraction of estrogens from complex aqueous samples. Finally, these encouraging results support ongoing research into molecular modeling of the governing interactions for rational understanding and designing the next generation of molecularly imprinted polymers with optimized selective retention properties[31].

3.3.5 References

1. Weigel, S.; Kallenborn, R.; Huhnerfuss, H., Simultaneous solid-phase extraction of acidic, neutral and basic pharmaceuticals from aqueous samples at ambient (neutral) pH and their determination by gas chromatography-mass spectrometry. *J. Chromatogr., A* **2004,** 1023, (2), 183-195.

2. Liu, R.; Zhou, J. L.; Wilding, A., Simultaneous determination of endocrine disrupting phenolic compounds and steroids in water by solid-phase extraction-gas chromatography-mass spectrometry. *J. Chromatogr., A* **2004,** 1022, (1-2), 179-189.

3. Mouatassim-Souali, A.; Tamisier-Karolak, S. L.; Perdiz, D.; Cargouet, M.; Levi, Y., Validation of a quantitative assay using GC/MS for trace determination of free and conjugated estrogens in environmental water samples. *J. Sep. Sci.* **2003,** 26, (1/2), 105-111.

4. Belfroid, A. C.; Van der Horst, A.; Vethaak, A. D.; Schafer, A. J.; Rijs, G. B. J.; Wegener, J.; Cofino, W. P., Analysis and occurrence of estrogenic hormones and their glucuronides in surface water and waste water in the Netherlands. *Sci. Total Environ.* **1999,** 225, (1,2), 101-108.

5. Lee, H.-B.; Peart, T. E., Occurrence and elimination of nonylphenol ethoxylates and metabolites in municipal wastewater and effluents. *Water Qual. Res. J. Can.* **1998,** 33, (3), 389-402.

6. Fine, D. D.; Breidenbach, G. P.; Price, T. L.; Hutchins, S. R., Quantitation of estrogens in ground water and swine lagoon samples using solid-phase extraction, pentafluorobenzyl/trimethylsilyl derivatizations and gas chromatography-negative ion chemical ionization tandem mass spectrometry. *J. Chromatogr., A* **2003,** 1017, (1-2), 167-185.

7. Jeannot, R.; Sabik, H.; Sauvard, E.; Dagnac, T.; Dohrendorf, K., Determination of endocrine-disrupting compounds in environmental samples using gas and liquid chromatography with mass spectrometry. *J. Chromatogr., A* **2002,** 974, (1-2), 143-159.

8. Ternes, T. A., Analytical methods for the determination of pharmaceuticals in aqueous environmental samples. *TrAC, Trends Anal. Chem.* **2001,** 20, (8), 419-434.

9. Ternes, T. A.; Andersen, H.; Gilberg, D.; Bonerz, M., Determination of estrogens in sludge and sediments by liquid extraction and GC/MS/MS. *Anal. Chem.* **2002,** 74, (14), 3498-504.

10. Mullett, W. M.; Walles, M.; Levsen, K.; Borlak, J.; Pawliszyn, J., Multidimensional on-line sample preparation of verapamil and its metabolites by a molecularly imprinted polymer coupled to liquid chromatography-mass spectrometry. *J. Chromatogr., B: Anal. Technol. Biomed. Life Sci.* **2004,** 801, (2), 297-306.

11. Xie, J.; Zhu, L.; Xu, X., Affinitive separation and on-line identification of antitumor components from Peganum nigellastrum by coupling a chromatographic column of target analogue imprinted polymer with mass spectrometry. *Anal. Chem.* **2002,** 74, (10), 2352-2360.

12. Koeber, R.; Fleischer, C.; Lanza, F.; Boos, K.-S.; Sellergren, B.; Barcelo, D., Evaluation of a Multidimensional Solid-Phase Extraction Platform for Highly Selective On-Line Cleanup and High-Throughput LC-MS Analysis of Triazines in River Water Samples Using Molecularly Imprinted Polymers. *Anal. Chem.* **2001,** 73, (11), 2437-2444.

13. Lagana, A.; Bacaloni, A.; De Leva, I.; Faberi, A.; Fago, G.; Marino, A., Analytical methodologies for determining the occurrence of endocrine disrupting chemicals in sewage treatment plants and natural waters. *Anal. Chim. Acta* **2004,** 501, (1), 79-88.

14. Vanderford, B. J.; Pearson, R. A.; Rexing, D. J.; Snyder, S. A., Analysis of Endocrine Disruptors, Pharmaceuticals, and Personal Care Products in Water Using Liquid Chromatography/Tandem Mass Spectrometry. *Anal. Chem.* **2003,** 75, (22), 6265-6274.

15. Farre, M.; Kloter, G.; Petrovic, M.; Alonso, M. C.; Lopez de Alda, M. J.; Barcelo, D., Identification of toxic compounds in wastewater treatment plants during a field experiment. *Anal. Chim. Acta* **2002,** 456, (1), 19-30.

16. Sole, M.; Lopez de Alda, M. J.; Castillo, M.; Porte, C.; Ladegaard-Pedersen, K.; Barcelo, D., Estrogenicity Determination in Sewage Treatment Plants and Surface Waters from the Catalonian Area (NE Spain). *Environ. Sci. Technol.* **2000,** 34, (24), 5076-5083.

17. Ternes, T. A.; Brenner-Weiss, G.; Eggert, T.; Muller, J.; Kirschhofer, F.; Nusser, M.; Wilken, R.-D.; Obst, U., Analysis of phytoestrogens and mycoestrogens in water using liquid chromatography-electrospray ionization/tandem mass spectrometry (LC-MSMS). *Vom Wasser* **1999,** 93, 255-263.

18. Baronti, C.; Curini, R.; D'Ascenzo, G.; Di Corcia, A.; Gentili, A.; Samperi, R., Monitoring natural and synthetic estrogens at activated sludge sewage treatment plants and in a receiving river water. *Environ. Sci. Technol.* **2000,** 34, (24), 5059-5066.

19. Peñalver, A.; Pocurull, E.; Borrull, F.; Marcé, R. M., SPME-HPLC-UV-Elctro Estrogenic compounds. *J. Chromatogr., A* **2002,** 964, 153-160.

20. Matsui, J.; Okada, M.; Tsuruoka, M.; Takeuchi, T., Solid-phase extraction of a triazine herbicide using a molecularly imprinted synthetic receptor. *Anal. Commun.* **1997,** 34, (3), 85-87.

21. These, A.; Reemtsma, T., Limitations of electrospray ionization of fulvic and humic acids as visible from size exclusion chromatography with organic carbon and mass spectrometric detection. *Anal. Chem.* **2003,** 75, (22), 6275-6281.

22. Fernandez, F. M.; Tudino, M. B.; Troccoli, O. E., Automatic on-line ultratrace determination of Cd species of environmental significance in natural waters by FI-ETAAS. *J. Anal. At. Spectrom.* **2000,** 15, (6), 687-695.

23. Zhao, L.; Lin, J.-M.; Li, Z.; Ying, X., Development of a highly sensitive, second antibody format chemiluminescence enzyme immunoassay for the determination of 17β-estradiol in wastewater. *Anal. Chim. Acta* **2006,** 558, (1-2), 290-295.

24. Rodriguez-Mozaz, S.; Lopez de Alda, M. J.; Barcelo, D., Monitoring of estrogens, pesticides and bisphenol A in natural waters and drinking water treatment plants by solid-phase extraction-liquid chromatography-mass spectrometry. *J. Chromatogr., A* **2004,** 1045, (1-2), 85-92.

25. Famiglini, G.; Palma, P.; Siviero, A.; Rezai, M. A.; Cappiello, A., Determination of Endocrine Disrupting Compounds in Marine Water by Nanoliquid Chromatography/Direct-Electron Ionization Mass Spectrometry. *Anal. Chem.* **2005,** 77, (23), 7654-7661.

26. Huang, C.-H.; Sedlak, D. L., Analysis of estrogenic hormones in municipal wastewater effluent and surface water using enzyme-linked immunosorbent assay and gas chromatography/tandem mass spectrometry. *Environ. Toxicol. Chem.* **2001,** 20, (1), 133-139.

27. Kuch, H. M.; Ballschmiter, K., Determination of endocrine-disrupting phenolic compounds and estrogens in surface and drinking water by HRGC-(NCI)-MS in the picogram per liter range. *Environ. Sci. Technol.* **2001,** 35, (15), 3201-3206.

28. Wei, S.; Huang, C.-H.; Fernandez, F. M.; Mizaikoff, B., Determination of Estrogens in River Water with SPE using 17β-Estradiol-Imprinted Polymers combined with LC-TOF-MS. *Anal. Chem.* **2007**, Submitted.

29. Meng, Z.; Chen, W.; Mulchandani, A., Removal of Estrogenic Pollutants from Contaminated Water Using Molecularly Imprinted Polymers. *Environ. Sci. Technol.* **2005,** 39, (22), 8958-8962.

30. Noir, M. L.; Lepeuple, A.-S.; Guieysse, B.; Mattiasson, B., Selective removal of 17β-estradiol at trace concentration using a molecularly imprinted polymer *Water Res.* **2007**, In press.

31. Molinelli, A.; O'Mahony, J.; Nolan, K.; Smyth, M. R.; Jakusch, M.; Mizaikoff, B., Analyzing the Mechanisms of Selectivity in Biomimetic Self-Assemblies via IR and NMR Spectroscopy of Prepolymerization Solutions and Molecular Dynamics Simulations. *Anal. Chem.* **2005,** 77, (16), 5196-5204.

CHAPTER 4

PROBING THE NATURE OF NON-COVALENT IMPRINTING MECHANISMS

4.1 Computational Modeling of MIPs

4.1.1 Introduction

The use of MIPs in SPE for selective pre-concentration is appealing to a wide variety of analytical applications given that sufficient selectivity and affinity of the synthesized MIPs to target compounds is provided. To achieve MIPs with high selectivity and binding capacity, the initial formulation of components for imprinting needs to be optimized by rational selection of functional monomers providing sufficiently strong interactions with the target molecule. Non-covalent imprinting is based on the co-polymerization of the non-covalently bonded template-functional monomer complex with an excess of cross-linker. However, non-covalent interactions are usually considered as weak interactions easily affected at different imprinting conditions, such as porogenic solvent and polymerization temperature. Furthermore, the selectivity and affinity of thus synthesized polymers are intimately related to the initial strength/integrity of the template - monomer complex[1]. Consequently, the optimization of a MIP formulation demands considering the governing interactions between template and functional monomer, as well as the porogenic solvent. Thereby, selection of the most suitable functional monomer with the potentially highest binding energy to the target molecule in the pre-polymerization solution is facilitated. To this end, computational predictions based on combinatorial screening approaches calculating the binding energies[2-4], or the

stabilization energies[5] of the selected template with different functional monomers have been described.

Recently, we have developed a general strategy targeting more fundamental understanding on the template-functional monomer interactions during molecular dynamics simulations[6]. We hypothesize that a suitable description of the electrostatic and van der Waals interactions governing non-covalent assembly of the pre-polymerization complex via appropriate choice of force field parameters provides a viable model for describing the pre-polymerization system (electrostatic interactions also represent hydrogen bonds with sufficient accuracy). In the present section, E2 was used as the model target molecule due to its relevance in ongoing studies related to endocrine disrupting compounds (EDCs)[7-12]. Molecular dynamics (MD) simulations is used for selecting the most suitable monomers via hydrogen bonding analysis, along with the accessibility of conformational changes of the template and/or monomer during the molecular dynamic simulations.

During preliminary studies, a library of nine monomers with different functionalities was screened. Experimental evidence from previously reported batch rebinding studies support that the selectivity of the synthesized MIP is strongly related to the initial stability of the template - monomer complex in the pre-polymerization solution. Hydrogen bonding analysis from molecular dynamics simulations, and ^{1}H-NMR analysis enable detailing the hydrogen bonding interaction between the template E2 and the functional monomer MAA. Both, the modeling results and ^{1}H-NMR experiments reveal that the dimerization of monomers plays a crucial role in optimizing this particular imprinting strategy. In the subsequence study, computational models including all the

imprinting species at the correct ratios were developed providing better understanding on the role of the different constituents during the imprinting process. Hydrogen bonding analysis and free energy calculation are combined to understand the interactions involved in the imprinting species. The π-π stacking interactions were investigated in detail for understanding the interaction between the aromatic moiety of cross-linker (DVB), and the template (E2).

4.1.2 Computational methods

4.1.2.1 Preliminary considerations on the modeling method for MIPs

The molecular modeling results reported in this thesis were obtained with the AMBER-8 package[13] using the ff99[14] and GAFF[15] force fields, respectively. The Antechamber tools with Leap are used to create topology and coordinate files for the template and monomers; the charge method is AM1-BCC[16]. The template - monomer pair (one template with one monomer: initially the functional group of the monomer is 3 Å to the 17β–OH of E2) was immersed in a periodic box of chloroform (CHCL3BOX10[13]), which was subject to periodic boundary conditions with 10 Å of solvent added around the complex in each direction. The particle-mesh Ewald (PME)[17, 18] procedure was used to handle long-range electrostatic interactions. Furthermore, bond length constraints were implemented for bonds involving hydrogen (SHAKE algorithm)[19]. Energy minimization and equilibration steps were followed by molecular dynamics simulations of the template - monomer system in explicit solvent using SANDER, a software component of the AMBER-8 package. Energy equilibrations with constant volume (5 ps), and constant pressure (5 ps×3) were performed, followed by energy equilibration with distance restraint (250 ps). The density of the system was

stabilized at 1.49 g/mL, which is the density of chloroform at the end of the equilibration. Distance restraint forces were introduced between template and monomer during the system equilibration, and removed for the simulation production run. The simulations resulted in molecular dynamics (MD) trajectories with durations of 1.8 ns, which were performed at constant volume and constant energy at time increments of 1 fs.

4.1.2.2 Advanced development of the modeling method

4.1.2.2.1 Understanding molecular recognition: theoretical modeling

To establish a simulation system close to the molar ratios of the experimental MIP preparation, a complex including 1 molecule of E2, 8 molecules of MAA or 4VP, 40 molecules of DVB, and 1 molecule of AIBN was modeled. The individual molecules were first placed in vacuum in an arbitrary configuration at distances of 10 Å from each other. To obtain a complex with reasonable internal distances, a short MD simulation was started, thereby pulling together individual molecules with increasing pair-wise distance restraints, while at the same time reducing the temperature from 300 to 0 K. In addition, an acetone solvent box was created by equilibrating a box of 20x20x20 $Å^3$ filled with acetone molecules until the density of the box was close to the experimental density of acetone (0.791 g/mL at 25 ^oC). The resulting equilibrated box was added to solvate the condensed initial complex, with particular attention to achieving the same concentration for all components as in the real MIP system (1 mmol template, 8 mmol functional monomer, and 40 mmol cross-linker in 6 mL of acetone).

This system was then equilibrated as follows. At the beginning of the equilibration procedure the intention was keeping the system close to the initial configuration for preventing the system to disintegrate, as it was still highly strained. First, strain resulting

from addition of the solvent was reduced by keeping the monomer complex fixed, and by relaxing acetone (minimization followed by 5 ps of a NVT MD run). Then, the complete system was strain minimized during a 50 ps NVT MD run, in which all molecules were free to move, however, distance restraints were kept between non-solvent molecules. This procedure was followed by a 3-step density equilibration at constant pressure and at decreasing pressure coupling (changing coupling constants from 0.05 ps over 0.5 ps to 5 ps). Finally, a simulated annealing protocol was executed by performing a NVT simulation of the system at 1200 K, from which every 17.5 ps snapshots were extracted and cooled to 0 K within a period of 13.5 ps. Thereby, 1000 low energy configurations were generated as input for the following studies.

4.1.2.2.2 Understanding inter-molecular interactions: hydrogen bonding and π-π stacking analysis

H-bond analysis was performed by using the ptraj program in AMBER-8 for tracking pair interactions within the set of simulated annealing snapshots produced from the previous modeling step. The hydrogen bond "donor" or "acceptor" were manually set (e.g., OH group in E2 was set as acceptor, and N in 4VP was set as donor), and a distance cut-off at 3.5 Å was defined. Resulting, the H-bond percentage is the percentage of snapshots where the H-bond is formed. Using the same definition as the hydrogen bond percentage, the π-π interaction percentage is defined as the percentage at which π-π stacking is formed and maintained (a benzene ring distance cut-off at 4.5 Å was defined) among the set of snapshots.

4.1.2.2.3 Understanding molecular recognition: free energy calculations

Free energies of complexes, as well as of individual molecules were calculated using the 'mm_pbsa' program from the AMBER suite. Reaction field energies and hydrophobic contributions to the solvation free energy were calculated with the Generalized Born – Surface Area (GB-SA) method using experimentally determined values for the dielectric constant and the surface tension of the MIP pre-polymerization solution (see below; for the MAA/DVB system ε_r = 8.67; σ = 26.99 dyn/cm, for 4VP/DVB: ε_r = 9.57; σ = 26.21 dyn/cm). Entropies were calculated via normal mode analysis with the program 'nmode' as implemented in 'mm_pbsa', with the exception that minimization prior to normal mode analysis was also done with 'nmode', as the minimization is necessary for the calculation of gas phase energies as well as the entropies. In order to make use of the Newton-Raphson minimization algorithm (which is a very efficient protocol to perform the energy minimization in AMBER) implemented therein, the code of 'mm_pbsa' was modified (see Appendix) in order to facilitate this step.

Complexes were extracted from the set of simulated annealing snapshots by considering the template, as well as any molecule that was closer to the template than a certain cut-off distance (in most cases 3.5 Å). In order to calculate average free energies of individual molecules, every instance of the molecule in any of the snapshots was taken into account.

4.1.2.2.4 Experimental determination of MIP pre-polymerization mixture bulk properties

The surface tension of pre-polymerization solutions was determined by the pendant drop method with a dynamic contact angle analyzer (FTÅ 200, First Ten Ångstroms, Portsmouth, VA, USA). The dielectric constant of the solutions was determined by a

network analyzer (HP8752A, Hewlett-Packard, Palo Alto, CA, USA) with a dielectric permittivity probe (HP 85070A, Hewlett-Packard, Palo Alto, CA, USA) at 60-1300 MHz. It was observed that the dielectric constant values of the studied systems remained constant in a range of 60-1300 MHz. The dielectric constant is used to calculate the reaction field energy, which is related to the rotation movement of the system, whose frequency range is close to 1300 MHz.

4.1.3 Results and discussion

4.1.3.1 Screening of a monomer library for imprinting of 17β-estradiol

For successful imprinting, it is essential that the functional monomer forms a stable complex with the template molecule ensuring the generation of selective binding cavities. In the present work, nine different monomers with acidic, basic, or neutral functionalities (Figure 4.1) were analyzed using MD simulations as for their potential serving as suitable functional monomers for imprinting E2.

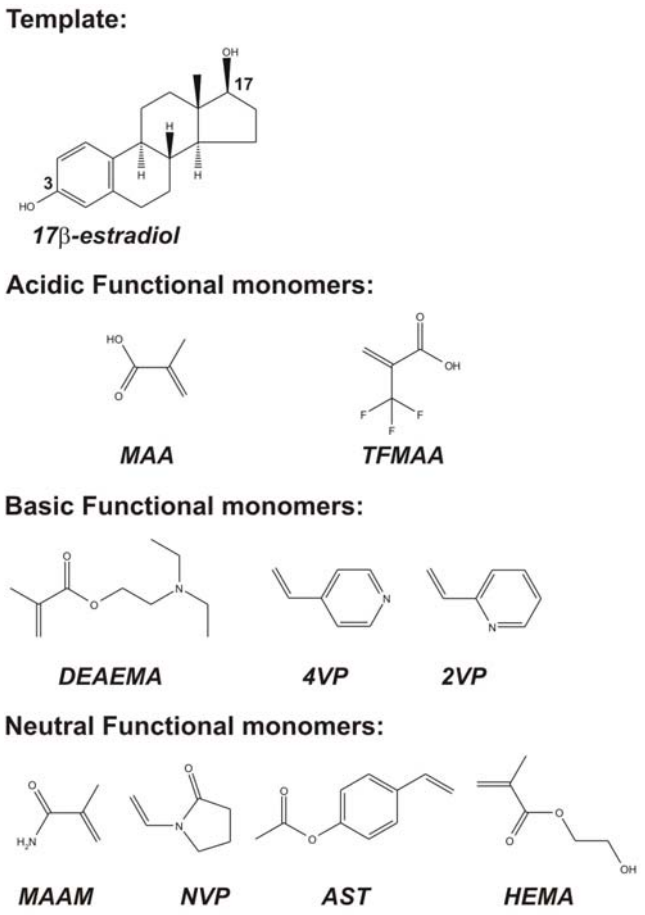

Figure 4.1 Molecular structures of the investigated templates and monomers.

Energy minimizations and equilibrations were performed prior to each simulation production run. Corresponding hydrogen bonding analysis results derived from 1.8 ns MD simulations are shown in Figure 4.2, with the hydrogen bond percentage calculated for both ends of E2. These results are in acceptable agreement with data from corresponding batch rebinding studies[20], where among all monomers displayed in Figure 4.1, the MIPs prepared with MAA, DEAEMA, and MAAM as functional monomers reveal the highest imprinting factors during batch rebinding experiments, thereby confirming that the acidic MAA, the basic DEAEMA, and the neutral MAAM exhibit the

highest hydrogen binding percentage, and are accordingly the most suitable monomers for imprinting of E2.

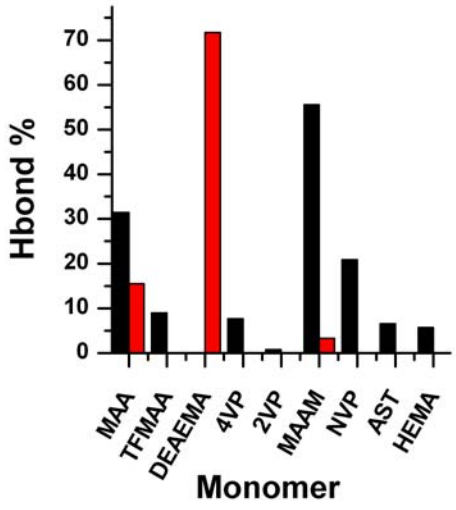

Figure 4.2 Hydrogen bonding percentage obtained from the monomer library using hydrogen bonding analysis in the MDS: hydrogen bond between 3OH of E2 with monomer (black); hydrogen bond between 17β-OH of E2 with monomer (red).

Furthermore, the obtained results indicate that E2 forms a stable complex with the monomer either at the phenol group (3-OH), or at the non-phenol OH-group (17-OH). Figure 4.3 illustrates the radial distribution functions (RDFs) of the E2 3-OH and 17-OH groups with the C=O and OH groups of MAA, respectively. The E2 (H_{3OH})-MAA (O_{CO}) and E2 (H_{17OH})-MAA (O_{CO}) RDFs exhibit significant peaks at around 2 Å, which confirms the strong tendency of the E2 H_{3OH} and H_{17OH} to form hydrogen bonds with the O_{CO} of MAA, whereas the E2 (O_{17})-MAA (H_{OH}), the E2 (O_3)-MAA (H_{OH}), the E2 (H_{3OH})-MAA (O_{OH}), and the E2 (H_{17OH})-MAA (O_{OH}) show less pronounced peaks at 2.2 Å, 5.5 Å, 3.7 Å, and 3.8 Å, respectively. In view of the selectivity of E2-imprinted

polymers to E2, the affinities of MAA to E2 at both molecular ends apparently plays an important role, although the difference in molecular shape certainly also contributes to the obtained selectivity.

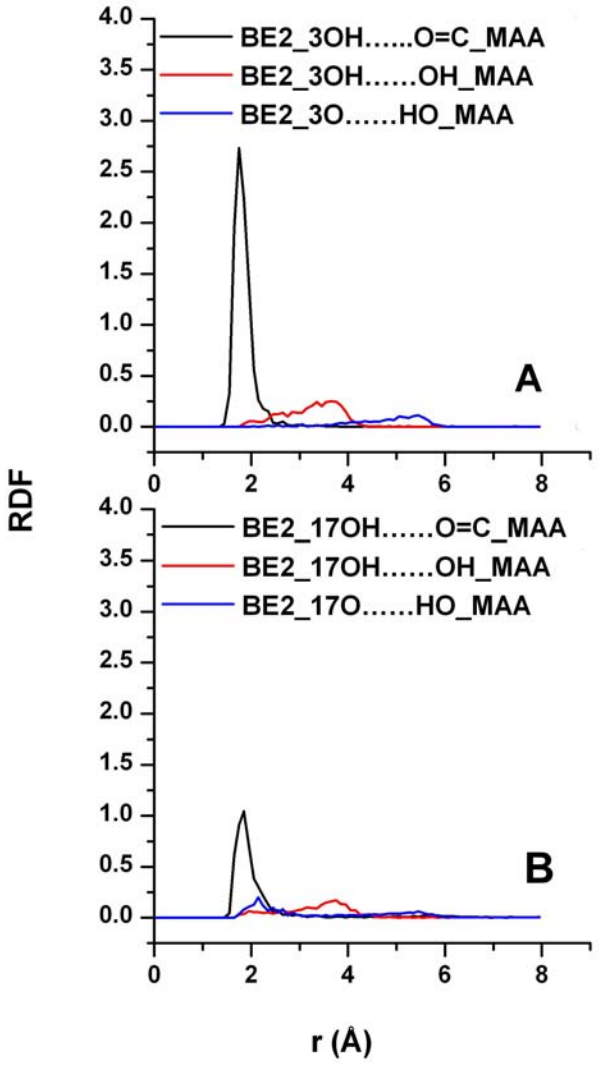

Figure 4.3 Radial distribution functions (RDFs) of the OH group of E2 (E2, A: 3-OH, B: 17β-OH), with the COOH group of MAA in $CHCl_3$.

4.1.3.2 Molecular modeling of all involved imprinting constituents for 17β-estradiol

4.1.3.2.1 Understanding molecular recognition: theoretical modeling

In order to evaluate the type and strength of the interactions between all involved imprinting components, it can be expected that establishing models including all species at correct experimental ratios will provide better understanding on the role of the different constituents during the imprinting process. The present work focuses on including the effects of cross-linker, solvent, and functional monomer at their experimental ratio into the simulation system, which provides a more realistic simulation environment in closer analogy to the experimental conditions present in the pre-polymerization solution. Another important aspect is that this study aims at avoiding bias from pre-determined assumptions on how structures of optimized pre-polymerization complexes would look like.

It is evident from Figure 4.2 that for imprinting of E2, MAA is apparently the favorable monomer compared to 4VP. It is also shown that only MAA has considerable affinities at both OH-groups of E2 compared to other monomers in the library. Two (or more)-point binding sites are essential to establishing sufficiently stable template-monomer complexes ensuring selective binding sites. Hence, MAA was selected as a representative for an optimized monomer, while 4VP was considered an inadequate monomer during establishing the modeling methodologies in this study. The investigated pre-polymerization solution is composed of DVB as cross-linker, along with acetone as porogenic solvent, and AIBN as initiator for the preparation of an E2 MIP, which was reported elsewhere[12]. The two systems were named “CPL1 (E2-MAA)” and “CPL2 (E2-4VP)”. The initial geometries were created by combining all the imprinting components

into a single ‘unit’ (AMBER terminology) in an arbitrary arrangement. To compress this structure and mix the molecules in a more realistic way, distance restraints between molecules were added, and a short MD simulation (50 ps) was carried out, while at the same time the system was cooled to 0 K. Further refinement of this initial structure was then performed in explicit solvent via energy and density equilibration steps, followed by a simulated annealing protocol, as previously described. 1000 snapshots were generated from simulated annealing runs yielding possible conformations of the entire pre-polymerization system, as exemplarily shown in Figure 4.4.

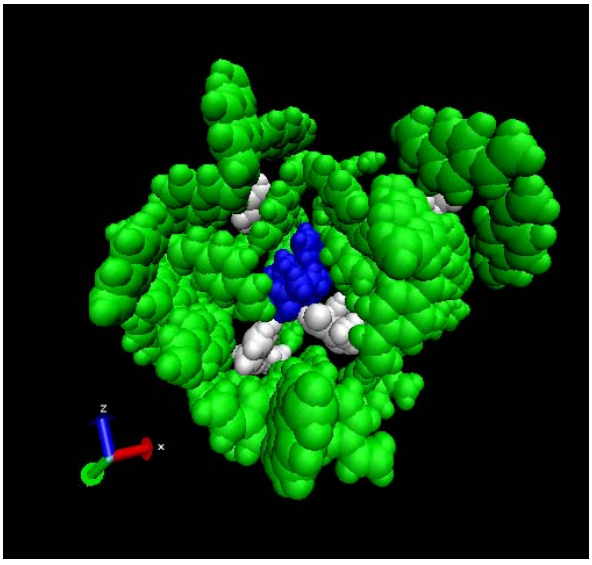

Figure 4.4 Example of one possible final structure of the complex arrangement after simulation (blue: E2; white: MAA; green: DVB, solvent was omitted for clarity).

In order to obtain an unbiased estimate on configurations yielding stable complexes vs. less stable configurations, the interaction energies between the template and other molecules were calculated, as well as the free energies of the complex formation. The

number of molecules involved in the calculation was reduced to an acceptable level by considering only the molecules in the first solvation shell during these first studies, which had to be appropriately defined.

Figure 4.5 A shows the radial distribution functions (RDF) of 17β-OH and 3-OH of E2 with MAA/4VP molecules as calculated from the simulated annealing snapshots. It is evident that the highest peaks are all located at around 2.8 Å. Hence, an appropriate cut-off value should be slightly larger than 2.8 Å accounting for functional monomers that provide H-bond interactions with the template molecule. To visualize the configuration of molecules in the first solvation shell of E2, different cut-off values (2.5 Å, 3.1 Å, 3.5 Å, and 4.5 Å) were selected. Figure 4.5 B shows that the configuration of the complex with a cut-off value of 3.5 Å includes most of the molecules in the first solvation shell. Therefore, in the present study 3.5 Å was selected as the cut-off value for defining complex structures during subsequent calculations.

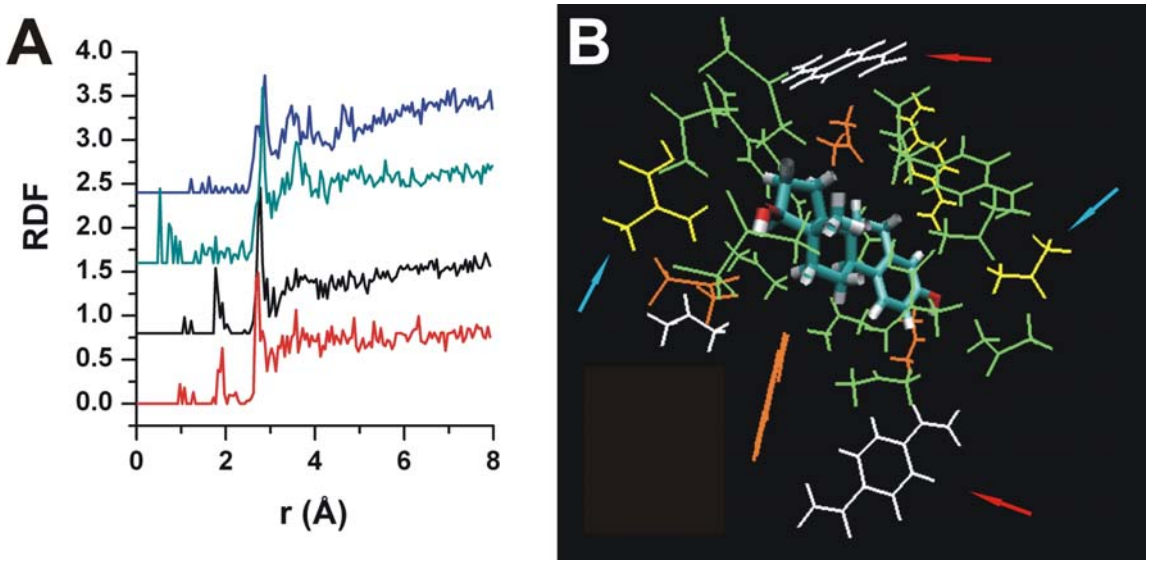

Figure 4.5 The determination of the cut-off used in the free energy calculation. A: The calculated radial distribution function (RDF) of the 17β-OH group of E2 with the 4VP (blue) and MAA (black), and 3-OH group of E2 with 4VP (green) and MAA (red), B: The selected complexes with different cut-off. Center: E2; cut-off = 2.5 Å, orange; cut-off = 3.1 Å, green, repeat molecules with previous shell didn't show; cut-off = 3.5 Å, yellow, repeat molecules with previous shell didn't show; cut-off = 4.5 Å, white, repeat molecules with previous shell didn't show. The blue arrows point out the molecules of the first solvation shell which are missing in the 3.1 Å layer, and the red arrows point out the molecules in the second solvation shell which are included in the 4.5 Å layer.

By analyzing the first solvation shell of the complex system, hydrogen bond percentages between E2 and functional monomers in the MAA and VP complex system were compared (Figure 4.6, green pie). Apparently, MAA is a significantly superior monomer for interacting with E2 via hydrogen bonding. The hydrogen bond percentage of 17β-OH of E2 with MAA and 4VP are 9.9 % and 4.9 %, respectively; the hydrogen bond percentage of 3-OH of E2 with MAA and 4VP are 10.4 % and 6.2 %, respectively. It is also evident that the E2-4VP interaction is slightly stronger at the 3-OH end, than at the 17β-OH end. It was also noticed that apparently more 4VP molecules are involved within the first solvation shell of the complex, than MAA molecules (Figure 4.6, red + green pie), which may due to the hydrophobic effects along with electrostatic interactions such as π-π stacking and Van der Waals interactions. If a larger cut-off value is selected, the 4VP molecules involved in the solvation shell may show an increasing trend, as the secondary aggregation of aromatic moieties (4VP-4VP) may occur.

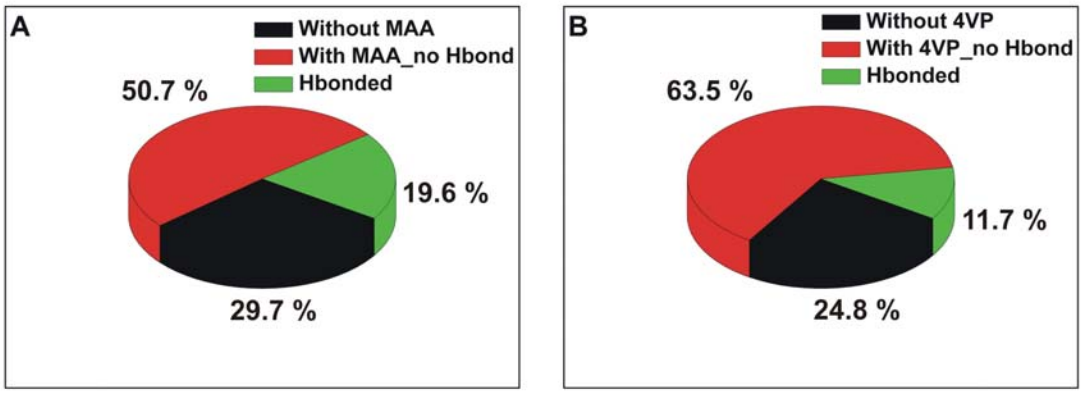

Figure 4.6 Comparison of the composition of the simulated complex from 1000 snapshots; A is for the E2-MAA system, and B is for the E2-4VP system.

Furthermore, it was expected that there could be additional π-π interactions between E2 and 4VP, as both E2 and 4VP provide aromatic moieties. To clarify the prevalence and strength of π-π interactions, the average distance (only distances smaller than 4.5 Å are considered) between the indicated atoms in Figure 4.7 was calculated based on Torimoto *et al*[21]. The proposed π- π interaction is of the edge-to-face type, which is considered to be among the most stable π-π interactions. The calculated π-π interaction percentage is approx. 4.4 %. Hence, it is likely that these weak interactions also contribute in part to the functionality of 4VP-E2 imprinting.

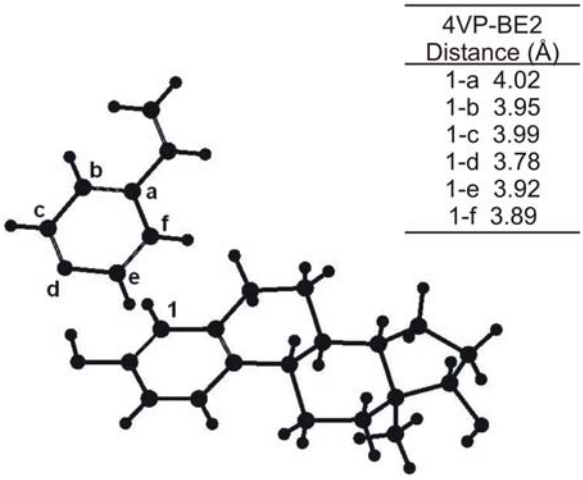

Figure 4.7 The distances between the A-ring of E2 and the benzene rings of 4-VP are shown. The π-π interaction between E2 and 4-VP is based on considerations by Torimoto *et al*[21].

To estimate the contribution of the cross-linker to the complex formation and to the subsequent imprinting process, average distances (only distances smaller than 4.5 Å are considered) between the benzene ring of E2 and DVB (Figure 4.8 A) were determined. The π-π percentage of E2-DVB for the CPL1 (E2-MAA) and CPL2 (E2-4VP) system are 16.8 % and 15.8 %, respectively. The small difference between the two systems is most likely related to the aromatic interaction of E2 with 4VP in CPL2, which reduces the probability of E2 to interact with DVB. It is evident that the distance between E2 and DVB is slightly larger than that between E2 and 4VP, indicating that π- π interactions between E2 and DVB are weaker. However, as there are a lot more DVB molecules than 4VP molecules in the system (40 mol DVB vs. 8 mol 4VP), the π-π percentage of E2-DVB is higher. Figure 4.8 B shows the configuration of the E2-DVB complex with π- π stacking interaction. Experimental data obtained during this thesis has shown that MIPs prepared with EDGMA are characterized by a lower separation factor E2/17α-E2, than

those prepared with DVB (1.65 vs. 2.04; template:functional monomer:cross-linker = 1:8:40, functional monomer: MAA). Hence, it is conceivable that the enhancement of the imprinting effect is in part explained by π- π interactions between E2 and DVB.

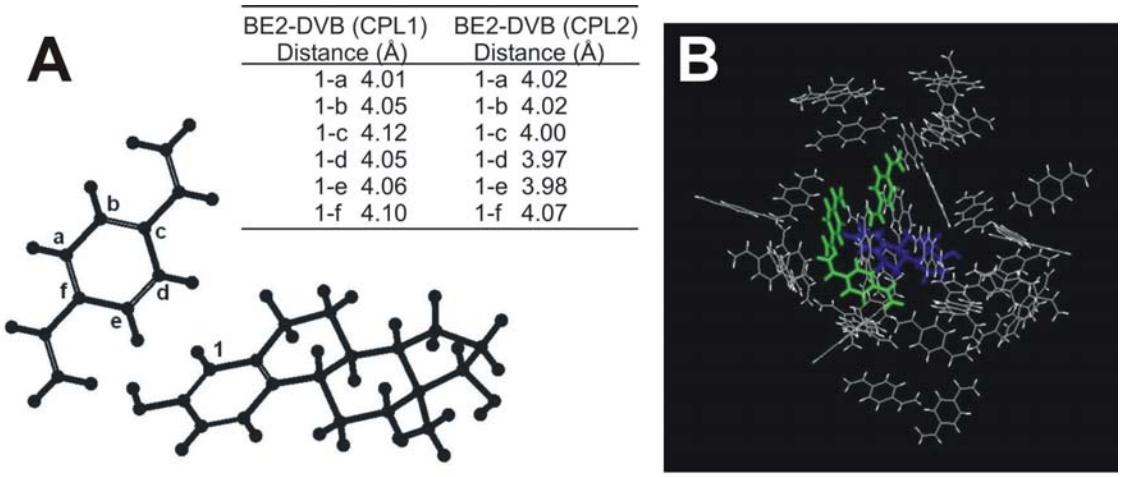

Figure 4.8 Template-cross-linker interaction: A: The distances between the A-ring of E2 and the benzene rings of DVB in the CPL1 (E2-MAA system) and CPL2 (E2-4VP system) are shown. The π-π interaction between E2 and 4-VP is based on the model proposed by Torimoto *et al*[21]. B: Configuration of the π- π interaction (edge-to-face) between E2 (blue) and DVB (green) in the simulated system. The white molecules are the remaining DVB molecules without interaction with E2. Other components (functional monomers, solvent, and initiator) are omitted for clarity.

Table 4.1 lists the average number of molecules involve in the 3.5 Å shell. It can be seen that hydrogen-bonded complexes involve more functional monomers in the first solvation shell, which facilitates the formation of template-monomer complexes. It is interesting that almost the same amount of DVB is present within H-bonded and non-bonded complexes of CPL1, but that there is significantly more DVB present within the H-bonded complexes vs. the non-bonded complexes of CPL2, which may again result

from π- π interactions between 4VP and DVB; if there is more 4VP in the hydrogen-bonded complexes, more DVB molecules are present within the 3.5 Å shell.

For both CPL1 and CPL2, it is evident that there are more acetone molecules involved in the non-bonded complexes vs. the H-bonded complexes, which indicates that acetone molecules apparently compete with functional monomers for interaction with template molecules by hydrogen bonding.

Table 4.1 Comparison of the imprinting components (functional monomers, cross-linker, solvent, initiator) involved in the first solvation shell (cut-off = 3.5 Å) of the complex with H-bond and without H-bond between the template and functional monomers molecules.

	Template-monomer with H-bond		Template-monomer without H-bond	
	E2-MAA (CPL1)	E2-4VP (CPL2)	E2-MAA (CPL1)	E2-4VP (CPL2)
MAA/4VP	1.9	2.0	1.0	1.2
DVB	7.3	8.0	7.4	7.6
ACN	10	9.6	10.7	10.2
ABN	0.2	0.2	0.2	0.2

The extended MM-GBSA method used in this study calculates and averages the contributions of gas-phase energies, solvation free energies, and solute entropies of each instance of a molecular component, which is found within the 1000 snapshots of the simulated annealing procedure. Here 'molecular components' refers to either single molecules (template, functional monomer, etc.), or complexes of the same stoichiometry. Average free energies of complex formation are then calculated for every complex stoichiometry as the difference between the average free energies of each complex and the individual molecules, if one assumes that a pre-polymerization complex is formed according to the general reaction

$$T + m\,M + c\,C + s\,S + i\,I \leftrightarrow CPL, \quad (1)$$

where T, M, C, S, I, and CPL stand for template, monomers, cross-linker, solvent, initiator, and complex, respectively (lower case characters denoting the stoichiometric coefficients), the molar free energy of complex formation would be given by

$$\Delta G = \langle G(CPL)\rangle - t\langle G(T)\rangle - m\langle G(M)\rangle - c\langle G(C)\rangle - s\langle G(S)\rangle - i\langle G(I)\rangle, \quad (2)$$

where $\langle G\cdots\rangle$ denotes an average of the respective absolute molar free energy accounting for all instances of the individual component found among the simulated annealing snapshots.

As generally done within the MM-GBSA framework, the absolute free energy of an individual component is calculated as the sum of gas phase energy and entropy, which are determined from the force field and via normal mode analysis (the 'MM' part), as well as a term for the free energy of solvation following

$$G = GBTOT - TSROT - TSVIB - TS\_trans\_gas \quad (3)$$

$$GBTOT = GBSOL + GAS \quad (4)$$

TSROT – Rotational entropy (as calculated by nmode) times temperature (5)

TSVIB – Vibrational entropy (as calculated by nmode) times temperature (6)

TS_trans_gas – the theoretical value for the translational entropy of an ideal gas (7)

The solvation term GBSOL in turn is made up of an electrostatic reaction field contribution calculated according to the Generalized Born (GB) model, and a hydrophobic contribution proportional to the solvent accessible surface area (SA) of the complex. It should be noted that the rationale of calculating free energies of complex formation by this strategy is based on the concept that molecules, which are prior to these calculations individually immersed in a continuum solvent of certain dielectric constant and surface tension, are brought together and form a complex that is again immersed in the same continuum solvent. While this assumption is not strictly valid from an experimental point of view, as the composition of the 'solvent' also changes during complex formation – at least for higher concentrations of the formed complex – this assumption is regarded sufficiently accurate for the purpose of this study, in particular if compared with other simplifications inherent to molecular mechanics calculations in general, and the MM-GBSA framework in particular. Nevertheless, in order to obtain reliable estimates of free energies, the dielectric constants and surface tensions of the modeled pre-polymerization solutions need to be known, and were experimentally determined in the course of this thesis.

The resulting binding free energies of the complex with and without hydrogen bond between template and functional monomer were separately binned (Figure 4.9). It can be seen from Figure 4.9 A that there is a significantly higher number of hydrogen-bonded complexes in case of CPL1 vs. CPL2. In contrast, for the non-bonded complexes there

are significantly higher frequencies in the main bins (Figure 4.9 B, 90, 100, 110 Kcal/mol) in case of CPL2 than in case of CPL1 (Figure 4.9 B). Consequently, also the free energy results indicate that MAA is a more favorable monomer than 4VP, which is again in agreement with the results of the previously performed hydrogen bonding analysis (Figure 4.2) derived from the E2-monomer distance. Experimentally, chromatographic data obtained from MIP-based HPLC studies have resulted in similar conclusions, which for the first time provides an arguable connection between experimental findings and molecular models of imprinted polymers. Finally, Figure 4.10 indicates that CPL1 provides significantly higher capacity factors, separation factors and imprinting factors than CPL2.

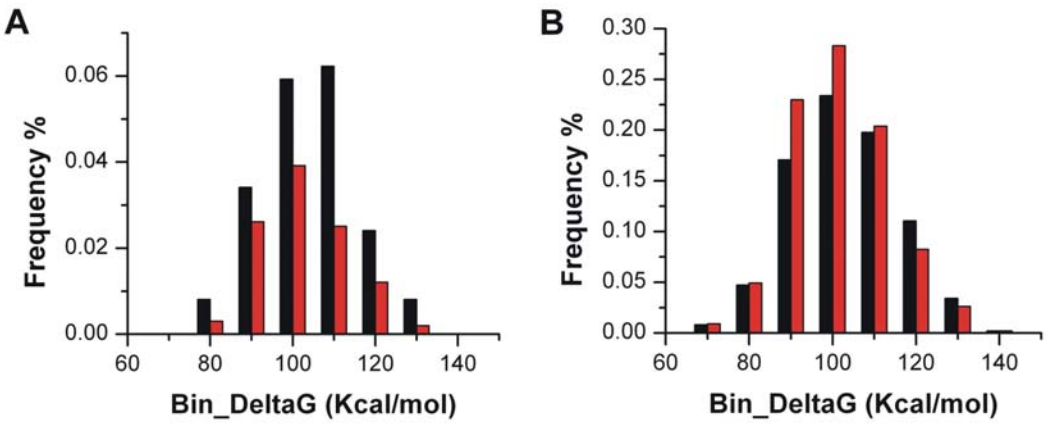

Figure 4.9 Energy distribution from the simulated complex with hydrogen bond (A) and without hydrogen bond (B) of E2-MAA (black) or E2-4VP (red).

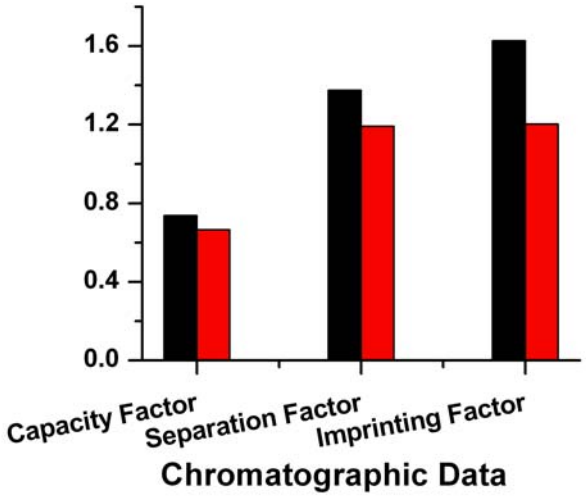

Figure 4.10 Capacity factor, separation factor and imprinting factor obtained from chromatographic data of MIP-based HPLC including the E2-MAA imprinted polymer (black) and E2-4VP imprinted polymer (red) on the analysis of E2 and 17α-E2. Capacity factor $K = (t-t_0)/t_0$; t and t_0 are the retention time of E2 and acetone (void marker), respectively; Separation factor = $(t_\beta - t_0)/ (t_\alpha - t_0)$; t_β and t_α are the retention time of E2 and 17α-E2, respectively; Imprinting factor = K_M/K_C; K_M and K_C are the capacity factor of E2 on the imprinted polymer and the control polymer, respectively.

4.1.4 Conclusions

A methodology based on molecular dynamic simulations and free energy calculations for more rational design of molecularly imprinted polymers (MIPs) has been developed. Computational models including all the imprinting species at the correct ratios were established, thereby providing better understanding on the role of the different constituents during the imprinting process. Hydrogen bonding analysis and free energy results indicate that methacrylic acid is a more favorable functional monomer than 4-vinylpyridine for imprinting E2, which has previously been confirmed during chromatographic studies. Furthermore, studying the modeled π-π stacking interactions indicates that the interaction between the aromatic moiety of divinylbenzene (cross-

linker) and E2 contributes to the functionality of the binding cavities in the resulting MIPs. Experimental HPLC separation analysis of the template and its structural analogues at the studied MIP systems confirms that the selected functional monomer (methacrylic acid), and the cross-linker (divinylbenzene) follow the theoretical predictions, and lead to the most efficient molecular recognition stationary phase material.

4.1.5 References

1. Andersson, H. S.; Nicholls, I. A., Spectroscopic evaluation of molecular imprinting polymerization systems. *Bioorg. Chem.* **1997,** 25, (3), 203-211.

2. Piletsky, S. A.; Karim, K.; Piletska, E. V.; Day, C. J.; Freebairn, K. W.; Legge, C.; Turner, A. P. F., Recognition of ephedrine enantiomers by molecularly imprinted polymers designed using a computational approach. *Analyst* **2001,** 126, (10), 1826-1830.

3. Chianella, I.; Lotierzo, M.; Piletsky, S. A.; Tothill, I. E.; Chen, B.; Karim, K.; Turner, A. P. F., Rational design of a polymer specific for microcystin-LR using a computational approach. *Anal. Chem.* **2002,** 74, (6), 1288-1293.

4. Wu, L.; Sun, B.; Li, Y.; Chang, W., Study properties of molecular imprinting polymer using a computational approach. *Analyst* **2003,** 128, (7), 944-949.

5. Dineiro, Y.; Menendez, M. I.; Blanco-Lopez, M. C.; Lobo-Castanon, M. J.; Miranda-Ordieres, A. J.; Tunon-Blanco, P., Computational approach to the rational design of molecularly imprinted polymers for voltammetric sensing of homovanillic acid. *Anal. Chem.* **2005,** 77, (20), 6741-6746.

6. Molinelli, A.; O'Mahony, J.; Nolan, K.; Smyth, M. R.; Jakusch, M.; Mizaikoff, B., Analyzing the Mechanisms of Selectivity in Biomimetic Self-Assemblies via IR and NMR Spectroscopy of Prepolymerization Solutions and Molecular Dynamics Simulations. *Anal. Chem.* **2005,** 77, (16), 5196-5204.

7. Ye, L.; Weiss, R.; Mosbach, K., Synthesis and Characterization of Molecularly Imprinted Microspheres. *Macromolecules* **2000,** 33, (22), 8239-8245.

8. Rachkov, A.; McNiven, S.; El'skaya, A.; Yano, K.; Karube, I., Fluorescence detection of b-estradiol using a molecularly imprinted polymer. *Anal. Chim. Acta* **2000,** 405, (1-2), 23-29.

9. Piscopo, L.; Prandi, C.; Coppa, M.; Sparnacci, K.; Laus, M.; Lagana, A.; Curini, R.; D'Ascenzo, G., Uniformly sized molecularly imprinted polymers (MIPs) for 17β-estradiol. *Macromol. Chem. Phys.* **2002,** 203, (10/11), 1532-1538.

10. Dong, H.; Tong, A.-j.; Li, L.-d., Syntheses of steroid-based molecularly imprinted polymers and their molecular recognition study with spectrometric detection. *Spectrochim. Acta, Part A* **2003,** 59A, (2), 279-284.

11. Sanbe, H.; Haginaka, J., Uniformly sized molecularly imprinted polymers for bisphenol A and b-estradiol: retention and molecular recognition properties in hydro-organic mobile phases. *J. Pharm. Biomed. Anal.* **2003,** 30, (6), 1835-1844.

12. Wei, S.; Molinelli, A.; Mizaikoff, B., Molecularly imprinted micro and nanospheres for the selective recognition of 17β-estradiol *Biosens. Bioeletron.* **2006,** 21, (10), 1943-1951.

13. Case, D. A.; Darden, T. A.; T.E. Cheatham, I.; Simmerling, C. L.; Wang, J.; Duke, R. E.; R.Luo; Merz, K. M.; Wang, B.; Pearlman, D. A.; Crowley, M.; Brozell, S.; Tsui, V.; Gohlke, H.; J.Mongan; Hornak, V.; Cui, G.; Beroza, P.; Schafmeister, C.; Caldwell, J. W.; Ross, W. S.; Kollman, P. A., amber8. **2004**, AMBER 8, University of California, San Francisco.

14. Wang, J.; Cieplak, P.; Kollman, P. A., How well does a restrained electrostatic potential (RESP) model perform in calculating conformational energies of organic and biological molecules? *J. Comput. Chem.* **2000,** 21, (12), 1049-1074.

15. Wang, J.; Wolf, R. M.; Caldwell, J. W.; Kollman, P. A.; Case, D. A., Development and testing of a general Amber force field. *J. Comput. Chem.* **2004,** 25, (9), 1157-1174.

16. Jakalian, A.; Bush, B. L.; Jack, B. D.; Bayly, C. I., Fast, Efficient Generation of High-Quality Atomic Charges. AM1-BCC Model: I. Method. *J. Comp. Chem.* **2000,** 21, 132-146.

17. Toukmaji, A.; Sagui, C.; Board, J.; Darden, T., Efficient particle-mesh Ewald based approach to fixed and induced dipolar interactions. *J. Chem. Phys.* **2000,** 113, (24), 10913-10927.

18. Sagui, C.; Pedersen, L. G.; Darden, T. A., Towards an accurate representation of electrostatics in classical force fields: Efficient implementation of multipolar interactions in biomolecular simulations. *J. Chem. Phys.* **2004,** 120, (1), 73-87.

19. Ryckaert, J. P.; Ciccotti, G.; Berendsen, H. J. C., Numerical integration of the Cartesian equations of motion of a system with constraints: molecular dynamics of n-alkanes. *J. Comput. Phys.* **1977,** 23, (3), 327-341.

20. Dirion, B.; Schillinger, E.; Sellergren, B., Development of a high throughput synthesis technique for the optimization of MIPs for 17β-Estradiol. *Mater. Res. Soc. Symp. Proc.* **2004,** 787, (Molecularly Imprinted Materials--2003), 53-60.

21. Torimoto, N.; Ishii, I.; Hata, M.; Nakamura, H.; Imada, H.; Ariyoshi, N.; Ohmori, S.; Igarashi, T.; Kitada, M., Direct Interaction between Substrates and Endogenous Steroids in the Active Site May Change the Activity of Cytochrome P450 3A4. *Biochemistry* **2003,** 42, (51), 15068-15077.

4.2 Probing the Nature of Template-MIP Interactions by Spectroscopic Analysis

4.2.1 Introduction

Experimental evidence from previously reported batch rebinding studies support that the selectivity of the synthesized MIP is strongly related to the initial stability of the template-monomer complex in the pre-polymerization solution. Methacrylic acid has been proven as an effective functional monomer for imprinting E2[1]. The nature of non-covalent interactions responsible for complex formation during imprinting of the template E2 with the functional monomer methacrylic acid was initially investigated by ^{1}H-NMR spectrometry. ^{1}H-NMR experiments and molecular dynamics simulations have revealed that the dimerization of monomers plays a crucial role in optimizing this particular imprinting strategy. Furthermore, infrared spectroscopic (IR) experiments confirm hydrogen bonding interaction between E2 and methacrylic acid within the imprinted polymers, which proves that the specific functionalities of the monomers responsible for assembling the initial pre-polymerization complex are retained as the prevalent rebinding mechanism after the polymerization. Infrared attenuated total reflection (IR-ATR) spectroscopy enables the evaluation of polymer powder samples via molecule-specific absorption of radiation in the evanescent field[2]. Complementarily, direct analysis in real time (DART)-mass spectrometry studies confirmed the presence of specific functionalities of the imprinted polymer to the template molecule by direct analysis at the imprinted and control polymer powder prior to and after template extraction. These spectroscopic results provide the fundamental analytical support for rationalizing the mechanisms of recognition during the imprinting process, and for probing the governing interactions for selective binding site formation at a molecular level. In addition, the

rebinding properties of imprinted polymers and the corresponding control polymers also prove that the specific functionalities of the monomers responsible for assembling the initial pre-polymerization complex are retained as the dominating rebinding mechanism when analytically applying the MIP matrix.

4.2.2 Experimental section

4.2.2.1 Chemicals

Deuterated solvents for NMR studies were obtained from Sigma-Aldrich (Milwaukee, WI), and used as supplied.

4.2.2.2 NMR titration and Job's plot analysis

^{1}H NMR measurements were performed at a Varian Mercury Vx 300 spectrometer at 300 MHz equipped with a 5-mm broadband probe head. Proton spectra were acquired with a spectral width of 4,500 and 16,384 data points. The titration study was performed by maintaining a constant amount of template (0.04 M) at increasing amounts of functional monomer (1 to 20 equivalents). The titration curve provides a $\delta_{complex}$ of 3.628 ppm. The complex stoichiometry was determined by Job's plot analysis. Stock solutions of E2 (0.16 M), and HAc (0.16 M) in acetone-d6 were prepared. Ten NMR tubes were filled with 0.75 mL solutions of E2 and HAc at the following volume ratios: 1:9, 2:8, 3:7, 4:6, 5:5, 6:4, 7:3, 8:2, and 9:1. ^{1}H NMR spectra were recorded, and the concentration of the complex was calculated as follows[3]: $[complex] = [template]_{tot} \times (\delta_{obs} - \delta_{template}) / (\delta_{complex} - \delta_{template})$, where $[template]_{tot}$ is the total concentration of the template in solution, δ_{obs} is the observed chemical shift, $\delta_{template}$ is the chemical shift of the 17-proton of E2, and $\delta_{complex}$ is the chemical shift of the 17-proton in the complex.

$\delta_{complex}$ use the chemical shift of the 17-proton of E2 where the E2: AA ratio is 1:16. As shown in Figure 4.11A, the increase of the chemical shift slows down after 1:16, which indicates that a secondary aggregation of the complex was probably formed. The studies in section 4.2.3.2 show that there is monomer dimerization in the imprinting system, which indicates the formation of a secondary aggregation of the complex because of the monomer-monomer association. In this case, it is difficult to determine the exact value of $\delta_{complex}$ as Job' plot is used for determining a simple system with only host-guest interaction; however, it is still possible to determine the right value of template:monomer ratio from the Job'plot, as ($\delta_{complex}$ - $\delta_{template}$) is a constant value independent of the value of $\delta_{complex}$, which therefore will not affect the x-coordinate of the intersection point in the Job's plot.

4.2.2.3 Monomer dimerization studies

^{1}H NMR measurements were performed at a Varian Mercury Vx 300 spectrometer at 300 MHz equipped with a 5-mm broadband probe head. Proton spectra were acquired with a spectral width of 4,500 and 16,384 data points. 56 μL of MAA was dissolved in 0.7 mL of $CDCl_3$ and acetone-d_6, respectively.

4.2.2.4 Mass spectrometric (MS) studies of the polymer matrix

MS measurements at MIP and control polymer powder samples were performed with an AccuTOF orthogonal acceleration TOF MS (JEOL, Peabody, MA, USA) equipped with a DART ion source (JEOL, Peabody, MA, USA). The mass scale was calibrated using poly(ethylene glycol) (PEG600) resulting in a $[M+H]^+$ ion series in positive-ion mode.

4.2.2.5 IR studies of the polymer matrix

Transmission-absorption IR data were recorded at a Bruker Equinox 55 Fourier transform infrared (FT-IR) spectrometer (Bruker Optics, Billerica, MA) equipped with a liquid nitrogen-cooled mercury-cadmium-telluride (MCT) detector in the spectral range of 4000-400 cm^{-1} at a spectral resolution of 4 cm^{-1}. The IR spectra of E2 (2×10^{-3} M in $CHCl_3$) and MAA (16×10^{-3} M in $CHCl_3$) were determined in a thin film liquid cell at room temperature with a 200 μm spacer and NaCl windows (PIKE Technologies, Madison, WI). The spectrometer was purged with dry air; 100 repetitive scans were averaged per spectrum.

IR-ATR spectra of the imprinted and control polymers were recorded at a Specac Gateway in-compartment horizontal ATR unit (Specac Inc, Woodstock, GA). Trapezoidal ZnSe ATR crystals (72 × 10 × 6 mm; 45 °; n = 2.43 @ 5 μm; MacroOptica, Moscow, Russia) with 6 effective reflection regions were used. IR-ATR spectra of polymer material deposited directly onto the waveguide surface were recorded at a spectral resolution of 4 cm^{-1} averaging 100 scans.

4.2.2.6 FIAD Analysis

The rebinding experiments for the imprinted polymers and control polymers are described in Section 3.2.2.2.1.

4.2.3 Results and discussion

4.2.3.1 Studying template - functional monomer interactions by NMR

To verify the obtained computational modeling results, NMR studies were performed for investigating the complex formation between the template molecule and the

functional monomer building blocks. As the solubility of E2 in $CDCl_3$ is very low, acetone-d6 was used as solvent instead. Previous results by our research group[4] have confirmed that template-functional monomer interactions in acetone could be based on hydrogen bonding. Furthermore, methacrylic acid has been experimentally confirmed as the most suitable monomer for imprinting E2. Hence, the E2-MAA system was selected as viable model system for fundamental NMR studies in the present work. Acetic acid (AA) was used as a substitute of MAA, as MAA readily polymerizes at room temperature. Although the association constant with the template molecule would be different given the difference in hydrophobicity between AA and MAA, AA has been established as an acknowledged substitute for MAA in spectroscopic studies owing to its photostability[5]. NMR titration studies of the E2-AA system reveal that the primary interaction is based on hydrogen bonding. Observations at the hydroxyl proton in polar media such as acetone with small amounts of water present are difficult, due to rapid exchange between the labile protons of E2 and the solvent deuterium atoms[6]. However, hydrogen interaction can be observed by monitoring the chemical shift of the neighboring protons at the carbon atoms to which the hydroxyl groups are bonded. The signal of the 17-proton of E2 migrates downfield as the titration progresses, in favor of a higher HAc concentration (Figure 4.11 A). Job's plot analysis of this interaction indicates a 6:4 template-monomer stoichiometry (Figure 4.11 B). As this system cannot be reduced to a 1:1 or 1:2 binding system, the binding constant cannot be derived. This analysis is based on the assumption that there is only template–functional monomer interactions in the system, without considering the monomer-monomer association. However, it still

provides some useful information such as the presence of hydrogen bonding interaction between E2 and the acetic acid group.

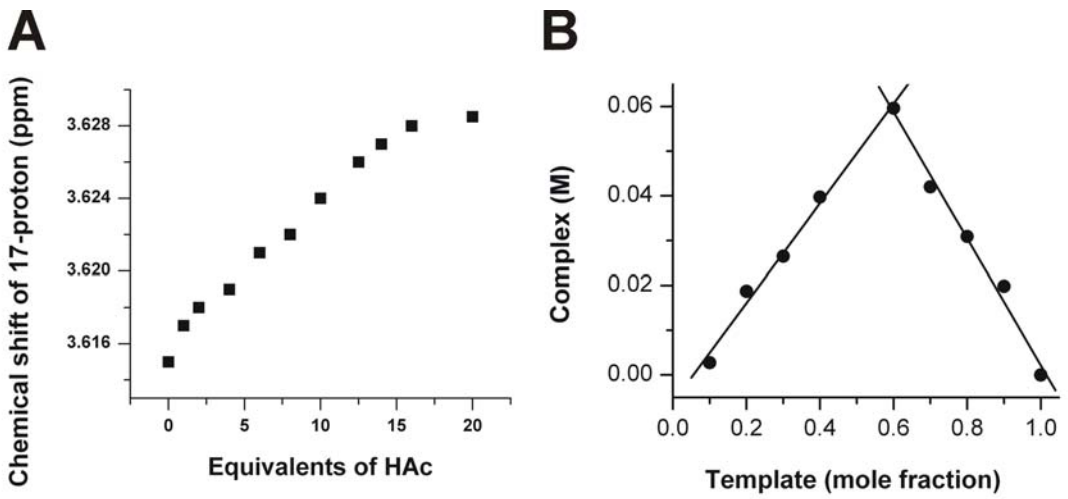

Figure 4.11 (A) Observed shift of the 17-proton of E2 (the proton at the D-ring) upon titration of HAc in acetone-d6 (^{1}H NMR at 25 ^{o}C, 16 scans); (B) Job's plot analysis of E2-HAc (HAc substituting of MAA) based on hydrogen bonding interaction (^{1}H NMR at 25 ^{o}C, 16 scans).

4.2.3.2 Dimerization of functional monomer building blocks

In the pre-polymerization solution, dimerization of monomer building blocks would affect the binding efficiency in forming template-monomer complexes. In non-covalent imprinting, a template-monomer ratio of 1:4 up to 1:10 is empirically applied throughout literature for ensuring complete template-monomer binding, if there are only one or two binding sites available at the template molecule. However, an exceedingly high concentration of monomer in the pre-polymerization solution facilitates monomer dimerization and multimerization.

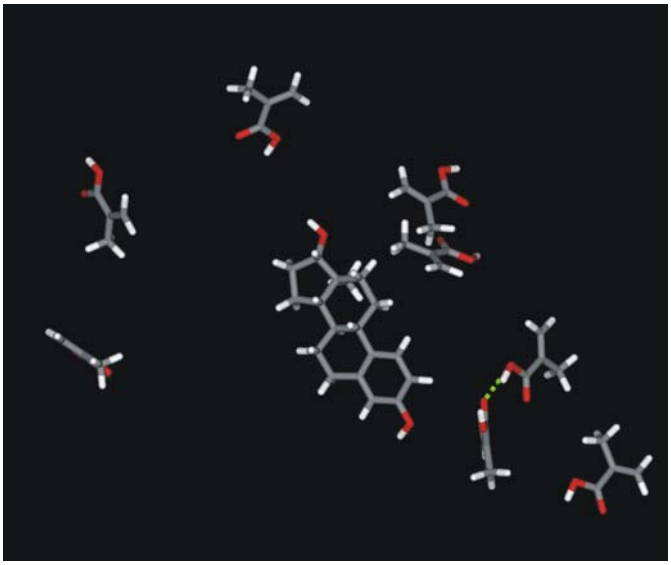

Figure 4.12 The observed MAA-MAA dimer in the modeling system with one molecule of E2 and eight molecules of methacrylic acid in acetone. Porogen molecules are not shown.

As clearly evident in Figure 4.12, at a monomer concentration of 0.61 M, one MAA-MAA dimer is formed in the pre-polymerization solution (E2:MAA = 1:8 in acetone; the concentration of E2 and MAA in the simulation are similar to the concentrations used for synthesizing the real MIP[1]), while the remaining six MAA molecules are free to interact with E2 for assembling the template-monomer complex. Consequently, precisely controlling the monomer concentration in the pre-polymerization solution enables minimizing dimerization of the functional monomer building blocks. Dimerization of monomers is not only related to the concentration of the monomers, but also to their interaction with the porogenic solvent used in the pre-polymerization solution. Figure 4.13 shows the NMR spectra of MAA in $CDCl_3$ (black), and acetone-d6 (red), respectively. Peak A is assigned to the proton shift of COOH, which can be used to monitoring the degree of dimerization for MAA, as MAA would dimerize by forming hydrogen bonds at the COOH position. It is evident that the MAA hydroxyl proton in

acetone-d6 shifts upfield in contrast to $CDCl_3$. As the interaction of MAA with acetone-d6 is stronger than with $CDCl_3$, MAA has a stronger tendency forming dimers in $CDCl_3$ rather than in acetone-d6. The comparatively weak dimerization tendency in acetone-d6 results in an upfield shift of the MAA hydroxyl proton.

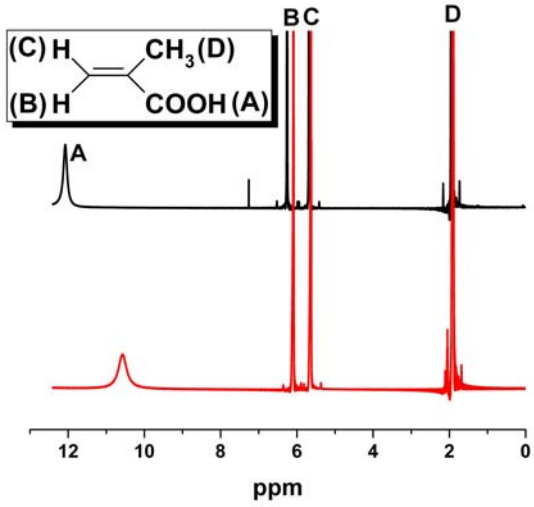

Figure 4.13 ^1H NMR of MAA in $CDCl_3$ (black), and acetone-d6 (red).

Hence, to eliminate, or at least control the extent of dimerization, it is essential considering the porogenic solvent properties, as well as the monomer concentration. It can be expected that in the E2-imprinted system, the E2-MAA ratio should not exceed 1:8 in a polar solvent such as acetone, and the ratio should be less than 1:8 in a non-polar solvent such as chloroform.

4.2.3.3 Template-polymer matrix interactions studied by IR

IR spectra of imprinted polymers, control polymers, and E2 in solution were compared. It is evident from Figure 4.14 that E2 is characterized by a pronounced and narrow O-H stretching peak at 3470 cm^{-1}, which shifts to 3241 cm^{-1} and broadens in the MIP sample prior to template extraction due to hydrogen bonding interaction of E2 with MAA. The O-H stretching vibration at 3241 cm^{-1} is significantly reduced in intensity after template extraction, however, does not entirely disappear. The continuing existence of O-H stretching signature indicates that the template molecules are not entirely removed after the extraction. As a comparison, there was no peak observed at 3241 cm^{-1} in the control polymers samples, as E2 was not present during synthesis. Figure 4.14 also shows the rather weak O-H stretching mode associated with the MAA control sample (red line, MAA in solution) at 3523 cm^{-1} (free O-H stretching). As proposed based on MD simulations, dimerization is very limited at MAA concentration of 0.61 M; consequently, no hydrogen-bonded O-H stretching band was observed in the IR spectrum of the MAA solution. In the polymer matrix, if all MAA molecules are associated with E2, the peak at 3523 cm^{-1} would shift to lower wavenumbers; however, this peak can still be observed in the MIP samples, which indicates that there is additional MAA contained in the polymer that did not participate in the E2-MAA interaction.

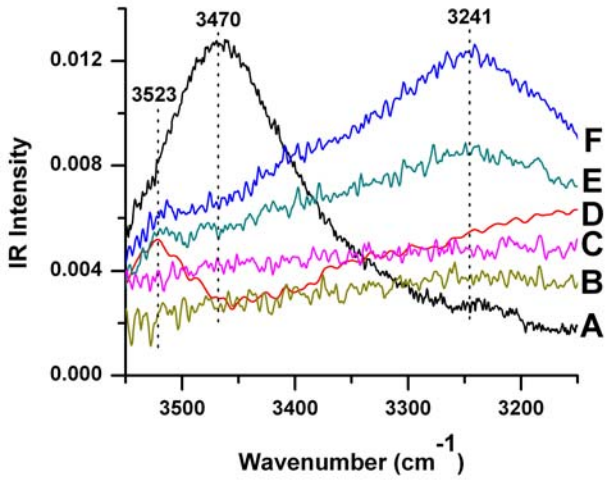

Figure 4.14 Transmission-absorption and attenuated total reflection infrared spectra for the O-H stretching region of: (A) 2×10^{-3} M E2 in $CHCl_3$ (black); (B) Control polymer after extraction (dark yellow); (C) Control polymer before extraction (magenta); (D) 16×10^{-3} M MAA in $CHCl_3$ (red); (E) E2-imprinted polymer after template extraction, E2: MAA= 1:8 (dark cyan); and (F) E2-imprinted polymer before template extraction, E2: MAA= 1:8 (blue).

It is evident in Figure 4.15B that both the E2 peak and a fragment of the E2 peak are present in the MIP sample prior to template extraction. These peaks disappear after template extraction (Figure 4.15C). For comparison, the standard E2 sample shows a strong E2 peak at $[M+H]^+$=273 (Figure 4.15A). As a comparison, the control polymer sample does not reveal any peak in the mass range of 268–275 (Figure 4.15D, E). It should also be noticed that there is no polymer signal observed in this mass spectrum, which indicates that the polymer (poly(MAA-co-DVB)) does not ionize at the MS conditions used in this study. Consequently, it is proposed that the peak at 271 is associated with a fragment of E2, which is absent from the standard E2 sample, and may therefore be induced by the formation of the complex between E2 and (polymerized) MAA. In addition, IR experiments prove the existence of hydrogen bonds between the

template molecule and the functional groups of the imprinted polymer, which are introduced via the functional monomer co-polymerized into the MIP matrix.

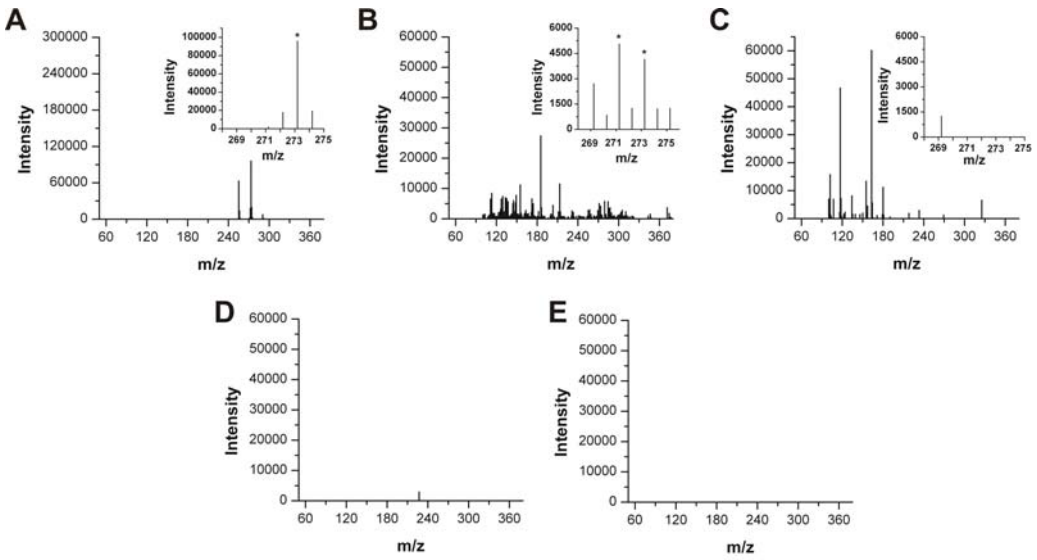

Figure 4.15 (A) Mass spectrum of the standard E2 sample (dry powder), the insert shows the zoom in spectrum: E2, $[M + H]^+ = 273$. (B) Mass spectrum of the MIP prior to template extraction, the insert shows the zoom in spectrum: E2, $[M + H]^+ = 273$, E2 fragment, $[M + H]^+ = 271$. (C) Mass spectrum of the MIP after template extraction, the insert shows the zoom in spectrum. (D) Mass spectrum of the CTL (control polymer) prior to extraction. (B) Mass spectrum of the CTL after extraction. All the mass spectra were obtained on a mass spectrometer with DART (Direct Analysis in Real Time) ion source.

The presence of specific functionalities of the imprinted polymer for binding the template molecule is additionally confirmed by the results obtained from the rebinding experiments discussed in this thesis. Figure 4.16A shows the rebinding isotherm with Freundlich fit for the imprinted polymer and the control polymer, respectively. In the range of 10-2000 μM, the median affinity constant for MIP and control polymer are 9 M^{-1} and 7.3×10^{-13} M^{-1}, respectively. Figure 4.16B shows the relationship of the binding site concentration *N(K)* and the affinity constant *K*. Evidently, the MIP is characterized

by numerous low affinity binding sites, and few high affinity binding sites. As for the control polymer, much less binding sites are distributed throughout the entire affinity range, which proves that specific binding sites are successfully created within the imprinted polymer matrix.

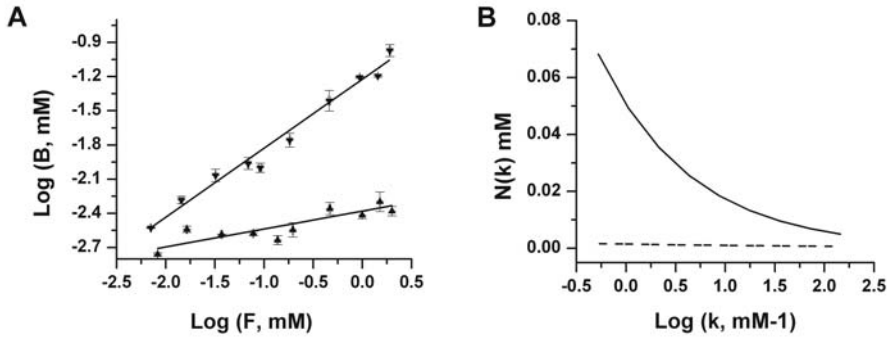

Figure 4.16. (A) Binding isotherm with Freundlich fit for the imprinted polymer (▼: experimental data; line: Freundlich fit) and control polymer (▲: experimental data; line: Freundlich fit). (B) Corresponding affinity distribution calculated using the Freundlich fitting parameters (solid line: imprinted polymer; dashed line: control polymer).

4.2.4 Conclusions

In conclusion, molecular dynamics simulations indicating monomer dimerization in the pre-polymerization solution correlate well with the nature of the porogenic solvent, which was confirmed by NMR studies on hydrogen bonding interactions of methacrylic acid in different solvents. IR experiments confirm that the specific interactions determined via ^{1}H-NMR and MD studies governing the initial formation of template-monomer complexes during MIP synthesis are retained after polymerization, and remain responsible for rebinding of the template molecules. The investigations performed in this

study serve as fundamental analytical support for modeling studies in the framework of this thesis focusing on molecular dynamics simulations of the imprinting system in explicit solvents. Furthermore, batch rebinding studies revealed that the specific functionalities of the monomers essential to rebinding are retained after polymerization, which proves that the application of spectroscopic analysis and computational methods for modeling the pre-polymerization solution provides useful information for optimizing real MIP systems.

4.2.5 References

1. Wei, S.; Molinelli, A.; Mizaikoff, B., Molecularly imprinted micro and nanospheres for the selective recognition of 17β-estradiol *Biosens. Bioeletron.* **2006,** 21, (10), 1943-1951.

2. Harrick, N. J., Internal Reflection Spectroscopy. John Wiley & Sons: New York, 1967; p 327.

3. O'Mahony, J.; Molinelli, A.; Nolan, K.; Smyth, M. R.; Mizaikoff, B., Towards the rational development of molecularly imprinted polymers: 1H NMR studies on hydrophobicity and ion-pair interactions as driving forces for selectivity. *Biosens. Bioelectron.* **2005,** 20, (9), 1884-1893.

4. Molinelli, A.; Weiss, R.; Mizaikoff, B., Advanced Solid Phase Extraction Using Molecularly Imprinted Polymers for the Determination of Quercetin in Red Wine. *J. Agric. Food Chem.* **2002,** 50, (7), 1804-1808.

5. Svenson, J.; Andersson, H. S.; Piletsky, S. A.; Nicholls, I. A., Spectroscopic studies of the molecular imprinting self-assembly process. *J. Mol. Recognit.* **1998,** 11, (1-6), 83-86.

6. Abrahams, R. J.; Fisher, J.; Loftus, P., **1988**, Introduction to NMR Spectroscopy,1st ed. Wiley, New York.

CHAPTER 5

CONCLUSIONS AND OUTLOOK

5.1 Analysis and application of MIPs

Molecularly imprinted polymers (MIPs) synthesized via the non-covalent route have increasingly been adopted as tailor-made synthetic materials capable of selectively re-binding a target analyte, or a group of structurally related compounds based on a combination of recognition mechanisms including size, shape, and functionality. Among the advantageous properties of MIPs are the achievable specific affinity, the relative ease of preparation, and their mechanical and chemical robustness, which renders them ideal materials for applications as stationary phase (e.g., affinity chromatography or solid phase extraction), or as antibody mimics (e.g., biomimetic assays)[1]. Nevertheless, many factors such as the choice of functional monomer, cross-linker, and porogenic solvent, as well as the ratio between template, functional monomer, and cross-linker will affect the resulting imprinting efficiency, polymer particle size, and particle morphology, as demonstrated by the example of imprinting the estrogen 17β-estradiol. A one-step precipitation polymerization method has been developed in this thesis for the preparation of micro- and nanospheres imprinted against E2[2]. With this synthetic strategy, the size and morphology of the imprinted spheres can be rationally controlled via the polymerization conditions, the nature of the cross-linker, the monomer concentration, and the polymerization temperature. It has been shown that thoroughly characterizing and consequently improving the binding characteristics of MIPs are an essential driving force toward next-generation MIP technology. Batch rebinding studies are useful characterization methods providing first insight into the binding properties of a specific

MIP. A comparison of the specific binding properties and porosities of imprinted polymers for E2 prepared by different synthetic routes yielding particulates generated from bulk polymers, microspheres, and nanospheres was obtained[3]. As a consequence, this thesis provides useful guidelines for controlling the particle properties for a desired application by providing detailed studies on the relationships of particle porosity, size, and morphology with the rebinding properties of different MIPs. As the optimization of imprinted materials is based on fundamental understanding of the binding site properties, the investigations presented here aid in establishing a more rational basis for further tailoring imprinted materials to the desired analytical application. MIPs for E2 offer an interesting alternative to natural antibodies used for sample pre-concentration in estrogen analysis. A cost-effective high-throughput analytical methodology for the determination of estrogens spiked into river water samples has been developed based on imprinted polymers for E2. Its use in liquid phase separations and solid phase extraction of a group of estrogens including E2, 17α-E2, E1, E3, and EE2 has been evaluated[4]. It was demonstrated that the loading and washing step requires careful optimization for suppressing non-specific interactions, and for achieving reproducible quantitative recovery rates. The developed MIP sorbents favorably compare to commercially available C18-based SPE materials in terms of selectivity and recovery, providing an advanced sample preparation tool for selective direct extraction of estrogens from complex aqueous samples. Finally, these encouraging results support research into molecular modeling of the governing interactions leading to more rational understanding and designing of the next generation of molecularly imprinted materials with optimized selective retention properties.

5.2 Fundamental modeling of non-covalent imprinting mechanisms

Computational modeling enables studying complex systems or processes by considering small replications of the investigated systems, generating optimized configurations, and providing structural and thermodynamic properties on the target complexes. Such approaches have demonstrated potential for rapid evaluation of molecular imprinting parameters, and for facilitating rational design of MIP synthesis strategies, which is particularly important when working with costly or rare templates. A novel strategy developed in the course of this thesis aims at studying the fundamental interactions of template molecules, functional monomer building blocks, and explicit solvent at molecular level detail using AMBER[5]. We have applied AMBER for the first time to simulating interactions between template and functional monomers, and for confirming hydrogen bonding and π-π stacking interactions during molecular dynamics simulations.

However, for modeling the entire molecular imprinting system, the effects of the cross-linker, and the correct ratio of the involved molecules need to be taken into account. This thesis focuses on modeling and analyzing such molecular systems including cross-linker, solvent, and functional monomer at their experimental ratios for providing close analogy to the experimental conditions present in the actual pre-polymerization solution. Initial studies on the applicability of AMBER for MIP modeling were reported on a pre-polymerization solution for the synthesis of 17β-estradiol MIPs[6]. Acceptable agreement between monomer selection based on computational predictions, and previously reported batch rebinding experiments and resulting capacity factor calculations provide evidence that the developed modeling strategy using molecular

dynamics simulations could in future lead toward a predictive tool providing guidelines for advanced functional monomer selection.

Further advanced methodology based on these initial studies have included 1 molecule of 17β-estradiol, 8 molecules of methacrylic acid (or 4-vinylpyridine), and 40 molecules of divinylbenzene (or ethylene glycol dimethacrylate) in explicit solvent[7]. Simulated annealing provides information on possible lowest energy conformations of the entire pre-polymerization system. It is concluded that a variety of parameters describing the interactions between template and monomers can be extracted providing fundamental understanding on the imprinting mechanisms of complex systems.

While computational predictions provide detailed insight on molecular interactions, the accuracy of these results needs to be confirmed by thorough experimental analysis establishing the validity of the developed models. So far, template-monomer interactions have predominantly been monitored via proton NMR for investigating the extent of complex formation in pre-polymerization solutions. IR spectroscopy experiments confirm that the specific interactions determined via ^{1}H-NMR and MD studies governing the initial formation of template-monomer complexes during MIP synthesis are retained after polymerization, and remain responsible for rebinding of the template molecules. X-ray crystallographic studies[8] were preformed to understand the conformation of pre-polymerization complexes, which may serve as initial configurations for computational modeling studies. In summary, currently applied analytical methods provide useful information for extensive systematic studies on the binding mechanisms involved in the pre-polymerization complex formation. Combining the results of spectroscopic studies with increasingly accurate computational molecular models

provides more conclusive information on binding interactions and stoichiometries ultimately governing the achievable selectivity, and is essential to the development of next-generation MIP technology.

5.3 Outlook

The presented studies on using MIPs as stationary phase material in liquid phase separations and solid phase extraction confirm the utility of MIPs in chromatographic applications. As discussed in Chapter 3.1, an area of growing interest is the use of MIPs as substitutes for natural antibodies in immunoassays. The successful synthesis of imprinted nanospheres, and the preliminary results with biomimetic radioligand binding assays using these imprinted nanospheres support future research on molecular imprinting in the context of assay development for environmental or biomedical analysis. For instance, the SPE extracts from environmental samples or poorly water soluble analytes can be assayed using the strategies of the biomimetic radioligand binding assays developed in this thesis.

An important aspect for characterizing the rebinding properties of MIPs, is to understand the pore structure of the final MIP matrix. Most studies on the pore structure are based on MIPs in dry state using gas sorption measurements. However, most applications of MIP sorbents are concerned with liquid sample media. Depending on the affinity of the MIP for a particular solvent and depending on the degree and distribution of cross-links, the MIP matrix will swell to varying extents. As a consequence, the porosity in swollen state should be of particular interest. Inverse size-exclusion chromatography (ISEC), a widely used chromatographic method for determining the pore size distribution of porous media[9], can be applied to provide more relevant information

on porosity of MIPs in swollen state. Furthermore, the pore geometry has rarely been characterized, which is an important parameter for understanding the binding behavior of MIPs at a molecular level. Consequently, the application of high-resolution sample preparation and imaging techniques operating at a single particle level such as e.g., focus ion-beam techniques should be explored, as they may aid in analyzing the interior structure of MIP particles.

Finally, the present computational modeling strategies for molecular imprinting of E2 need to be further validated and generalized by application to other imprinting systems. The 4-nitrophenol imprinting system previously studied by our research group could be an interesting starting point to continue these studies considering that it is a well-understood synthetic strategy[10-13]. 2-, 3-, and 4-nitrophenol can be included in this system to explore the resulting differences in molecular interactions in detail. Firstly, the number of molecules involved in the modeling system should be increased for including template-template associations, however, such calculations need to use more efficient algorithms or simplifications for achieving acceptable computation times. Secondly, the modeling system needs to be expanded for considering the next synthetic step in the pre-polymerization solution, that is, the molecular interactions during the polymerization process. Thirdly, experimental validation of the observed interactions in the modeling system requires enhanced support by accompanying analytics for increasing confidence in the modeling strategy and potentially establishing predictive calculations for reducing the experimental efforts.

5.4 References

1. Wei, S.; Mizaikoff, B., Recent Advances on Non-covalent Molecular Imprints for Affinity Separations. *J. Sep. Sci.* **2007**, Accepted.

2. Wei, S.; Molinelli, A.; Mizaikoff, B., Molecularly imprinted micro and nanospheres for the selective recognition of 17b-estradiol. *Biosens. Bioelectron.* **2006,** 21, (10), 1943-1951.

3. Wei, S.; Mizaikoff, B., Binding Site Characteristics of 17β-Estradiol Imprinted Polymers. *Biosens. Bioeletron.* **2007**, In press.

4. Wei, S.; Huang, C.-H.; Fernandez, F. M.; Mizaikoff, B., Determination of Estrogens in River Water with SPE using 17β-Estradiol-Imprinted Polymers combined with LC-TOF-MS. *Anal. Chem.* **2007**, Submitted.

5. Wei, S.; Jakusch, M.; Mizaikoff, B., Capturing molecules with templated materials - Analysis and rational design of molecularly imprinted polymers. *Anal. Chim. Acta* **2006,** 578, (1), 50-58.

6. Wei, S.; Jakusch, M.; Mizakoff, B., Investigating the Mechanisms of 17b-Estradiol Imprinting by Computational Prediction and Spectroscopic Analysis. *Anal. Bioanal. Chem.* **2007**, In press.

7. Wei, S.; Jakusch, M.; Mizaikoff, B., Understand the Mechanism of Selectivity in Molecular Imprinted Polymers by Molecular Dynamic Simulation. manuscript in preparation.

8. O'Mahony, J.; Wei, S.; Molinelli, A.; Mizaikoff, B., Imprinted Polymeric Materials. Insight into the Nature of Prepolymerization Complexes of Quercetin Imprinted Polymers. *Anal. Chem.* **2006,** 78, (17), 6187-6190.

9. Yao, Y.; Lenhoff Abraham, M., Determination of pore size distributions of porous chromatographic adsorbents by inverse size-exclusion chromatography. *J. Chromatogr. A* **2004,** 1037, (1-2), 273-82.

10. Masque, N.; Marce, R. M.; Borrull, F.; Cormack, P. A. G.; Sherrington, D. C., Synthesis and Evaluation of a Molecularly Imprinted Polymer for Selective On-Line Solid-Phase Extraction of 4-Nitrophenol from Environmental Water. *Anal. Chem.* **2000,** 72, (17), 4122-4126.

11. Janotta, M.; Weiss, R.; Mizaikoff, B.; Bruggemann, O.; Ye, L.; Mosbach, K., Molecularly imprinted polymers for nitrophenols - an advanced separation material for environmental analysis. *Int. J. Environ. Anal. Chem.* **2001,** 80, (2), 75-86.

12. Caro, E.; Masque, N.; Marce, R. M.; Borrull, F.; Cormack, P. A. G.; Sherrington, D. C., Non-covalent and semi-covalent molecularly imprinted polymers for selective on-line solid-phase extraction of 4-nitrophenol from water samples. *J. Chromatogr., A* **2002,** 963, (1-2), 169-178.

13. Huang, X.; Kong, L.; Li, X.; Zheng, C.; Zou, H., Molecular imprinting of nitrophenol and hydroxybenzoic acid isomers: Effect of molecular structure and acidity on imprinting. *J. Mol. Recognit.* **2003,** 16, (6), 406-411.

APPENDIX A

THE AMBER 8 PACKAGE FOR MIP MODELING

- **AMBER 8:**

The AMBER 8 package consists of a suite of programs that allow users to perform molecular dynamics simulations, and is particularly tailored toward biomolecules. Figure 6.1 shows the information flow within the amber 8 package.

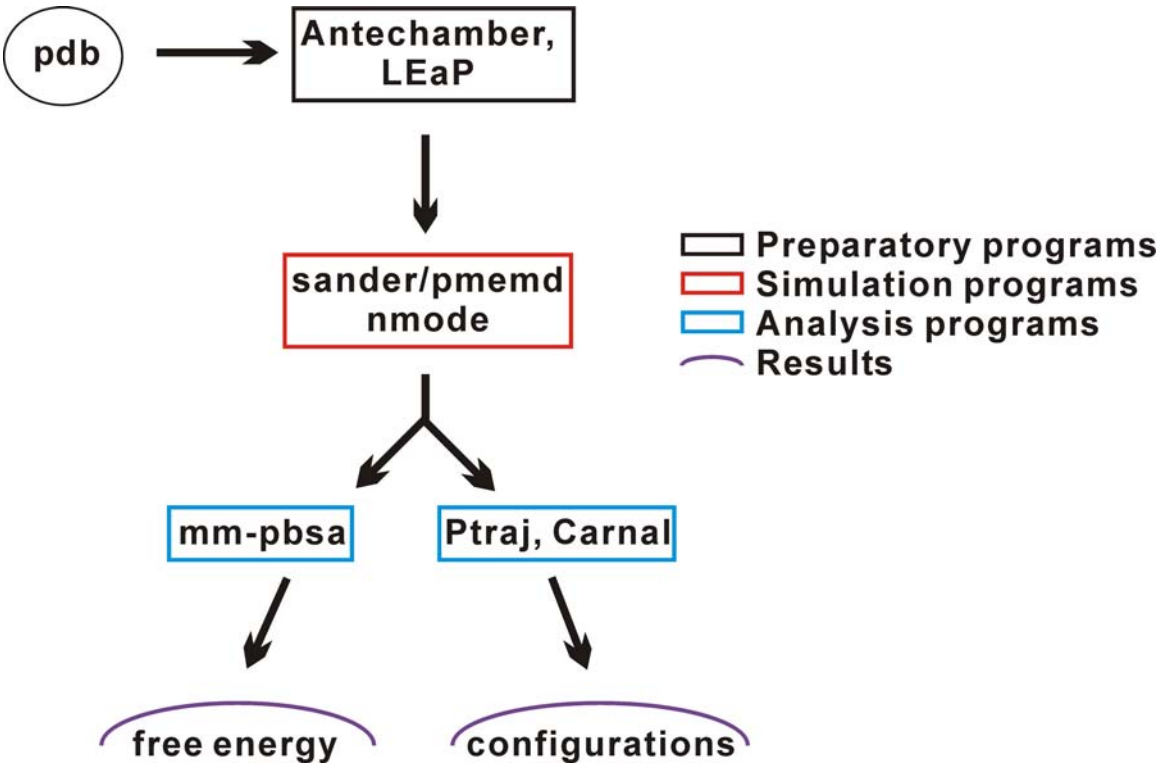

Figure A.1 Information flow in AMBER 8.

- Preparatory programs: *antechamber, LEaP*

Building the simulation model starts with obtaining the Cartesian coordinates for each atom in the system in Protein Databank (PDB) format. These coordinates usually derive from X-ray crystallography, NMR spectroscopy, or model-building. The program *antechamber* is used to convert an input pdb file into a "prep input" file ready for *LEaP*, and the missing parameters are written out by *Parmchk*. *LEaP* provides a platform for building residues and manipulating molecules, and for creating the parameter/topology input files (*prmtop*) and coordinate files (*inpcrd*) for the dynamics simulations.

- Simulation programs: *sander, pmemd, nmode*

Sander and *pmemd* are the main programs for energy minimization and molecular dynamics simulations. *Pmemd* is a new version of *sander* that is optimized for performance in speed and parallel scaling. The energy minimization is done by relaxing the structure by iteratively moving the atoms down an energy gradient until a sufficiently low average gradient is obtained. The molecular dynamics portion will sample an increased configurational space compared to the minimization, and will allow the structure to cross over small potential energy barriers, thereby generating configurations of the system by integrating Newtonian equations of motion. Configurations may be saved at regular intervals during the simulation for later analysis.

Nmode performs molecular mechanics calculations using first and second derivative information to find local minima, transition states, and to perform vibrational analysis. *Nmode* can be used to calculate the entropy (translational, rotational, and vibrational) of the modeling system.

- - Analysis programs: *mm-pbsa, ptraj*

The *mm-pbsa* is a script that automates the energy analysis of snapshots from a molecular dynamics simulation, thereby representing the post-processing method to evaluate free energies of binding, or to calculate absolute free energies of molecules in solution. *mm-pbsa* can be included with *Nmode* to estimate the Gibbs free energy of the modeling system.

Ptraj is a program to analyze and process trajectory or coordinate files created from MD simulations (or from various other sources), carrying out superpositions, extractions of coordinates, calculation of bond/angle/dihedral values, atomic positional fluctuations, correlation functions, analysis of hydrogen bonds, etc..

- **AMBER 8 input files:**

1. The input files for simulations with *sander/pmemd* used in this thesis are listed below:

Table A.1 The input/ouput files of *sander/pmemd.*

file	**in/out**	**purpose**
mdin	input	control data for the minimization/molecular dynamic run
prmtop	input	molecular topology, force field, periodic box type, atom and residue names
inpcrd	input	initial coordinates and (optionally) velocities and periodic box size
refc	input	(optional) reference coords for position restraints; also used for targeted MD

Table A.1 continued

mdcrd	output	coordinate sets saved over trajectory
restrt	output	final coordinates, velocity, and box dimensions if any - for restarting run
mdout	output	user readable state info and diagnostics -o stdout will send output to stdout (to the terminal) instead of to a file

2. The input files for analysis programs *mm-pbsa* and *ptraj* used in this thesis are listed below:

Table A.2 The input/ouput files of *mm-pbsa* and *ptraj*.

program	**file**	**in/out**	**purpose**
ptraj	ptraj.in	in	process and analyze sets of 3-D coordinates read in from a series of input coordinate files
	ptraj.out	out	print out the processing and resulting data
	various output files	out	reprocess the input trajectory to give various output such as atom distance, angle distance, etc.
mm-pbsa	.in	in	the edited input file which specify “receptor”, “ligand” and “complex”
	.out	out	summaries of various energy quantities

- **Generating the initial structure and arranging the molecular topology/parameter and coordinate files:**

The initial individual structures of the template/monomers in the current studies have been obtained from the SciFinder Scholar (Chemical Abstracts Service, Columbus, Ohio). Since no experimentally determined structure or 3D molecular model for the pre-polymerization complex was available, the initial complex (Figure A.2) was built by hand in *xleap*, as described in detail in Chapter 4.1.

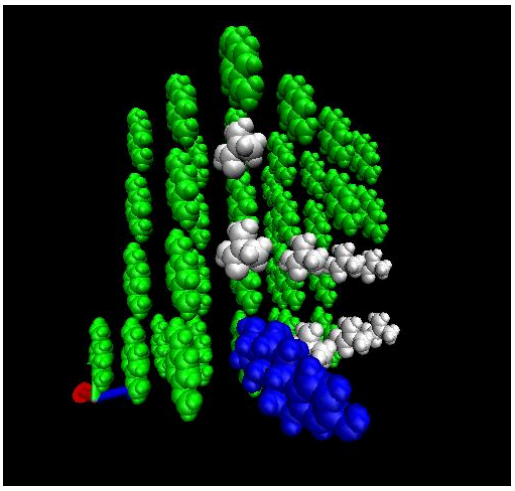

Figure A.2 Initial configuration of the template-functional monomer-crosslinker-initiator complex (blue: template E2, white: functional monomer MAA; green: cross-linker DVB).

To solvate the complex with explicit solvent, a rectangular box of solvent was added around the complex. The complex and the solvent should be saved in *prmtop* and *inpcrd* files. *Prmtop* is the parameter/topology file, which defines the connectivity and parameters for the solvated complex model. This information does not change during the

simulation. *Inpcrd* is the coordinates (and box coordinates and velocities) file, and changes during the simulations.

- **Performing energy minimization and molecular dynamics (MD) simulations**

1. ***Minimization Stage 1 - Creating the target complex***

To compress the complex during the initial minimization, "positional restraints" were used on each of the atoms for holding them together. Such restraints work by adding restraints between atoms, or by gradually changing the temperature; in this case we slowly add restraints from 0 to 1, along with a temperature decrease from 300 K to 10 K, and then compress the complex to a minimized structure.

Below is the sample input for the initial minimization:

```
molecular dynamics run for holding the complex fixed
&cntrl
  imin=0, irest=0, ntx=1,
  nstlim=500000,
  ntwx=1000, ntpr=50,
  ntt=1, tautp=2, tempi=0
  ntp=0, taup=0.2,
  ntb=0, cut=30
  ntc=2, ntf=2,dt=0.002
  iwrap=0,
  nmropt=1
/
```

```
&wt
  type='REST',
  istep1=1,
  istep2=500000,
  value1=0,
  value2=1
/
&wt
  type='TEMP0',
  istep1=1,
  istep2=500000,
  value1=300,
  value2=10
/
&wt
   type='END'
/
LISTIN=POUT
LISTOUT=POUT
DISANG=RST.dist
```

The *RST.dist* file specifies the restraint conditions that have been added to this simulation. In these simulations, restraints were added between the final atom of the first molecule and the first atom of the second molecule; the final atom of the third molecule and the first atom of the fourth molecule; and so on. Then, restraints were also added between the final atom of the first molecule and the first atom of the ninth molecule; the final atom of the second molecule and the first atom of the eleventh molecule; and so on.

```
&rst
 ixpk= 0, nxpk= 0, iat=44 , 45, 0, 0, r1= 0, r2= 0, r3= 3.4, r4= 5.4,
 rk2=0, rk3=20.0, ialtd=0
/
&rst
 ixpk= 0, nxpk= 0, iat=56 , 57, 0, 0, r1= 0, r2= 0, r3= 3.4, r4= 5.4,
 rk2=0, rk3=20.0, ialtd=0
/
&rst
 ixpk= 0, nxpk= 0, iat=68 , 69, 0, 0, r1= 0, r2= 0, r3= 3.4, r4= 5.4,
 rk2=0, rk3=20.0, ialtd=0
/
&rst
 ixpk= 0, nxpk= 0, iat=80 , 81, 0, 0, r1= 0, r2= 0, r3= 3.4, r4= 5.4,
 rk2=0, rk3=20.0, ialtd=0
/
&rst
 ixpk= 0, nxpk= 0, iat=92 , 93, 0, 0, r1= 0, r2= 0, r3= 3.4, r4= 5.4,
 rk2=0, rk3=20.0, ialtd=0
/
&rst
 ixpk= 0, nxpk= 0, iat=104 , 105, 0, 0, r1= 0, r2= 0, r3= 3.4, r4= 5.4,
 rk2=0, rk3=20.0, ialtd=0
/
&rst
 ixpk= 0, nxpk= 0, iat=116 , 117, 0, 0, r1= 0, r2= 0, r3= 3.4, r4= 5.4,
 rk2=0, rk3=20.0, ialtd=0
/
&rst
 ixpk= 0, nxpk= 0, iat=128 , 129, 0, 0, r1= 0, r2= 0, r3= 3.4, r4= 5.4,
 rk2=0, rk3=20.0, ialtd=0
/
&rst
 ixpk= 0, nxpk= 0, iat=140 , 141, 0, 0, r1= 0, r2= 0, r3= 3.4, r4= 5.4,
 rk2=0, rk3=20.0, ialtd=0
/
&rst
 ixpk= 0, nxpk= 0, iat=164 , 165, 0, 0, r1= 0, r2= 0, r3= 3.4, r4= 5.4,
 rk2=0, rk3=20.0, ialtd=0
/
&rst
 ixpk= 0, nxpk= 0, iat=192 , 193, 0, 0, r1= 0, r2= 0, r3= 3.4, r4= 5.4,
 rk2=0, rk3=20.0, ialtd=0
/
&rst
 ixpk= 0, nxpk= 0, iat=220 , 221, 0, 0, r1= 0, r2= 0, r3= 3.4, r4= 5.4,
 rk2=0, rk3=20.0, ialtd=0
/
&rst
 ixpk= 0, nxpk= 0, iat=248 , 249, 0, 0, r1= 0, r2= 0, r3= 3.4, r4= 5.4,
 rk2=0, rk3=20.0, ialtd=0
/
&rst
 ixpk= 0, nxpk= 0, iat=276 , 277, 0, 0, r1= 0, r2= 0, r3= 3.4, r4= 5.4,
 rk2=0, rk3=20.0, ialtd=0
/
&rst
 ixpk= 0, nxpk= 0, iat=304 , 305, 0, 0, r1= 0, r2= 0, r3= 3.4, r4= 5.4,
 rk2=0, rk3=20.0, ialtd=0
/
&rst
 ixpk= 0, nxpk= 0, iat=332 , 333, 0, 0, r1= 0, r2= 0, r3= 3.4, r4= 5.4,
 rk2=0, rk3=20.0, ialtd=0
/
&rst
 ixpk= 0, nxpk= 0, iat=360 , 361, 0, 0, r1= 0, r2= 0, r3= 3.4, r4= 5.4,
 rk2=0, rk3=20.0, ialtd=0
```

```
/
&rst
 ixpk= 0, nxpk= 0, iat=388 , 389, 0, 0, r1= 0, r2= 0, r3= 3.4, r4= 5.4,
 rk2=0, rk3=20.0, ialtd=0
/
&rst
 ixpk= 0, nxpk= 0, iat=416 , 417, 0, 0, r1= 0, r2= 0, r3= 3.4, r4= 5.4,
 rk2=0, rk3=20.0, ialtd=0
/
&rst
 ixpk= 0, nxpk= 0, iat=444 , 445, 0, 0, r1= 0, r2= 0, r3= 3.4, r4= 5.4,
 rk2=0, rk3=20.0, ialtd=0
/
&rst
 ixpk= 0, nxpk= 0, iat=472 , 473, 0, 0, r1= 0, r2= 0, r3= 3.4, r4= 5.4,
 rk2=0, rk3=20.0, ialtd=0
/
&rst
 ixpk= 0, nxpk= 0, iat=500 , 501, 0, 0, r1= 0, r2= 0, r3= 3.4, r4= 5.4,
 rk2=0, rk3=20.0, ialtd=0
/
&rst
 ixpk= 0, nxpk= 0, iat=528 , 529, 0, 0, r1= 0, r2= 0, r3= 3.4, r4= 5.4,
 rk2=0, rk3=20.0, ialtd=0
/
&rst
 ixpk= 0, nxpk= 0, iat=556 , 557, 0, 0, r1= 0, r2= 0, r3= 3.4, r4= 5.4,
 rk2=0, rk3=20.0, ialtd=0
/
&rst
 ixpk= 0, nxpk= 0, iat=584 , 585, 0, 0, r1= 0, r2= 0, r3= 3.4, r4= 5.4,
 rk2=0, rk3=20.0, ialtd=0
/
&rst
 ixpk= 0, nxpk= 0, iat=612 , 613, 0, 0, r1= 0, r2= 0, r3= 3.4, r4= 5.4,
 rk2=0, rk3=20.0, ialtd=0
/
&rst
 ixpk= 0, nxpk= 0, iat=640 , 641, 0, 0, r1= 0, r2= 0, r3= 3.4, r4= 5.4,
 rk2=0, rk3=20.0, ialtd=0
/
&rst
 ixpk= 0, nxpk= 0, iat=668 , 669, 0, 0, r1= 0, r2= 0, r3= 3.4, r4= 5.4,
 rk2=0, rk3=20.0, ialtd=0
/
&rst
 ixpk= 0, nxpk= 0, iat=696 , 697, 0, 0, r1= 0, r2= 0, r3= 3.4, r4= 5.4,
 rk2=0, rk3=20.0, ialtd=0
/
&rst
 ixpk= 0, nxpk= 0, iat=724 , 725, 0, 0, r1= 0, r2= 0, r3= 3.4, r4= 5.4,
 rk2=0, rk3=20.0, ialtd=0
/
&rst
 ixpk= 0, nxpk= 0, iat=752 , 753, 0, 0, r1= 0, r2= 0, r3= 3.4, r4= 5.4,
 rk2=0, rk3=20.0, ialtd=0
/
&rst
 ixpk= 0, nxpk= 0, iat=780 , 781, 0, 0, r1= 0, r2= 0, r3= 3.4, r4= 5.4,
 rk2=0, rk3=20.0, ialtd=0
/
&rst
 ixpk= 0, nxpk= 0, iat=808 , 809, 0, 0, r1= 0, r2= 0, r3= 3.4, r4= 5.4,
 rk2=0, rk3=20.0, ialtd=0
/
&rst
 ixpk= 0, nxpk= 0, iat=836 , 837, 0, 0, r1= 0, r2= 0, r3= 3.4, r4= 5.4,
 rk2=0, rk3=20.0, ialtd=0
/
&rst
```

```
 ixpk= 0, nxpk= 0, iat=864 , 865, 0, 0, r1= 0, r2= 0, r3= 3.4, r4= 5.4,
 rk2=0, rk3=20.0, ialtd=0
/
&rst
 ixpk= 0, nxpk= 0, iat=892 , 893, 0, 0, r1= 0, r2= 0, r3= 3.4, r4= 5.4,
 rk2=0, rk3=20.0, ialtd=0
/
&rst
 ixpk= 0, nxpk= 0, iat=920 , 921, 0, 0, r1= 0, r2= 0, r3= 3.4, r4= 5.4,
 rk2=0, rk3=20.0, ialtd=0
/
&rst
 ixpk= 0, nxpk= 0, iat=948 , 949, 0, 0, r1= 0, r2= 0, r3= 3.4, r4= 5.4,
 rk2=0, rk3=20.0, ialtd=0
/
&rst
 ixpk= 0, nxpk= 0, iat=976 , 977, 0, 0, r1= 0, r2= 0, r3= 3.4, r4= 5.4,
 rk2=0, rk3=20.0, ialtd=0
/
&rst
 ixpk= 0, nxpk= 0, iat=1004 , 1005, 0, 0, r1= 0, r2= 0, r3= 3.4, r4= 5.4,
 rk2=0, rk3=20.0, ialtd=0
/
&rst
 ixpk= 0, nxpk= 0, iat=1032 , 1033, 0, 0, r1= 0, r2= 0, r3= 3.4, r4= 5.4,
 rk2=0, rk3=20.0, ialtd=0
/
&rst
 ixpk= 0, nxpk= 0, iat=1060 , 1061, 0, 0, r1= 0, r2= 0, r3= 3.4, r4= 5.4,
 rk2=0, rk3=20.0, ialtd=0
/
&rst
 ixpk= 0, nxpk= 0, iat=1088 , 1089, 0, 0, r1= 0, r2= 0, r3= 3.4, r4= 5.4,
 rk2=0, rk3=20.0, ialtd=0
/
&rst
 ixpk= 0, nxpk= 0, iat=1116 , 1117, 0, 0, r1= 0, r2= 0, r3= 3.4, r4= 5.4,
 rk2=0, rk3=20.0, ialtd=0
/
&rst
 ixpk= 0, nxpk= 0, iat=1144 , 1145, 0, 0, r1= 0, r2= 0, r3= 3.4, r4= 5.4,
 rk2=0, rk3=20.0, ialtd=0
/
&rst
 ixpk= 0, nxpk= 0, iat=1172 , 1173, 0, 0, r1= 0, r2= 0, r3= 3.4, r4= 5.4,
 rk2=0, rk3=20.0, ialtd=0
/
&rst
 ixpk= 0, nxpk= 0, iat=1200 , 1201, 0, 0, r1= 0, r2= 0, r3= 3.4, r4= 5.4,
 rk2=0, rk3=20.0, ialtd=0
/
&rst
 ixpk= 0, nxpk= 0, iat=1228 , 1229, 0, 0, r1= 0, r2= 0, r3= 3.4, r4= 5.4,
 rk2=0, rk3=20.0, ialtd=0
/
&rst
 ixpk= 0, nxpk= 0, iat=1256 , 1257, 0, 0, r1= 0, r2= 0, r3= 3.4, r4= 5.4,
 rk2=0, rk3=20.0, ialtd=0
/
&rst
 ixpk= 0, nxpk= 0, iat=1284 , 1, 0, 0, r1= 0, r2= 0, r3= 3.4, r4= 5.4,
 rk2=0, rk3=20.0, ialtd=0
/
&rst
 ixpk= 0, nxpk= 0, iat=44 , 129, 0, 0, r1= 0, r2= 0, r3= 3.4, r4= 5.4,
 rk2=0, rk3=20.0, ialtd=0
/
&rst
 ixpk= 0, nxpk= 0, iat=56 , 141, 0, 0, r1= 0, r2= 0, r3= 3.4, r4= 5.4,
 rk2=0, rk3=20.0, ialtd=0
```

```
/
&rst
 ixpk= 0, nxpk= 0, iat=68 , 165, 0, 0, r1= 0, r2= 0, r3= 3.4, r4= 5.4,
 rk2=0, rk3=20.0, ialtd=0
/
&rst
 ixpk= 0, nxpk= 0, iat=80 , 193, 0, 0, r1= 0, r2= 0, r3= 3.4, r4= 5.4,
 rk2=0, rk3=20.0, ialtd=0
/
&rst
 ixpk= 0, nxpk= 0, iat=92 , 221, 0, 0, r1= 0, r2= 0, r3= 3.4, r4= 5.4,
 rk2=0, rk3=20.0, ialtd=0
/
&rst
 ixpk= 0, nxpk= 0, iat=104 , 249, 0, 0, r1= 0, r2= 0, r3= 3.4, r4= 5.4,
 rk2=0, rk3=20.0, ialtd=0
/
&rst
 ixpk= 0, nxpk= 0, iat=116 , 277, 0, 0, r1= 0, r2= 0, r3= 3.4, r4= 5.4,
 rk2=0, rk3=20.0, ialtd=0
/
&rst
 ixpk= 0, nxpk= 0, iat=128 , 305, 0, 0, r1= 0, r2= 0, r3= 3.4, r4= 5.4,
 rk2=0, rk3=20.0, ialtd=0
/
&rst
 ixpk= 0, nxpk= 0, iat=140 , 285, 0, 0, r1= 0, r2= 0, r3= 3.4, r4= 5.4,
 rk2=0, rk3=20.0, ialtd=0
/
&rst
 ixpk= 0, nxpk= 0, iat=164 , 333, 0, 0, r1= 0, r2= 0, r3= 3.4, r4= 5.4,
 rk2=0, rk3=20.0, ialtd=0
/
&rst
 ixpk= 0, nxpk= 0, iat=192 , 361, 0, 0, r1= 0, r2= 0, r3= 3.4, r4= 5.4,
 rk2=0, rk3=20.0, ialtd=0
/
&rst
 ixpk= 0, nxpk= 0, iat=220 , 389, 0, 0, r1= 0, r2= 0, r3= 3.4, r4= 5.4,
 rk2=0, rk3=20.0, ialtd=0
/
&rst
 ixpk= 0, nxpk= 0, iat=248 , 417, 0, 0, r1= 0, r2= 0, r3= 3.4, r4= 5.4,
 rk2=0, rk3=20.0, ialtd=0
/
&rst
 ixpk= 0, nxpk= 0, iat=276 , 445, 0, 0, r1= 0, r2= 0, r3= 3.4, r4= 5.4,
 rk2=0, rk3=20.0, ialtd=0
/
&rst
 ixpk= 0, nxpk= 0, iat=304 , 473, 0, 0, r1= 0, r2= 0, r3= 3.4, r4= 5.4,
 rk2=0, rk3=20.0, ialtd=0
/
&rst
 ixpk= 0, nxpk= 0, iat=332 , 501, 0, 0, r1= 0, r2= 0, r3= 3.4, r4= 5.4,
 rk2=0, rk3=20.0, ialtd=0
/
&rst
 ixpk= 0, nxpk= 0, iat=360 , 529, 0, 0, r1= 0, r2= 0, r3= 3.4, r4= 5.4,
 rk2=0, rk3=20.0, ialtd=0
/
&rst
 ixpk= 0, nxpk= 0, iat=388 , 557, 0, 0, r1= 0, r2= 0, r3= 3.4, r4= 5.4,
 rk2=0, rk3=20.0, ialtd=0
/
&rst
 ixpk= 0, nxpk= 0, iat=416 , 585, 0, 0, r1= 0, r2= 0, r3= 3.4, r4= 5.4,
 rk2=0, rk3=20.0, ialtd=0
/
&rst
```

```
 ixpk= 0, nxpk= 0, iat=444 , 613, 0, 0, r1= 0, r2= 0, r3= 3.4, r4= 5.4,
 rk2=0, rk3=20.0, ialtd=0
/
&rst
 ixpk= 0, nxpk= 0, iat=472 , 641, 0, 0, r1= 0, r2= 0, r3= 3.4, r4= 5.4,
 rk2=0, rk3=20.0, ialtd=0
/
&rst
 ixpk= 0, nxpk= 0, iat=500 , 669, 0, 0, r1= 0, r2= 0, r3= 3.4, r4= 5.4,
 rk2=0, rk3=20.0, ialtd=0
/
&rst
 ixpk= 0, nxpk= 0, iat=528 , 697, 0, 0, r1= 0, r2= 0, r3= 3.4, r4= 5.4,
 rk2=0, rk3=20.0, ialtd=0
/
&rst
 ixpk= 0, nxpk= 0, iat=556 , 725, 0, 0, r1= 0, r2= 0, r3= 3.4, r4= 5.4,
 rk2=0, rk3=20.0, ialtd=0
/
&rst
 ixpk= 0, nxpk= 0, iat=584 , 753, 0, 0, r1= 0, r2= 0, r3= 3.4, r4= 5.4,
 rk2=0, rk3=20.0, ialtd=0
/
&rst
 ixpk= 0, nxpk= 0, iat=612 , 781, 0, 0, r1= 0, r2= 0, r3= 3.4, r4= 5.4,
 rk2=0, rk3=20.0, ialtd=0
/
&rst
 ixpk= 0, nxpk= 0, iat=640 , 809, 0, 0, r1= 0, r2= 0, r3= 3.4, r4= 5.4,
 rk2=0, rk3=20.0, ialtd=0
/
&rst
 ixpk= 0, nxpk= 0, iat=668 , 837, 0, 0, r1= 0, r2= 0, r3= 3.4, r4= 5.4,
 rk2=0, rk3=20.0, ialtd=0
/
&rst
 ixpk= 0, nxpk= 0, iat=696 , 865, 0, 0, r1= 0, r2= 0, r3= 3.4, r4= 5.4,
 rk2=0, rk3=20.0, ialtd=0
/
&rst
 ixpk= 0, nxpk= 0, iat=724 , 893, 0, 0, r1= 0, r2= 0, r3= 3.4, r4= 5.4,
 rk2=0, rk3=20.0, ialtd=0
/
&rst
 ixpk= 0, nxpk= 0, iat=752 , 921, 0, 0, r1= 0, r2= 0, r3= 3.4, r4= 5.4,
 rk2=0, rk3=20.0, ialtd=0
/
&rst
 ixpk= 0, nxpk= 0, iat=780 , 949, 0, 0, r1= 0, r2= 0, r3= 3.4, r4= 5.4,
 rk2=0, rk3=20.0, ialtd=0
/
&rst
 ixpk= 0, nxpk= 0, iat=808 , 977, 0, 0, r1= 0, r2= 0, r3= 3.4, r4= 5.4,
 rk2=0, rk3=20.0, ialtd=0
/
&rst
 ixpk= 0, nxpk= 0, iat=836 , 1005, 0, 0, r1= 0, r2= 0, r3= 3.4, r4= 5.4,
 rk2=0, rk3=20.0, ialtd=0
/
&rst
 ixpk= 0, nxpk= 0, iat=864 , 1033, 0, 0, r1= 0, r2= 0, r3= 3.4, r4= 5.4,
 rk2=0, rk3=20.0, ialtd=0
/
&rst
 ixpk= 0, nxpk= 0, iat=892 , 1061, 0, 0, r1= 0, r2= 0, r3= 3.4, r4= 5.4,
 rk2=0, rk3=20.0, ialtd=0
/
&rst
 ixpk= 0, nxpk= 0, iat=920 , 1089, 0, 0, r1= 0, r2= 0, r3= 3.4, r4= 5.4,
 rk2=0, rk3=20.0, ialtd=0
```

```
/
&rst
 ixpk= 0, nxpk= 0, iat=948 , 1117, 0, 0, r1= 0, r2= 0, r3= 3.4, r4= 5.4,
 rk2=0, rk3=20.0, ialtd=0
/
&rst
 ixpk= 0, nxpk= 0, iat=744 , 885, 0, 0, r1= 0, r2= 0, r3= 3.4, r4= 5.4,
 rk2=0, rk3=20.0, ialtd=0
/
&rst
 ixpk= 0, nxpk= 0, iat=764 , 905, 0, 0, r1= 0, r2= 0, r3= 3.4, r4= 5.4,
 rk2=0, rk3=20.0, ialtd=0
/
&rst
 ixpk= 0, nxpk= 0, iat=784 , 925, 0, 0, r1= 0, r2= 0, r3= 3.4, r4= 5.4,
 rk2=0, rk3=20.0, ialtd=0
/
&rst
 ixpk= 0, nxpk= 0, iat=804 , 945, 0, 0, r1= 0, r2= 0, r3= 3.4, r4= 5.4,
 rk2=0, rk3=20.0, ialtd=0
/
&rst
 ixpk= 0, nxpk= 0, iat=824 , 45, 0, 0, r1= 0, r2= 0, r3= 3.4, r4= 5.4,
 rk2=0, rk3=20.0, ialtd=0
/
&rst
 ixpk= 0, nxpk= 0, iat=844 , 57, 0, 0, r1= 0, r2= 0, r3= 3.4, r4= 5.4,
 rk2=0, rk3=20.0, ialtd=0
/
&rst
 ixpk= 0, nxpk= 0, iat=864 , 69, 0, 0, r1= 0, r2= 0, r3= 3.4, r4= 5.4,
 rk2=0, rk3=20.0, ialtd=0
/
&rst
 ixpk= 0, nxpk= 0, iat=884 , 81, 0, 0, r1= 0, r2= 0, r3= 3.4, r4= 5.4,
 rk2=0, rk3=20.0, ialtd=0
/
&rst
 ixpk= 0, nxpk= 0, iat=904 , 93, 0, 0, r1= 0, r2= 0, r3= 3.4, r4= 5.4,
 rk2=0, rk3=20.0, ialtd=0
/
&rst
 ixpk= 0, nxpk= 0, iat=924 , 105, 0, 0, r1= 0, r2= 0, r3= 3.4, r4= 5.4,
 rk2=0, rk3=20.0, ialtd=0
/
&rst
 ixpk= 0, nxpk= 0, iat=944 , 117, 0, 0, r1= 0, r2= 0, r3= 3.4, r4= 5.4,
 rk2=0, rk3=20.0, ialtd=0

&end
```

A detailed explanation for each parameter can be found in the AMBER 8 manual

2. Minimization Stage 2 - Minimizing the entire system

After the initial minimization of the complex, a rectangular box of solvent was added around the complex to solvate the structure. The solvent box (acetone) in the present

work was created by using one acetone molecule as center, and adding acetone molecules around this center molecule. This can be done in *xleap* with the "solvatebox" function. The resulting acetone box (Figure A.3A) is then equilibrated in *sander* until the density of the box is close to the experimentally determined density of acetone (Figure A.3B).

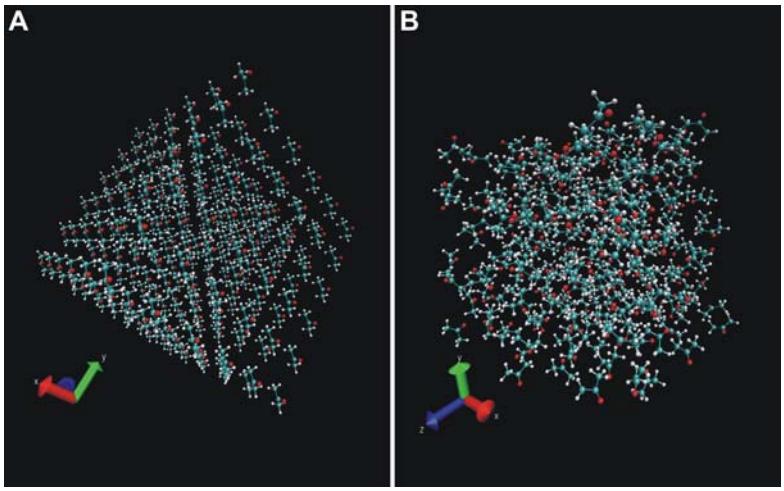

Figure A.3 A: The initial acetone box created in *xleap*. B: The equilibrated acetone box.

The next stage of our minimization is to minimize the entire system with solvent. First, the minimized complex as shown in Figure A.3 was solvated with the acetone box. Then, during this minimization the solvent was allowed to move, and the coordinates of the complex were frozen by using the *ibelly* run, and the *bellymask* command specifying the residue number of the complex. Below, the sample input file is shown:

```
minimization
 &cntrl
   imin=1,
   ntc=1, ntb=1,
   maxcyc=500,ntpr=25,
   ibelly=1, bellymask=:51-130


 &end
```

3. Molecular dynamics simulations - Equilibration

The minimized system must be equilibrated using volume, pressure, and temperature control to adjust e.g., the density of the solvent to experimental values prior to executing the real dynamics runs. The system must be equilibrated first at constant volume to a temperature close to the final temperature prior to implementing constant pressure. In the present system, equilibration was performed at constant volume with the *belly* setting and distance restraint, respectively, which are used to ensure that the complex structure does not disintegrate during the initial MD runs. The sample input files are shown below:

```
Equilibration-constant Volume with belly setting
 &cntrl
   imin=0, irest=0, ntx=1,
   ntt=1, temp0=300.0, tautp=2,
   ntp=0, taup=0.2,
   ntb=1, ntc=2, ntf=2,
   nstlim=5000,
   iwrap=1,
   ntwx=200, ntpr=50,
   ibelly=1, bellymask=:51-130


 &end
```

```
Equilibration-constant Volume with restraints
&cntrl
   imin=0, irest=0, ntx=7,
   ntt=1, temp0=300, tautp=2,
   ntp=0, taup=0.2,
   ntb=1, ntc=2, ntf=2,dt=0.002,
   nstlim=50000,
   iwrap=1,
```

```
  ntwx=200, ntpr=50,
    nmropt=1
/
&wt
  type='REST',
  istep1=1,
  istep2=50000,
  value1=0,
  value2=1,

/
&wt
   type='END'
/
LISTIN=POUT
LISTOUT=POUT
DISANG=RST2.dist


&end
```

The system is then equilibrated at constant pressure for achieveing an appropriate density. The pressure may be maintained at a constant defined value by e.g., scaling the volume. Equilibrations at constant pressure were performed at three pressure relaxation times (*taup*). It can be seen that with lower values, the pressure restraint increases. Therefore, this value is set to 0.05, 0.5, and 5 for the performed equilibrations to gradually decrease the pressure restraint. The sample input file is:

```
Equilibration-constant pressure
molecular dynamics run
 &cntrl
  imin=0, irest=0, ntx=7,
  ntt=1, temp0=300.0, tautp=2,
  ntp=1, taup=0.05,
  ntb=2, ntc=2, ntf=2,
  nstlim=50000,
  iwrap=1,
  ntwx=200, ntpr=50,
 nmropt=1
/
&wt
  type='REST',
  istep1=1,
  istep2=50000,
  value1=0,
  value2=1,

/
&wt
   type='END'
/
LISTIN=POUT
LISTOUT=POUT
DISANG=RST2.dist
```

```
 &end
```

4. Molecular dynamics simulations - Simulation annealing

The next stage is to perform *simulation annealing* on the modeled system. First, the system is slowly heated up over a period of 100 ps to 1200 K at constant volume using following input file:

```
&cntrl
  imin=0
  nstlim=200000,dt=.0005
  ntx=5
  ntpr=50,ntwe=50,ntwx=500
  ntb=1,cut=9,scee=1.2
  ntt=1, tautp=.2
  temp0=1200
  ntc=2, ntf=2
  ibelly=0
&end
```

The next step is to keep the heated system at the same temperature (1200 K), while executing dynamics runs over 350 ps. Individual *mdcrd* files (coordinates) are extracted every 8.75 ps for subsequent simulated annealing using following commands:

```
&cntrl
  imin=0
  nstlim=700000,dt=.0005
  ntx=7
  ntpr=50,ntwe=50,ntwx=2000
  ntwr=-17500
  ntb=1,cut=9,scee=1.2
  ntt=1, tautp=.2
  temp0=1200
  ntc=2, ntf=2
  ntcm=1, nscm=10000, ndfmin=6
  ibelly=0
&end
```

Each *mdcrd* file was used as input file to the final cooling step. The system was slowly down over 13.5 ps in a total of 4 stages. Performing the cooling in stages reduces the probability that the system will be come unstable by becoming extremely un-equilibrated by allowing stepwise equilibration at each temperature. Since the initial structure in these particular simulations is a manually modeled structure rather than an experimental crystal structure, it is likely to be initially much less stable than a validated experimentally obtained structure. In order to allow the initial system to relax in a controlled fashion, a very short time step of 1.0 fs was applied for the cooling stage. Furthermore, the coordinate (mdcrd) write frequency was set to 50 here (ntwx = 50). Setting a low number of steps for writing each coordinate is a preventive measure; if problems occur, the operator should be able to determine those and to identify where the problem results from. Hence, the cooling protocol for the system was defined as follows:

Step 1 - 10,000 steps, 1.0 fs time step (10 ps), initial temperature coupling constant = 4.0 ps, target temperature coupling constant = 3.8 ps

Step 2 - 2,000 steps, 1.0 fs time step (2 ps), initial temperature coupling constant = 3.8 ps, target temperature coupling constant = 0.5 ps

Step 3 - 1,000 steps, 1.0 fs time step (1 ps), initial temperature coupling constant = 0.5 ps, target temperature coupling constant = 0.01 ps

Step 4 - 500 steps, 1.0 fs time step (0.5 ps), temperature coupling constant = 0.01 ps

Here is the input file:

```
&cntrl
  imin=0
  nstlim=13500, dt=.001
  ntx=5
  ntpr=50,ntwe=50,ntwx=500
  ntb=1,cut=9,scee=1.2
  ntt=1
  tempi=1200
  ntc=2, ntf=2
  ibelly=0
  nmropt=1
  iwrap=1
&end
&wt
  type='TEMP0'
  istep1=0, istep2=500
  value1=1200, value2=1200.
&end
&wt
  type='TEMP0'
  istep1=501, istep2=13500
  value1=0, value2=0
&end
&wt
  type='TAUTP'
  istep1=0, istep2=10000
  value1=4., value2=3.8
&end
&wt
  type='TAUTP'
  istep1=10001, istep2=12000
  value1=3.8, value2=0.5
&end
&wt
  type='TAUTP'
  istep1=12001, istep2=13000
  value1=0.5, value2=0.01
&end
&wt
  type='TAUTP'
  istep1=13001, istep2=13500
  value1=0.01, value2=0.01
&end
&wt
  type='END'
&end
```

5. Analysis the MD results

Ptraj is used to process the configurations of the simulated system. *Ptraj* it is necessary to (1) read in a parameter/topology file (*prmtop)*, (2) set up a list of input

coordinate files (*inpcrd*), (3) optimally specify an output file, and (4) specify a series of actions to be performed at each coordinate set that is read in.

The *Ptraj* program contains a generic facility for keeping track of lists of pair interactions useful for the calculation of e.g., hydrogen bonding or π-π stacking interactions. It is furthermore designed to track specific interactions once the hydrogen bond "donor/acceptor" for hydrogen bonding or aromatic rings for π-π stacking interactions are identified.

Here is the sample input for calculating the hydrogen bonding interactions:

```
trajin cpl_maa_configs_cooled.pseudo_mdcrd
donor mask :BE2@O1
donor mask :BE2@O2
donor mask :2-9@O1
donor mask :2-9@O2
acceptor mask :BE2@O1 :BE2@H14
acceptor mask :BE2@O2 :BE2@H24
acceptor mask :MAA@O2 :MAA@H6
hbond distance 3.5 series Hbond
```

In this input file, the hydrogen bonding between 17β-estradiol (BE2) and MAA are calculated with a cut-off distance of 3.5 Å.

Distance command is used to calculate the π-π distance of the aromatic rings of the target molecules. The edge-to-face distance is calculated by measuring the distance of an atom in E2 with the atoms of the aromatic rings of the other molecule (e.g., DVB, 4VP, etc.). The sample input file is:

```
trajin cpl_maa_configs_cooled.pseudo_mdcrd
distance end_to_end :BE2@C16 :11@C6 out  dist_end_to_end.list
```

To visualize the resulting modeling system, it is necessary to center the interested atoms based on the center of geometry of the atomic arrangement in the mask to the center of the periodic box, or the origin. Below is the sample input file:

```
trajin cpl_maa_configs_cooled.pseudo_mdcrd
center :1-2
image origin center
```

In order to count the number of molecules within the first solvation shell of the template molecule, the *WATERSHELL* function in *ptraj* is used:

```
trajin cpl_maa_configs_cooled.pseudo_mdcrd
watershell :1 watershellMAA_maa.list :MAA
```

The RDF function in *ptraj* enables the description of how - on average - the atoms in a system are radially packed around each other. This procedure can be used to calculate the relationship of the density of MAA with the cut-off of the solvation shell of E2. The sample input file for calculating the density of MAA around the O1and O2 atom of E2 reads as:

```
trajin cpl_maa_configs_cooled_all.pseudo_mdcrd
```

```
image origin
rms first
radial rdf_BE2_O1-MAA 0.05 8.0 :MAA :BE2@O1 density 0.0070999
radial rdf_BE2_O2-MAA 0.05 8.0 :MAA :BE2@O2 density 0.0070999
go
```

The density value 0.0068908 is calculated by 1.015*6.022/(10*86.09), in which 1.015 is the standard density of MAA, and 86.09 is the molecular weight of MAA.

The MM_GBSA approach represents the post-processing method to evaluate free energies of binding, or to calculate absolute free energies of molecules in solution. In the present work, the system after simulated annealing was analyzed by MM_GBSA to calculate the binding energy of template molecules to the rest of the system. Although this method has been well established for DNA/RNA, there has no application of this model for MIPs been reported to date. Therefore, the MM_GBSA code has been modified in the present work to adjust to the needs of MIP calculations. Here is the script for mm_gbsa.pl:

```
#!/usr/bin/perl -w

use strict;
use POSIX;
use File::Path;
use Class::Struct;


# data structure definitions

struct ComplexData => {
  residues => '%',
  pdbtemp => '$',
  pdbfile => '$',
  crdfile => '$',
  prmtopstr => '$',
  mpberr => '$'
};


# global variables

my %globals;
```

```
my %complex_info;
my %results;


### main
&init;

#&print_globals();

&define_complexes;
#&print_info_all_complexes;
&run_mm_pbsa;
&print_header;
&print_results;
&archive_structures;
$globals{FINISHED_CLEAN}=1;


############################
#
# TODOs:
#
# (none)
#
############################
### print "There are open TODOs!\n";

### end of main



sub usage{
   print &version() . "\n";
   print "\nusage: " . &basename($0) . " inputfile\n\n" ;
   exit 1;
}


sub version{
   my $id='$Id: mip_pbsa.pl,v 1.18 2006-07-26 19:10:30+02 jakuschm Exp $';
}

sub dirname{
   my ($path)=@_;
   $path =~ s?[^/]+$??
   $path;
}

sub basename{
   my ($path)=@_;
   $path =~ s  .*/Ë;
   $path;
}


sub init{
   &set_defaults;
   &read_input(@ARGV);
   &check_globals;
   &init_temp;
}



sub init_temp{

   my $dir=$globals{TEMPDIR};

   -d $dir && die "Temporary dir $dir already exists - try again!\n stopped";
```

```
   mkdir $dir,0777
            or die "can't create temporary directory $dir: $!, stopped";

   $globals{TEMP_EXISTS} = 1;
}



sub set_defaults{
   %globals = (
                        INPUT_PRMTOP       => "",
                        INPUT_LEAPRC       => "",
                        INPUT_MDCRD        => "",
                        TEMPLATE_MM_PBSA_IN => "",
                        PATH_LEAPDATA      => "",
                        CENTRAL_RESIDUES    => 1,
                        CUTOFF_CMPLX       => 2.0,
                        NUM_CMPLX_MAX      => 0,
                        CARNAL    => "/opt/modelling/programs/amber7/exe/carnal",
                        PATH_PRMTOPS_COMPLEXES    => "./prmtops",
#                       OVERWRITE_OUTPUT_MM_PBSA   => 0,
                        KEEP_TEMPFILES            => 0,
                        TEMPDIR           => "/tmp/temp_mip_pbsa_$$",
                        MAX_CPL_IN_DIR     => 1000,
#                       VAR => val,
                        DUMMY => ""
                        );
}

sub read_input{
   my $infile = shift @ARGV;

   defined $infile or &usage();

   open INFILE, $infile or
            die "cannot open file \"$infile\" for reading: $!\n";

   while (<INFILE>) {
#            $n_read++;
#            print "$n_read\n";

            s/\"\'//g;  # remove quotes
            s/\#.*$// ; # remove comments
            next if( /^\s*$/ ); # empty line
            s/^\s+//;   # remove whitespace
            s/\s+$//;

#            print "$_\n";

            my @fields=split /\s+/;

            assert(@fields>0);

            if(@fields==1){
               warn "warning: ignoring line with only one input field:\n >$_<\n ";
               next;
            }

            if(@fields>2){
               warn "warning: only first two fields are used from\n >$_<\n ";
            }

            my ($key,$val)=@fields;

            if(!defined $globals{$key}){
               warn "warning: ignoring unknown key \"$key\"\n";
               next;
            }

            $globals{$key}=$val;
```

```
    }
    close INFILE;

    # set some other global vars
    my $cwd=getcwd;
    $globals{WORKDIR}=$cwd;

    my $pref=&basename($infile);
    $pref =~ s/\.[^.]*$// ;

    $globals{OUTPUT_PREFIX}=$pref;
    $globals{MM_PBSA_OUT_CPIO}=$globals{OUTPUT_PREFIX} ."_mmpbo.cpio";
    $globals{DIR_STRUCTFILES}=$globals{OUTPUT_PREFIX} . "_structfiles";


}



sub check_globals{

    my $cwd=$globals{WORKDIR};

    die "Please set environment variable AMBERHOME!\nstopped"
            if (!defined $ENV{AMBERHOME});

    die "Please set environment variable MMPBSAMODHOME!\nstopped"
            if (!defined $ENV{MMPBSAMODHOME});


    # check for readable files
    foreach my $fil ( $globals{INPUT_PRMTOP},
                      $globals{INPUT_LEAPRC},
                      $globals{INPUT_MDCRD} ,
                      $globals{TEMPLATE_MM_PBSA_IN}
                      ){

            die "$fil: no such file or directory, stopped"
               if ( ! -e $fil );

            die "File $fil not readable, stopped"
               if ( ! -r $fil );
    }


    # check for existing dirs
    foreach my $dir ( $globals{PATH_LEAPDATA}
                      ){
            die "no such directory: \"$dir\", stopped"
               if ( ! -d $dir );
    }


    # check for writable dirs
    foreach  my $dir (
                       $globals{PATH_PRMTOPS_COMPLEXES}
                       ){

            die "no such directory: \"$dir\", stopped"
               if ( ! -d $dir );

            die "directory $dir not writable, stopped"
               if ( ! -w $dir );
    }


    die "character '? not allowed in OUTPUT_PREFIX, stopped"
            if ( $globals{OUTPUT_PREFIX} =~ m/? );
```

```
   die "carnal binary $globals{CARNAL} \nnot found or no execute permission,
stopped.\n(CWD=$cwd)\n"
            if ( ! -x $globals{CARNAL} );

   die "illegal value CENTRAL_RESIDUES, must be RES1[-RES2], stopped"
            if ( ! ( $globals{CENTRAL_RESIDUES} =~ /^\d*(\d|-)\d*$/ ) );


   die "Cutoff value \"$globals{CUTOFF_CMPLX}\" is not numeric, stopped"
            if ( ! ( $globals{CUTOFF_CMPLX} =~ /^\d*(\d|\.)\d*$/ ) );


   if( -f $globals{MM_PBSA_OUT_CPIO}){
               die "archive $globals{MM_PBSA_OUT_CPIO} already exists,"
                     . " stopped";
   }
}




sub print_globals{
   foreach my $key (sort { $a <=> $b } keys %globals ){
            printf "%-20s=> %s\n", $key, $globals{$key};
   }
}

sub new_tempfile {
   my ($prefix)=@_;

   my $dir=$globals{TEMPDIR};

   my $num=0;

   my $fname = "$dir/$prefix.$num";

   while ( -e $fname ){
            $num++;
            if ($num > 10000) {
               die "Could not find a temporary file name, stopped "
            }
            $fname = "$dir/$prefix.$num";
   }

   &touch($fname);

   return $fname;
}


sub new_tempsubdir {
   my ($prefix)=@_;

   my $dir=$globals{TEMPDIR};

   my $num=0;

   my $dname = "$dir/$prefix.$num";

   while ( -e $dname ){
            $num++;
            if ($num > 10000) {
               die "Could not create a temporary subdir, stopped "
            }
            $dname = "$dir/$prefix.$num";
   }

   mkdir $dname,0777
            or die "can't create temporary subdir $dname: $!, stopped";
```

```
    return $dname;
}


sub touch{
    foreach my $file (@_) {
            open FIL, ">$file"
               or die "cannot create file $file: $!\n stopped";
            close FIL;
    }
}



sub define_complexes{
    my $prmtop=$globals{INPUT_PRMTOP};
    my $mdcrd=$globals{INPUT_MDCRD};

    my $maxcplnum=$globals{NUM_CMPLX_MAX};


    foreach my $rnum (&expand_reslist($globals{CENTRAL_RESIDUES})){

            my $lastcount=keys %complex_info;
#       my @tmp=sort keys %complex_info;
#       print STDERR "@tmp\n";
#
#       print STDERR "xxxxx $maxcplnum $lastcount \n";

            last if( $maxcplnum > 0 && $lastcount >= $maxcplnum  ) ;

            my $pdbtempdir=&new_tempsubdir("pdbs");

            print STDERR "Extracting complexes with central residue $rnum\t" ;
            printf STDERR "time: %d\n",time();

            my $analout=&run_carnal($prmtop,
                                    $mdcrd,
                                    $rnum,
                                    $pdbtempdir);

            &parse_analout($analout,$pdbtempdir);
    }

    print STDERR "Writing coordinate files\t";
    printf STDERR "time: %d\n",time();
    &make_coorfiles();

    print STDERR "Updating prmtop cache\t";
    printf STDERR "time: %d\n",time();
    &update_prmtop_cache;
}


sub expand_reslist {
    my $string=shift;

    my ($start,$end) = split /-/,$string;

    if (! defined $end) {
            $end=$start;
    }

    die "In 'RES1-RES' value 'RES2' must not be lower than 'RES1'; stopped.\n"
            if (! ($end >= $start) );

    return ($start..$end);
}
```

```
sub make_coorfiles{

   my $fpref=$globals{OUTPUT_PREFIX} .
            "_cmplx";

   my $maindir=
            $globals{TEMPDIR} . "/" . $globals{DIR_STRUCTFILES};

   mkdir $maindir,0777
            or die "error creating dir $maindir, stopped";


   foreach my $cplnum (sort { $a <=> $b } keys %complex_info){

            printf STDERR "cplnum: %d\t time: %d\n",$cplnum,time();

            my $dirnum = int( $cplnum / $globals{MAX_CPL_IN_DIR} );

            my  $dirnam = $maindir . "/" . $dirnum;

            if( ! -d $dirnam ){
               mkdir $dirnam,0777
                        or die "can't create directory $dirnam: $!, stopped";
            }


            my $infile = ${$complex_info{$cplnum}}->pdbtemp();
            my $fbase = $dirnam . "/" . $fpref . "_" . $cplnum;
            my $pdbout = $fbase . ".pdb";
            my $crdout = $fbase . ".crd";

            my @atoms_in;
            my @atoms_out;


            &read_pdb($infile,\@atoms_in);
            &select_residues(\@atoms_in,\@atoms_out,$cplnum);
            &write_pdb($pdbout,\@atoms_out);
            ${$complex_info{$cplnum}}->pdbfile($pdbout);
            &write_crd($crdout,\@atoms_out);
            ${$complex_info{$cplnum}}->crdfile($crdout);

   }
}

sub run_carnal{
   my ($prmtop,
            $mdcrd,
            $resnum,
            $pdbtempdir) = @_;

   my $analin=&new_tempfile("analin");
   my $analout=&new_tempfile("analout");

   my $pdbpref=$pdbtempdir . "/pdb";

   open ANALIN, ">$analin";
   print ANALIN qq{
            FILES_IN
               PARM p1 $prmtop;
            STREAM s1 $mdcrd;
            FILES_OUT
               COORD c1 $pdbpref PDB;
            DECLARE
               GROUP tpl ( RES $resnum );
            CUTRES cr1 tpl $globals{CUTOFF_CMPLX};
            OUTPUT
               COORD c1 s1;
            END
            };
```

```
   close ANALIN;

   my $command =
            $globals{CARNAL} . " " .
            "<$analin >$analout";

   system($command) && die "error running carnal, stopped";

   return $analout;
}


sub parse_analout{
   my $analout=shift;
   my $pdbtempdir=shift;

#    my @tmp=sort { $a <=> $b } keys %complex_info;
#    my $cplnum=$tmp[-1];

   my $cplnum=keys %complex_info;

   my $maxcplnum=$globals{NUM_CMPLX_MAX};

   my $framenum=0;
   my $flag;
   my @resids;
   my @flds;


   open ANALOUT, "<$analout";

   while (<ANALOUT>) {
            if (m/^--CUTRES/) {
               @resids=();
               $cplnum++;

#              print STDERR "mmmm $cplnum\n";

               $framenum++;
               $flag=1;
            }
            if (m/^RES / && $flag) {
               @flds=split;
               push @resids, ($flds[1]..$flds[2]);
            }
            if (m/^--$/) {
               $flag=0;
#              print "$cplnum @resids\n";

               &register_resids($cplnum,\@resids);
               ${$complex_info{$cplnum}}->pdbtemp($pdbtempdir .
                                                  "/pdb." .
                                                  $framenum);

               if( $maxcplnum > 0 && $cplnum >= $maxcplnum ) {
                        print STDERR "Maximum number of complexes reached; " .
                           "stopping extraction\n";
                        close ANALOUT;
                        return;
               }
            }
   }
   close ANALOUT;
}


sub register_resids{
   my ($n,$resref) = @_;

   my $data = new ComplexData;
```

```
    foreach (@$resref){
            $data->residues($_,'');
    }

    $complex_info{$n}=\$data;
}


sub print_info_all_complexes {

    foreach my $cpl (sort { $a <=> $b } keys %complex_info){

            print "============================\n";
            print "complex number: $cpl\n";
            print "----------------------\n";

            foreach my $res (
                                    sort { $a <=> $b }
                                    keys %{${$complex_info{$cpl}}->residues()}
                                    ) {
               print "$res\t"
                        . ${$complex_info{$cpl}}->residues($res)
                        . "\n";
            }
            print "----------------------\n";
            print "prmtopstr: " . ${$complex_info{$cpl}}->prmtopstr() . "\n";
            print "pdbfile: " . ${$complex_info{$cpl}}->pdbfile() . "\n";
            print "crdfile: " . ${$complex_info{$cpl}}->crdfile() . "\n";
    }
    print "============================\n";
}



sub read_pdb {
    my $infile = shift;
    my $ref_atoms= shift;

    # read the pdb file
    open INFILE, "<$infile" or die "opening $infile for reading: $!, stopped";

    while (<INFILE>) {
            push @{$ref_atoms}, $_;
    }

    close INFILE;
}

sub update_prmtop_cache {
    my $dir=$globals{PATH_PRMTOPS_COMPLEXES};

    foreach my $cpl (sort { $a <=> $b } keys %complex_info){

            &gen_prmtopstring($cpl);
            my $prmtopfile=
               $dir . "/"
               . ${$complex_info{$cpl}}->prmtopstr()
               . ".prmtop";

            next if ( -r $prmtopfile );

            my $pdbfile=${$complex_info{$cpl}}->pdbfile();

            &make_prmtop($pdbfile,$prmtopfile);
    }
}

sub gen_prmtopstring{
    my $cpl=shift;
```

```
    my $string="";
    my %rescounter;

    foreach my $res (
                                sort { $a <=> $b }
                                keys %{${$complex_info{$cpl}}->residues()}
                                ) {
                $rescounter{${$complex_info{$cpl}}->residues($res)}++;
    }

    foreach my $res (sort keys %rescounter) {
                $string .= $res . "_" . $rescounter{$res}. ":";
    }
    chop $string;
    ${$complex_info{$cpl}}->prmtopstr($string);
}


sub select_residues {
    my $ref_atoms_in = shift;
    my $ref_atoms_out = shift;
    my $i = shift;

    my @resids=
                sort { $a <=> $b } keys %{${$complex_info{$i}}->residues()};

    my $len;
    foreach (@resids) {
                $len=length;
                die "residue number out of range, stopped" if ($len==0 || $len > 4);

                # take the residues we are interested in
                my $leadlen=4-$len;
                my $pat= "^.{22}" .  "[ 0]{$leadlen}" . $_;
                push(@{$ref_atoms_out},grep(m/$pat/,@{$ref_atoms_in}));

                # find the residue name in the last matching line and store it
                my $resname=substr($ref_atoms_out->[-1],17,3);
                ${$complex_info{$i}}->residues($_,$resname);

                # put a 'TER' line between residues
                push(@{$ref_atoms_out},"TER\n");
    }
}


sub write_pdb{
    my $out=shift;
    my $ref_atoms=shift;

    # write the pdb output
    open OUT, ">$out" or die "cannot open file $out for writing: $!, stopped";

    $"="";

    print OUT @{$ref_atoms};

    $"=" ";

    close OUT;

}


sub write_crd{
    my $out=shift;
    my $ref_atoms=shift;

    # remove 'TER' lines
```

```
    for(my $i=0; $i < @{$ref_atoms} ; $i++){
            if ($ref_atoms->[$i] =~ /^TER/){
               splice(@{$ref_atoms}, $i, 1);
            }
    }

    my $num=@{$ref_atoms};

    # write the crd output
    open OUT, ">$out" or die "cannot open file $out for writing: $!, stopped";

    print OUT "\n";
    printf OUT "%5d\n", $num;

    my ($x, $y, $z);
    my $i=0;

    foreach(@{$ref_atoms}){

            $x=substr($_,30,8);
            $y=substr($_,38,8);
            $z=substr($_,46,8);

            printf OUT "%12.7f%12.7f%12.7f", $x, $y, $z;
            print OUT "\n" if ($i % 2);

            $i++;
    }

    close OUT;
}


sub  make_prmtop{
    my ($pdbin,$prmtopout)=@_;

    my $leaprc=$globals{INPUT_LEAPRC};
    my $leappath=$globals{PATH_LEAPDATA};


    my $tmpcrd=&new_tempfile("crd");
    my $leapin=&new_tempfile("leapin");
    my $leapout=&new_tempfile("leapout");
    my $leaplog=&new_tempfile("leaplog");

    open  LEAPIN, ">$leapin";
    print LEAPIN "logfile $leaplog\n";
    print LEAPIN "addpath $leappath\n";
    print LEAPIN "source $leaprc\n";
    print LEAPIN "sys = loadpdb $pdbin\n";
    print LEAPIN "saveAmberParm sys $prmtopout $tmpcrd\n";
    print LEAPIN "quit\n";
    close LEAPIN;

    my $command =
            "$ENV{'AMBERHOME'}/exe/tleap -s -f $leapin"
            . ">$leapout";


    system($command) && die "error running tleap, stopped";


#    print "$prmtopout $tmpcrd\n";

    -z $prmtopout  &&
            die "error running tleap (empty parameter file),"
            . " stopped";

}
```

```
sub run_mm_pbsa {
   my $dir=&new_tempsubdir("mm_pbsa_out");

   # directory erzeugen oder leeren

   my $cpiofile=$globals{MM_PBSA_OUT_CPIO};

   if( -f $cpiofile ){
            if( ! $globals{OVERWRITE_OUTPUT_MM_PBSA} ){
               die "archive $cpiofile already exists,\n"
                        . "-> use OVERWRITE_OUTPUT_MM_PBSA to overwrite!\n"
                        . "stopped";
            }
            unlink $cpiofile;
   }


   # cpiofile initialisieren
   my $cmd="cpio -o </dev/null >$cpiofile 2>" .
            $globals{TEMPDIR} . "/cpio.err";

   system($cmd)
            && die "error initialising cpio file $cpiofile, stopped";


   # Pfade zu den prmtop- und crd-files bestimmen

   die if ( ! $dir =~ /^\// );

   my $workdir=$globals{WORKDIR} . "/";
   my $tempdir=$globals{TEMPDIR} . "/";

   my $path_prmtops =
            $workdir .
            $globals{PATH_PRMTOPS_COMPLEXES} .
            "/";

   my $crd_prefix = $globals{OUTPUT_PREFIX} . "_cmplx";


   # die eigentlichen MM-PBSA-runs durchf黨ren

   chdir $dir;

   print STDERR "Running MM-PBSA\t";
   printf STDERR "time: %d\n",time();

   foreach my $cplnum (sort { $a <=> $b } keys %complex_info){

            printf STDERR "cplnum: %d\t time: %d\n",$cplnum,time();

            my $crdfullpath =
               ${$complex_info{$cplnum}}->crdfile();

            my $crdname=basename($crdfullpath);

            my $crdlink = $crdname . "_com.crd.1";

            symlink $crdfullpath , $crdlink;

            my $prmtopfullpath =
               $path_prmtops .
               ${$complex_info{$cplnum}}->prmtopstr() .
               ".prmtop";

            my $prmtop=&basename($prmtopfullpath);
```

```
            symlink $prmtopfullpath, $prmtop;

            my $mpbin="mpbin.$cplnum";

            my $ref_subst_pats =
               [
                ["=MPBI_PREFIX=",$crdname],
                ["=MPBI_COMPT=" ,$prmtop]
               ];



            &fill_template_file($workdir . $globals{TEMPLATE_MM_PBSA_IN},
                                $mpbin,
                                $ref_subst_pats);


            my $mpbout=$crd_prefix . "_" . $cplnum . ".mpbout";
            my $mpberr=$crd_prefix . "_" . $cplnum . ".mpberr";

            my $command =
               "$ENV{'MMPBSAMODHOME'}/mm_pbsa.pl $mpbin"
               . ">$mpbout 2>$mpberr";

            system($command) && die "error running mm_pbsa.pl, stopped";

            &check_mpberr($mpberr) ||
               ${$complex_info{$cplnum}}->mpberr(1);


            &parse_statistics_file($crdname . "_statistics.out",$cplnum);

            my $sandout="sander_com.1.out" ;

            if ( -f $sandout ) {
               rename $sandout, $crdname . "_sander.out"               ;
            }

            rename "restrt", $crdname . "_rest.crd";

            if( ! $globals{KEEP_TEMPFILES} ) {
               unlink $crdlink, $mpbin, "mdinfo";
            }

            if( !( $cplnum % $globals{MAX_CPL_IN_DIR} ) ) {
               &move_all_to_cpio("$workdir/$cpiofile");
            }
   }

   &move_all_to_cpio("$workdir/$cpiofile");

   chdir $workdir;
}


sub move_all_to_cpio {
   my $cpiofile=shift;

#    my $cpiolink=".cpiolink";

#    symlink $cpiofile,$cpiolink;

   my $cmd = "ls|cpio -o --append " .
#                "-O $cpiolink 2>cpio.err";
                "-F $cpiofile 2>cpio.err";

#    print "$cmd\n";

   system($cmd)
```

```
            && die "error running cpio, stopped";

   unlink glob "*";
#   unlink $cpiolink;
}


sub fill_template_file{
   my($template,$output,$ref_substpats)=@_;

   open TEMPLATE, $template or
            die "cannot open file \"$template\" for reading: $!\n";

   open OUT, ">$output" or
            die "cannot open file \"$template\" for writing: $!\n";

   while (<TEMPLATE>){
            my $line = $_;

            my $pat_ref;
            foreach $pat_ref ( @$ref_substpats  ){
#              print "$pat_ref->[0] $pat_ref->[1]\n";
               $line =~ s{$pat_ref->[0]}{$pat_ref->[1]};

            }
            print OUT $line;
   }

   close OUT;
   close TEMPLATE;
}

sub parse_statistics_file{
   my ($infile,$cplnum) = @_;

   my $store_labels = 0;

   if (! defined $results{LABELS} ) {
            $store_labels = 1 ;
   }


   open INFILE, $infile;
   while (<INFILE>) {
            s/\#.*$// ; # remove comments
            next if( /^\s*$/ ); # empty line

            my @flds = split /\s+/;

            my $label=$flds[0];
            my $value=$flds[1];

            $results{$label}->[$cplnum]=$value;

            if ( $store_labels ) {
               push @{$results{LABELS}}, $label;
            }
   }
   close INFILE;
}


sub check_mpberr {
   my $file = shift;

   if ( -z $file )  {
            unlink $file;
            return 1;
   }
```

```
    return 0;
}



sub print_results {

    print "\n";
    print "MM-PBSA results:\n\n";

    my @labels = @{$results{LABELS}};

    $"="\t";
    print "#\t\t@labels\tSTOICHIOMETRY\n";

    foreach my $cplnum (sort { $a <=> $b } keys %complex_info){
                print "$cplnum\t";
                if ( ${$complex_info{$cplnum}}->mpberr()) {
                   print "w!"
                }
                print "\t";
                foreach my $lb (@labels){
                   print $results{$lb}->[$cplnum] . "\t";
                }
                print ${$complex_info{$cplnum}}->prmtopstr() . "\n"
    }
}


sub print_header{

    print "=====================================================\n";
    printf "Output of %s\n", &basename($0);
    printf "( %s )\n", &version();
    print "=====================================================\n";
    print "\n";
    print "Parameters controlling the run:\n\n";



    my @keys = qw{
                            INPUT_PRMTOP
                            INPUT_LEAPRC
                            INPUT_MDCRD
                            PATH_PRMTOPS_COMPLEXES
                            OUTPUT_PREFIX
                            TEMPLATE_MM_PBSA_IN
                            CUTOFF_CMPLX
                    };


   foreach my $key (@keys ){
                printf "%-20s=> %s\n", $key, $globals{$key};
    }

    print "\n";
    print "=====================================================";
    print "\n";

}

sub archive_structures {

    chdir $globals{TEMPDIR};

    my $structdir=$globals{DIR_STRUCTFILES};
    my $cpiofile=$globals{WORKDIR} . "/" . $structdir . ".cpio" ;

    if( system("find $structdir|cpio -o -O $cpiofile 2>cpio.err") ) {
                chdir $globals{WORKDIR};
```

```
            die "error running cpio, stopped";
    }

    chdir $globals{WORKDIR};
}



sub move_tempdir{

    return if ( ! $globals{TEMP_EXISTS} );

    my $tempdir=$globals{TEMPDIR};
    my $workdir=$globals{WORKDIR};


    if ( ! $globals{REMOVE_TEMPFILES} ) {

            if( $globals{KEEP_TEMPFILES}
                ||
                ! $globals{FINISHED_CLEAN}) {

                if( system("cp -r $tempdir $workdir") ) {
                        warn "Could not copy temporary dir $tempdir" .
                            "to working directory $workdir";
                } else {
                        print STDERR
                            "Temporary files are left in directory " .
                            basename($tempdir) . ".\n";
                }
            }
    }

    rmtree "$tempdir"
            or die "error removing temporary directory $tempdir: $!";
}


sub END {
    &move_tempdir;
}
```

The input parameters for mm_pbsa.pl are specified in the file MM_GBSA_IN_NMODE:

```
#
# Input parameters for mm_pbsa.pl
# This example uses snapshots from ../01_GenerateSnapshots, and computes
#    continuum free energy estimates, using both GB and PB models
#
# Holger Gohlke
# 08.01.2002
#
###############################################################################
```

```
@GENERAL
#
# General parameters
#   0: means NO; >0: means YES
#
#   mm_pbsa allows to calculate (absolute) free energies for one molecular
#     species or a free energy difference according to:
#
#     Receptor + Ligand = Complex,
#     DeltaG = G(Complex) - G(Receptor) - G(Ligand).
#
#   PREFIX - To the prefix, "{_com, _rec, _lig}.crd.Number" is added during
#           generation of snapshots as well as during mm_pbsa calculations.
#   PATH - Specifies the location where to store or get snapshots.
#
#   COMPLEX - Set to 1 if free energy difference is calculated.
#   RECEPTOR - Set to 1 if either (absolute) free energy or free energy
#             difference are calculated.
#   LIGAND - Set to 1 if free energy difference is calculated.
#
#   COMPT - parmtop file for the complex (not necessary for option GC).
#   RECPT - parmtop file for the receptor (not necessary for option GC).
#   LIGPT - parmtop file for the ligand (not necessary for option GC).
#
#   GC - Snapshots are generated from trajectories (see below).
#   AS - Residues are mutated during generation of snapshots from trajectories.
#   DC - Decompose the free energies into individual contributions
#        (only works with MM and GB).
#
#   MM - Calculation of gas phase energies using sander.
#   GB - Calculation of desolvation free energies using the GB models in sander
#        (see below).
#   PB - Calculation of desolvation free energies using delphi (see below).
#   MS - Calculation of nonpolar contributions to desolvation using molsurf
#        (see below).
#        If MS == 0, nonpolar contributions are calculated with the LCPO method
#        in sander.
#   NM - Calculation of entropies with nmode.
#
PREFIX              =MPBI_PREFIX=
PATH               ./
#
COMPLEX             1
RECEPTOR            0
LIGAND              0
#
COMPT               =MPBI_COMPT=
RECPT               XXX
LIGPT               XXX
#
GC                 0
AS                 0
DC                  0
#
MM                  1
GB                 1
PB                 0
MS                  0
#
NM                  1
#
###############################################################################
@PB
#
# PB parameters (this section is only relevant if PB = 1 above)
#
#   The following parameters are passed to the PB solver.
#   Additional parameters (e.g. SALT) may be added here.
#   For further details see the delphi and pbsa documentation.
#
```

```
#   PROC - Determines which method is used for solving the PB equation:
#         If PROC = 1, the delphi program is applied. If PROC = 2,
#          the pbsa program of the AMBER suite is used.
#   REFE - Determines which reference state is taken for PB calc:
#         If REFE = 0, reaction field energy is calculated with EXDI/INDI.
#           Here, INDI must agree with DIELC from MM part.
#         If REFE > 0 && INDI > 1.0, the difference of total energies for
#           combinations EXDI,INDI and 1.0,INDI is calculated.
#           The electrostatic contribution is NOT taken from sander here.
#   INDI - Dielectric constant for the molecule.
#   EXDI - Dielectric constant for the surrounding solvent.
#   SCALE - Lattice spacing in no. of grids per Angstrom.
#   LINIT - No. of iterations with linear PB equation.
#   PRBRAD - Solvent probe radius in A (e.g. use 1.4 with the PARSE parameter set
#     and 1.6 with the radii optimized by R. Luo)
#
#   Parameters for pbsa only
#
#   RADIOPT - Option to set up atomic avity radii for molecular surface calculation
#     and dielectric assignment. A value of 0 uses the cavity radii from the prmtop file.
#     A value of 1 sets up optimized cavity radii at the pbsa initialization phase.
#     The latter radii are optimized for model compounds of proteins only; use cautions
#     when applying these radii to nucleic acids.
#
#   Parameters for delphi only
#
#   FOCUS - If FOCUS > 0, subsequent (multiple) PERFIL and SCALE parameters are
#     used for multiple delphi calculations using the focussing technique.
#     The # of _focussing_ delphi calculations thus equals the value of FOCUS.
#   PERFIL - Percentage of the lattice that the largest linear dimension of the
#           molecule will fill.
#   CHARGE - Name of the charge file.
#   SIZE - Name of the size (radii) file.
#
#   SURFTEN / SURFOFF - Values used to compute the nonpolar contribution Gnp to
#                 the desolvation according to Gnp = SURFTEN * SASA + SURFOFF.
#
#
PROC               2
REFE               0
INDI              1.0
EXDI              80.0
SCALE              2.0
LINIT             500
PRBRAD              1.6
#
RADIOPT             1
#
FOCUS              0
PERFIL             80.0
CHARGE               ./my_amber94_delphi.crg
SIZE              ./my_parse_delphi.siz
#
SURFTEN             0.005
SURFOFF             0.0
#
##############################################################################
@MM
#
# MM parameters (this section is only relevant if MM = 1 above)
#
#   The following parameters are passed to sander.
#   For further details see the sander documentation.
#
#   DIELC - Dielectricity constant for electrostatic interactions.
#           Note: This is not related to GB calculations.
#
DIELC              1.0
MAXCYC                    10000
#
```

```
##############################################################################
@GB
#
# GB parameters (this section is only relevant if GB = 1 above)
#
#   The first group of the following parameters are passed to sander.
#   For further details see the sander documentation.
#
#   IGB - Switches between Tsui's GB (1), Onufriev's GB (2, 5).
#   GBSA - Switches between LCPO (1) and ICOSA (2) method for SASA calc.
#         Decomposition only works with ICOSA.
#   SALTCON - Concentration (in M) of 1-1 mobile counterions in solution.
#   EXTDIEL - Dielectricity constant for the solvent.
#   INTDIEL - Dielectricity constant for the solute
#
#   SURFTEN / SURFOFF - Values used to compute the nonpolar contribution Gnp to
#                 the desolvation according to Gnp = SURFTEN * SASA + SURFOFF.
#
IGB                2
GBSA               1
SALTCON            0.00
EXTDIEL            20.7
INTDIEL            1.0
#
SURFTEN            0.00
SURFOFF            0.00
#
##############################################################################
@MS
#
# Molsurf parameters (this section is only relevant if MS = 1 above)
#
#   PROBE - Radius of the probe sphere used to calculate the SAS.
#         Since Bondi radii are already augmented by 1.4A, PROBE should be 0.0
#
PROBE              0.0
#
##############################################################################
@NM
#
# Parameters for sander/nmode calculation (this section is only relevant if NM = 1 above)
#
#   The following parameters are passed to sander (for minimization) and nmode
#     (for entropy calculation using gasphase statistical mechanics).
#   For further details see documentation.
#
#   DIELC - (Distance-dependent) dielectric constant
#   MAXCYC - Maximum number of cycles of minimization.
#   DRMS - Convergence criterion for the energy gradient.
#
DIELC              4
MAXCYC             1
DRMS               0.0001
#
##############################################################################
@PROGRAMS
#
# Program executables
#
DELPHI             /home/gohlke/src/delphi.98/exe/delphi
#
##############################################################################
```

The input file for the calculation of free energy is:

```
INPUT_PRMTOP            CPL_ACN.prmtop
INPUT_MDCRD             maa_lowest101_200.mdcrd
INPUT_LEAPRC            leap/parmspreps.leaprc

TEMPLATE_MM_PBSA_IN     mm_pbsa_in_Nmode
CUTOFF_CMPLX            3.5

NUM_CMPLX_MAX                   1000

PATH_PRMTOPS_COMPLEXES          prmtops_Nmode

CARNAL              ./carnal
#KEEP_TEMPFILES     1
PATH_LEAPDATA       leap/
```

The free energies were individually calculated in the present work. For establishing the binding free energy of the template to the rest of the system, a ΔG value needs to be obtained. As for the 1000 snapshots created from the simulated annealing procedure, the number of each species included in the first solvation shell is different, which requires writing a script to extract ΔG for each snapshot. The code for calculating ΔG is:

```
#!/usr/bin/perl -w

use strict;
use POSIX;
#use File::Path;
#use Class::Struct;

my ($file_mippbo_out,$file_tab_gs_mols);
my @clabels;
my %gs_mols;
my $warnings;

### main

&parse_cmdline;
&read_gs_mols;
&work_on_input;

# foreach my $mol ( keys %gs_mols ) {
```

```
#     print "$mol:\t@{$gs_mols{$mol}}\n";
# }


### end of main

sub parse_cmdline {

   ($file_mippbo_out,$file_tab_gs_mols) = @ARGV;

   defined $file_tab_gs_mols or &usage;

   -r $file_mippbo_out
            or die "file $file_mippbo_out does " .
            "not exist or is not readable, stopped";
   -r $file_tab_gs_mols
            or die "file $file_tab_gs_mols does " .
            "not exist or is not readable, stopped";
}


sub usage{
   print &version() . "\n";
   print "\nusage: " . &basename($0) .
            " mip_pbsa_output table_with_gs_of_mols\n\n" ;
   exit 1;
}


sub version{
   my $id='$$';
}

sub basename{
   my ($path)=@_;
   $path =~ s  .*/Ë;
   $path;
}


sub read_gs_mols {
   my $infile=$file_tab_gs_mols;

     open INFILE, $infile or
            die "cannot open file \"$infile\" for reading: $!\n";

   my $line;

   while (<INFILE>) {
            next if( /^\s*$/ ); # empty line

            s/^\s+//;
            $line++;

            next if($line==1);

            if( $line==2 ){
               @clabels=split /\s+/;
            } else {
               &store_gs($_);
            }
   }

   close INFILE;
}

sub store_gs {
   $_=shift;

   my @flds=split /\s+/;
```

```
    my $mol=$flds[0];
    my @vals=@flds[1 .. $#flds];

    $gs_mols{$mol}=\@vals;
}


sub work_on_input{

    my $infile=$file_mippbo_out;

    open INFILE, $infile or
            die "cannot open file \"$infile\" for reading: $!\n";

    my ($flag,$line);

    while (<INFILE>) {
            next if( /^\s*$/ ); # empty line

            $flag++ if( /^MM-PBSA results:/ );

            next if( ! $flag );

            $line++;

            next if($line==1);

            if( $line==2 ){
               &check_and_print_clabels($_);
            } else {
               &calc_and_print_results($_);
            }
    }

    close INFILE;

    if($warnings) {
            print STDERR "there have been $warnings warnings\n";
    }
}

sub check_and_print_clabels {
    $_=shift;

    /^\#\s+.*STOICHIOMETRY\s*$/ or die "strange format, stopped";

    s/^#\s+//;

    my @flds=split /\s+/;

    my @theselabels=@flds[0 .. $#flds-1];

    $"='xxx';

    my $check1="@clabels";
    my $check2="@theselabels";

    if( ! ( $check1 eq $check2) ) {
            die "column label mismatch";
    }

    $"="\t";

    print "Results for Delta_G:\n\n#\t\t@clabels\n"

}


sub calc_and_print_results{
```

```
    $_=shift;

    my $wstr="";


    /^\d+\s+/ or die "strange format, stopped";


    if( /w!/){
            $wstr="w!";
            $warnings++;
            s/w!//;
    }

    my @flds=split /\s+/;

    my $cplnum=$flds[0];
    my @results=@flds[1 .. $#flds-1];
    my $stoechstr=$flds[-1];

    $"="\t";
#   print "$cplnum\t$wstr\t@vars\n";

    ( $#results == $#clabels ) or
            die "strange format, stopped";

    my $ref_stoich=&parse_stoichiometry($stoechstr);

    foreach my $mol ( keys %$ref_stoich ) {

            defined $gs_mols {$mol}
               or die "Values for $mol not found in table, stopped";

            my $mult = $$ref_stoich{$mol};

            my @gs_mol = @{$gs_mols{$mol}};

            my @tmp=@{&multiply(\@gs_mol,$mult)};

            @results=@{&subtract(\@results,\@tmp)};
    }

    my @results_formatted=@{&sprintf_array("%1.4g",\@results)};

    print
            $cplnum    . "\t" .
            $wstr      . "\t" .
            "@results_formatted" . "\t" .
            $stoechstr . "\n";
}



sub parse_stoichiometry{

    $_=shift;

    my %stoich;

    my @parts=split ':';

    foreach ( @parts ) {
            my($mol,$num)=split '_';
            $stoich{$mol}=$num;
    }
    return \%stoich;
}
```

```
sub subtract{
   my($ref1,$ref2)=@_;

   my @result;

   $#$ref1 == $#$ref2 or die "differing vector lengths, stopped";

   foreach my $i ( 0 .. $#$ref1 ) {
            $result[$i]=$$ref1[$i]-$$ref2[$i];
   }

   return \@result;
}


sub multiply{
   my($aref,$fact)=@_;

   my @result;


   foreach my $i ( 0 .. $#$aref ) {
            $result[$i]=$$aref[$i]*$fact;
   }

   return \@result;
}


sub sprintf_array {

   my($format,$aref)=@_;

   my @results;

            foreach ( @$aref ) {

               push @results, sprintf($format,$_);

            }

   return \@results;
}
```

APPENDIX B

LIST OF PUBLICATIONS

[1] **Wei, S.**; Molinelli, A.; Mizaikoff, B., Molecularly imprinted micro and nanospheres for the selective recognition of 17β-estradiol. *Biosens. Bioelectron.* **2006,** 21, (10), 1943-1951.

[2] **Wei, S.**; Jakusch, M.; Mizaikoff, B., Capturing molecules with templated materials - Analysis and rational design of molecularly imprinted polymers. *Anal. Chim. Acta* **2006,** 578, (1), 50-58.

[3] O'Mahony, J.; **Wei, S.**; Molinelli, A.; Mizaikoff, B., Imprinted Polymeric Materials. Insight into the Nature of Prepolymerization Complexes of Quercetin Imprinted Polymers. *Anal. Chem.* **2006,** 78, (17), 6187-6190.

[4] **Wei, S.**; Mizaikoff, B., Binding Site Characteristics of 17β-Estradiol Imprinted Polymers. *Biosens. Bioeletron.* **2007**, In press.

[5] **Wei, S.**; Jakusch, M.; Mizakoff, B., Investigating the Mechanisms of 17β-Estradiol Imprinting by Computational Prediction and Spectroscopic Analysis. *Anal. Bioanal. Chem.* **2007**, In press.

[6] **Wei, S.**; Mizaikoff, B., Recent Advances on Non-covalent Molecular Imprints for Affinity Separations. *J. Sep. Sci.* **2007**, In press.

[7] **Wei, S.**; Huang, C.-H.; Fernandez, F. M.; Mizaikoff, B., Determination of Estrogens in River Water with SPE using 17β-Estradiol-Imprinted Polymers combined with LC-TOF-MS. *Anal. Chem.* **2007**, Submitted.

[8] **Wei, S.**; Jakusch, M.; Mizaikoff, B., Understand the Mechanism of Selectivity in Molecular Imprinted Polymers by Molecular Dynamic Simulation. Manuscript in preparation.

[9] **Wei, S.**, Park, S.-H., Huang, C.-H., Taylor, A. E., Aral, M. Mizaikoff, B., Effect of Environmental Aging of Water-Plant Polymers on N-nitrosodimethylamine (NDMA) Formation. Manuscript in preparation.